ISSN 2622-9374 (Online)

Asian Institute of Research

Engineering and Technology Quarterly Reviews

Vol. 2, No.1 June 2019

Asian Institute of Research
Connecting Scholars Worldwide

Asian Institute of Research
Engineering and Technology Quarterly Reviews
Vol.2, No.1 June 2019

Engineering and Technology
Quarterly Reviews
ISSN 2622-9374 (Online)

Engineering and Technology
Quarterly Reviews
ISSN 2622-9374 (Online)

ASIAN INSTITUTE OF RESEARCH
Connecting Scholars Worldwide

The Asian Institute of Research
Engineering and Technology Quarterly Reviews
Vol.2, No.1, 2019: 1-15
ISSN 2622-9374

Effect of Height on Retrofitting of Existing Steel Frames Using Buckling Restrained Brace Frames

Sara Seyedfarizani[1]

[1] Sharif University of Technology, International Campus, Kish Island. Email: farizani@kish.sharif.edu

Abstract
Recent earthquakes indicate the importance of retrofitting existing structures to achieve an acceptable level of performance. Several different methods for retrofitting of existing structures were used by structural designers; Use of bracing systems is a cost-effective method for seismic retrofitting of existing steel frames. In particular, Buckling Restrained Braces (BRBs) are workable choices to be used because of their large energy dissipation capacity especially under moderate to severe earthquakes. Buckling restrained braces yield in tension and compression, exhibits stable and predictable hysteretic behavior. In this paper two existing structure with different heights are retrofitted with BRB. At next stage vulnerability assessment is done according to ASCE 41-06 with pushover analysis by SAP2000 software and compare the seismic parameters with each other to evaluate effect of height in retrofitted buildings with BRB. By having focus on results, it's observed that, Stiffness of four story building that retrofitted with BRB is larger than eight story but Earthquake energy that dissipated by eight story BRB is more also, four story BRB may undergo less lateral displacements than eight story BRBF and ductility of eight story is larger, so with increasing height, effective stiffness will decrease but ductility will increase. So it's better to use of BRB for retrofitting high raise building in moderate to high seismicity regions.

Key Words: Bracing System, BRB, Ductile, Retrofit, Steel Frame

1. Introduction

The hazard to life in case of earthquake is almost entirely associated with man-made structures such as buildings, dams, bridges etc. Prevention of disasters caused by earthquake has become increasingly important in recent years (Uang et al., 2001). Disaster prevention includes the reduction of seismic risk through retrofitting existing buildings in order to meet seismic safety requirements. The planning of alterations to existing buildings differs from new planning through an important condition; the existing construction must be taken as the basis for all planning and building actions (Prinz, 2007).

Many existing buildings do not meet the seismic strength requirement. The need for seismic retrofitting in existing building can arise due to any of the following reasons: (1) building not designed to code (2) subsequent updating of code and design practice (3) subsequent upgrading of seismic zone (4) deterioration of strength and aging (5) modification of existing structure (6) change in use of the building, etc. These buildings are more vulnerable, and in the event of a major earthquake, there is likely to be substantial loss of lives and property (Roeder et al., 2011).

Retrofit specifically aims to enhance the structural capacities (strength, stiffness, ductility, stability and integrity) of a building that is found to be deficient or vulnerable. In the specific context of enhancing the resistance of a

vulnerable building to earthquakes, the term seismic retrofit is used. Sometimes, the terms 'seismic rehabilitation', 'seismic up gradation' and 'seismic strengthening' are used in lieu of 'seismic retrofit'. Seismic retrofit is primarily applied to achieve public safety, with various levels of structure and material survivability determined by economic considerations.

Several techniques have been used to retrofit buildings that have experienced structural damage as a consequence of moderate or severe earthquake shaking, or for the seismic upgrading of outdated existing buildings. Among these techniques, diagonal steel bracing has been considered attractive to enhance the lateral strength and stiffness of existing multi-story steel buildings. Nevertheless, it should be kept in mind that traditional braces (ductile or not) tend to exhibit global buckling when subjected to compressive strains, which in turn results in local buckling, fracture of the base material, and a highly unstable behavior under cyclic loading.

2. Buckling Restrained Braced Frames (BRBF)

The concept of buckling-restrained braces was introduced about thirty years ago in Japan by Uang and Nakashima in 2003. The idea behind a buckling-restrained brace is to fabricate a structural element that is able to work in a stable manner when it is subjected to compressive deformations (because braces are normally able to behave in a stable manner when subjected to tensile forces**.** The concept of eliminating the compression buckling failure mode in intermediate and slender compression elements has long been a subject of discussion. The theoretical solution for eliminating the buckling failure mode is very simple: laterally brace a compression element, at close regular intervals, so that the compression element's un-braced length effectively approaches zero (Bozorgnia and Bertero, 2004).

2.1 Components of BRBF:

BRBF composed of following components, as it is shown in figures 1 and 2.

- *Restrained yielding segment:* This steel segment can be rectangular or cruciform in cross section. Although it is common that a steel plate be surrounded in a casing, more than one plate can be used, if it is desired. Because this segment is designed to yield under cyclic loading, mild steel that exhibits high ductility is desirable. Also desirable are steel materials with predictable yield strength with small variations.

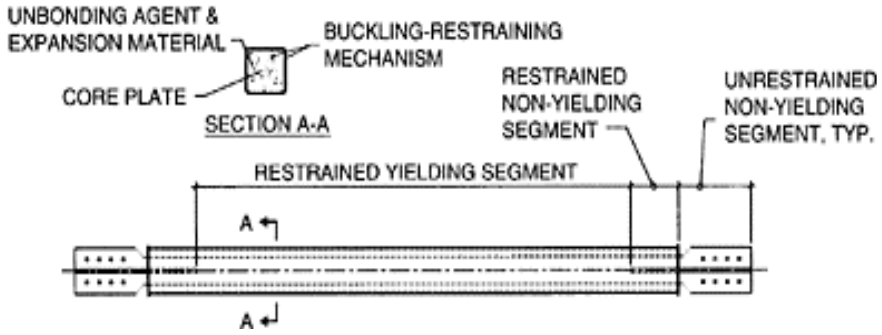

Figure 1. *Components of buckling restrained brace (Bozorgnia and Bertero, 2004)*

- *Restrained non yielding segment:* This segment, which is surrounded by the casing and mortar, is usually an extension of the restrained yielding segment but with an enlarged area to ensure elastic response.

- *Unrestrained non yielding segment*: This segment is usually an extension of the restrained non yielding segment, except that it projects from the casing and mortar for connection to the frame. This segment is also called the steel core projection.

- *Unhanding agent and expansion material:* Inert material that can effectively minimize or eliminate the transfer of shear force between the restrained steel segment and mortar can be used; materials like rubber, polyethylene, silicon grease and mastic tape have been reported.

- *Buckling-restraining mechanism:* This mechanism is typically composed of mortar and steel casing (Bozorgnia and Bertero, 2004).

The single-diagonal configuration is also an effective way to take advantage of the high strengths possible for BRBs. Note that neither X-bracing nor K-bracing is an option for BRBF. K-braced frames are not permitted for BRBF due to the possibility of inelastic flexural demands on columns. The chevron (V or Inverted-V) configuration is also popular for BRBF, as it maintains some openness for the frame. Because of the balance between brace tension and compression strength, the beam is required to resist only modest loads (Seismic Provisions, 2010)

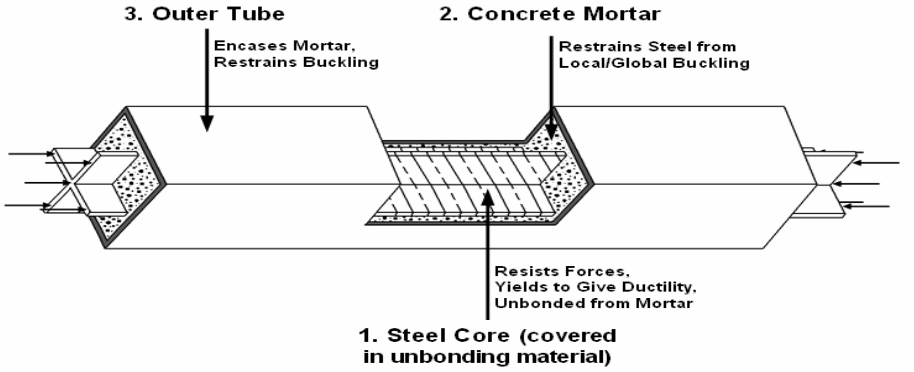

Figure 2. *Buckling-restrained brace cross section view (Prinz, 2007).*

3. Methodology

In this paper two existing structure with different height is retrofitted with BRB. At next stage vulnerability assessment is done according to ASCE 41-06 with pushover analysis by SAP2000 software and compare the seismic parameters with each other to evaluate effect of height in retrofitted buildings with BRB.

3.1 Design Methodology

According to AISC-2010, the steel core of BRBF is composed of a yielding segment and steel core projections; it may also contain transition segments between the projections and yielding segment. The length and area of the yielding segment, in conjunction with the lengths and areas of non-yielding segments, determine the stiffness of the brace. The steel core shall be designed to resist the entire axial force in the brace. The brace design axial strength, φP_{ysc} (LRFD), in tension and compression, in accordance with the limit state of yielding, shall be determined as follows:

$P_{ysc} = F_{ysc} A_{sc}$ (φ=0.90 (LRFD)) **(Eq. 1)**

Where; (A_{sc}): cross-sectional area of the yielding segment of the steel core, in^2 (mm^2) and (F_{ysc}): specified minimum yield stress of the steel core, or actual yield stress of the steel core as determined from a coupon test, (MPa).

3.2 Nonlinear Static Procedure (NSP)

The NSP is generally a more reliable approach to characterizing the performance of a structure than are linear procedures. The control node shall be located at the center of mass at the roof of a building. If the Nonlinear Static Procedure (NSP) is selected for seismic analysis of the building, a mathematical model directly incorporating the nonlinear load-deformation characteristics of individual components and elements of the building shall be subjected to monotonically increasing lateral loads representing inertia forces in an earthquake until a target displacement is exceeded.

Separate mathematical models representing the framing along two orthogonal axes of the building shall be developed for two-dimensional analysis. A mathematical model representing the framing along two orthogonal axes of the building shall be developed for three-dimensional analysis. Independent analysis along each of the two orthogonal principal axes of the building shall be permitted unless concurrent evaluation of multidirectional effects is required. The target displacement (δ_t) at each floor level shall be calculated in accordance with Equation 2:

$$\delta_t = C_0 C_1 C_2 S_a \frac{T_e^{\,2}}{4\pi^2} g \qquad \textbf{(Eq. 2)}$$

Where, (C_0): modification factor to relate spectral displacement of an equivalent single-degree of freedom (SDOF) system to the roof displacement of the building multi-degree of freedom (MDOF) system. (C_1): modification factor to relate expected maximum inelastic displacements to displacements calculated for linear elastic response. (C_2): modification factor to represent the effect of pinched hysteresis shape, cyclic stiffness degradation, and strength deterioration on maximum displacement response. (T_e): effective fundamental period of the building in the direction under consideration, in seconds. (S_a): response spectrum acceleration at the effective fundamental period and damping ratio of the building in the direction under consideration ($S_a = A \times B$). g: acceleration of gravity. (C_0) coefficient is modification factor to relate spectral displacement of an equivalent single-degree of freedom (SDOF) system to the roof displacement of the building multi-degree of freedom is calculated using of the following table 1.

Table 1. Values for modification factor C_0 [1] (ASCE 41-06, Table 3-2)

	Shear building [2]		Other building
Number of stories	Triangular load pattern	Uniform load pattern	Any load pattern
1	1.0	1.0	1.0
2	1.2	1.15	1.2
3	1.2	1.2	1.3
5	1.3	1.2	1.4
10+	1.3	1.2	1.5

[1] Linear interpolation shall be used to calculate intermediates values

[2] Buildings in which, inter-story drift decreasing with increasing height.

According to ASCE 41-06, C_1 is calculated for linear elastic response shall be calculated in accordance with following equation:

$$C_1 = 1 + \frac{R-1}{aT_e^2} \qquad \textbf{(Eq. 3)}$$

Where; a = site class factor: =130 site Class A,
B; = 90 site Class
C; = 60 site Class D, E, and F;

C_2 for periods greater than 0.7 seconds, C_2=1.0. So C_2 shall be calculated in accordance with equation 4, as follow:

$$C_2 = 1 + \frac{1}{800}\left(\frac{R-1}{T_e}\right)^2 \qquad \textbf{(Eq. 4)}$$

4. Description and geometry of existing structure

A four-story residential building in Iran, Tehran was assumed as the sample building. This structure will be rehabilitated with some retrofitting techniques including BRBFs that are added as structural elements to the existing sample structure. For designing the sample building, a common place plan of a residential building in Tehran, which has been built before the Islamic revolution of Iran about years of 1975, is assumed. The configuration and plan of the sample building is shown in figure 3 and 4. The height of stories is assumed to be 3.2 meters.

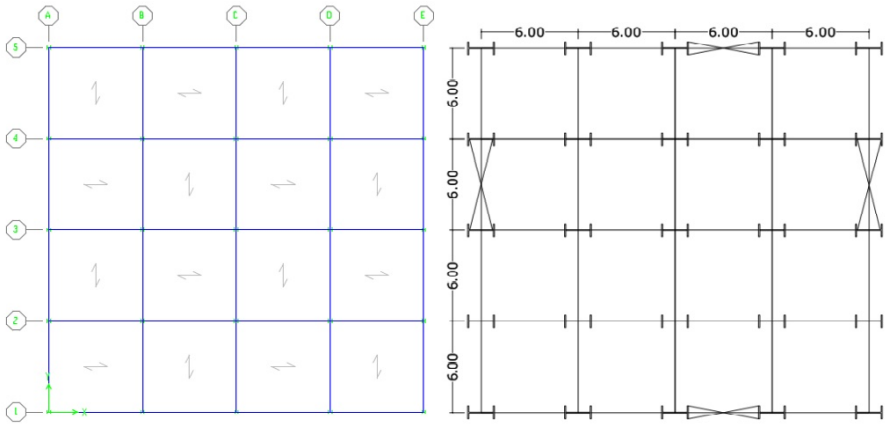

Figure 3. Plan of the sample building

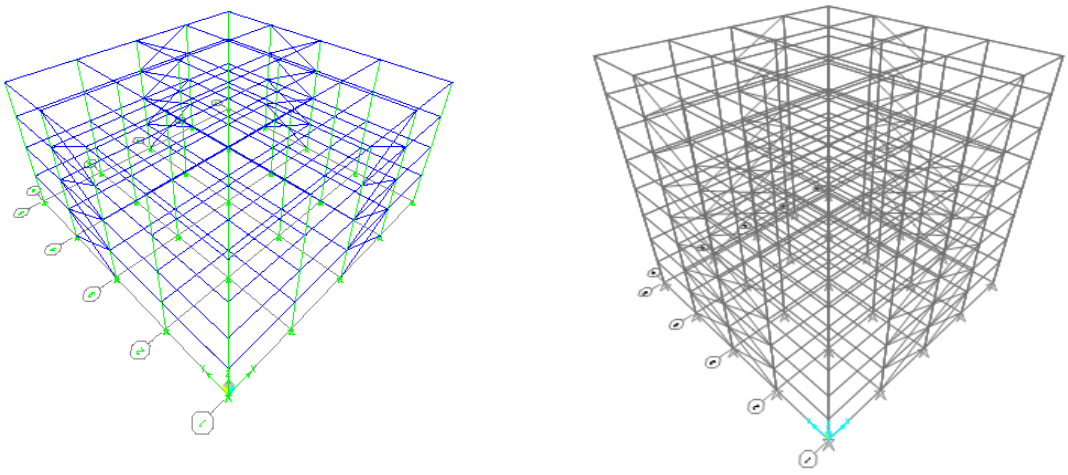

Figure 4. General view of the sample buildings

4.1 Material properties of structure

By Using St-37 steel, the yield strength of columns, beams and braces are assumed to be 240 MPa and the ultimate strength of columns, beams and braces are assumed to be 370 MPa. The details of material properties are shown in Table 2.

Table 2. Material properties data

F_y (MPa)	F_u (MPa)	E (GPa)
240	370	210

4.2 Computer model description

The building is analyzed and designed by means of commercial SAP 14.1 software and following procedures are used:

1. Floor diaphragms are assumed to be rigid.
2. Frame columns are modeled as pinned at their bases.
3. Beams to columns connections are pinned.
4. Brace connections to adjacent beams and columns are pinned.
5. HE-B (IPB) sections are used as columns.
6. IPE sections are used as beams.
7. Double angles (2L) sections are used as braces in sample buildings
8. Plate sections are used as core of braces in BRBFs system for retrofitted buildings.
9. Box sections are used as casing of braces in BRBFs system for retrofitted buildings.

4.3 Frame sections properties

Beams and columns of buildings with BRBFs are similar to the sample building with braces configuration, except those columns that adjacent to the braces that were strengthened with plates and are shown in tables. Plate section is used as brace's core of BRBF building, as shown in table 4. Table 3 and figure 5 show frame sections of sample building**.**

Table 3. Frame sections properties for four (left) and eight story (right) sample building

Column sections (mm)	**Beam sections (mm)**	**Brace sections (mm)**
IPB 160	IPE 360	2L120x120x12
IPB 180	IPE 330	2L150x150x12
IPB 200	IPE 220	
IPB 220	IPE 180	
IPB 240		
IPB 260		
IPB 280		
IPB 320		
IPB 340		
IPB 360		
IPB 400		

Table 4. Plate section for four (right) and eight story (left) building

	BRBF brace sections
Story	steel core section (mm)
1	Plate 110x40
2	Plate 110x40
3	Plate 100x40
4	Plate 100x40

	BRBF brace sections
Story	steel core section (mm)
1,2	Plate 160x40
3,4	Plate 160x40
5,6	Plate 140x40
7,8	Plate 140x40

Column-sections (mm)	Beam-sections (mm)	Brace-sections (mm)
IPB 160	IPE 360	2L120 x 120 x 12
IPB 180	IPE 330	2L100 x 100 x 10
IPB 200	IPE 220	-
IPB 220	IPE 180	-
IPB 240	-	-

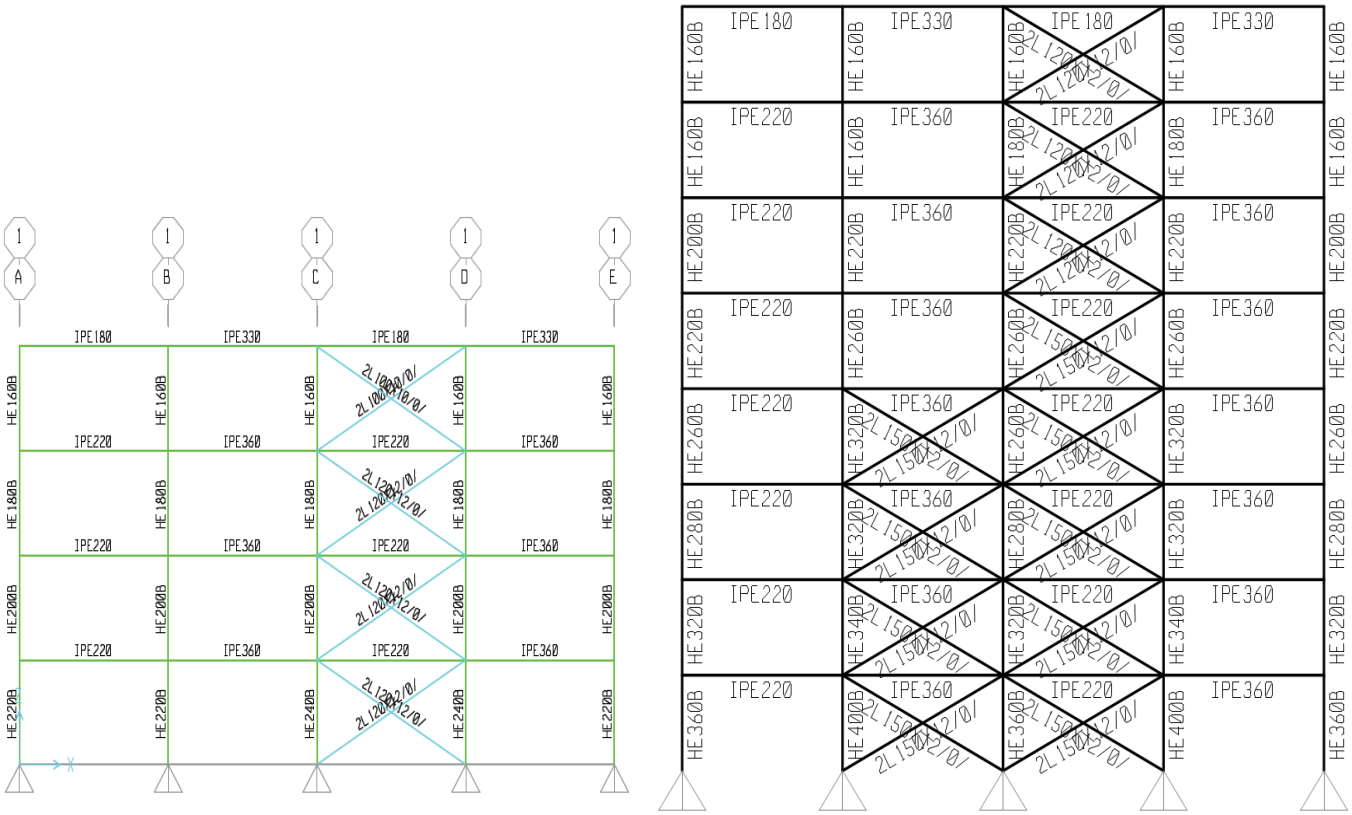

Figure 5. Illustration of frame sections at elevation

4.4 Calculating of equivalent static procedure for BRBF

Equivalent static procedure for four and eight story BRBFs are done according to STD NO.2800-3. Design base acceleration ratio, A, is equal to 0.35g. T_0 Coefficient is equal to 0.15. Fundamental period of vibration, T, is equal to 0.338 Second for four story and equals to 0.56 second for eight story structure. Building importance factor, I, is equal to 1.0. Building behavior factor, R, is equal to 8.0 for BRBF, according to ASCE/SEI7-10.

5. Design of four and eight story buildings with BRBFs

Design lateral loads that is applied to the structure by means of equivalent static procedure. BRBs Design control of steel core is according to AISC 2010, that shown in table 5 for four story and table 6 for eight story building as follow:

Table 5. Design control of steel core in four-story BRBFs building

Story	Steel core section, (mm)	A_{sc} (mm^2)	F_y (MPa)	ϕ	P_{ysc} (kN)	$P_{allowed} = \phi P_{ysc}$ (kN)	$P_{available}$ (kN)	$P_{allowed} \rangle P_{available}$
1	PL 110 x 40	4400	2400	0.9	1035.6	932.05	620.58	ok
2	PL 110 x 40	4400	2400	0.9	1035.6	932.05	570.31	ok
3	PL 100 x 40	4000	2400	0.9	941.47	847.32	450.27	ok
4	PL 100 x 40	4000	2400	0.9	941.47	847.32	244.50	ok

Table 6. Design control of steel core in eight-story BRBFs building

Story	Steel core section (mm)	A_{sc} (mm^2)	F_y (MPa)	ϕ	p_{ysc} (kN)	$P_{allowed} = \phi\ P_{ysc}$ (kN)	Pavalible (kN)	$P_{allowed} \rangle P_{available}$
1	PLATE 160X40	6400	240	0.9	1506.56	1355.9	1193.04	ok
2	PLATE 160X40	6400	240	0.9	1506.56	1355.9	1168.76	ok
3	PLATE 160X40	6400	240	0.9	1506.56	1355.9	1120.98	ok
4	PLATE 160X40	6400	240	0.9	1506.56	1355.9	1056.95	ok
5	PLATE 140X40	5600	240	0.9	1318.24	1186.41	906.39	ok
6	PLATE 140X40	5600	240	0.9	1318.24	1186.41	764.84	ok
7	PLATE 140X40	5600	240	0.9	1318.24	1186.41	576.53	ok
8	PLATE 140X40	5600	240	0.9	1318.24	1186.41	309.53	ok

6. Calculation of story drifts for BRBF

According to ASCE/SEI 7-10, the design story drift (Δ) shall be computed as the difference of the deflections at the centers of mass at the top and bottom of the story under consideration. The deflection at level *x* (δ_x) (in. or mm) used to compute the design story drift, Δ, shall be determined in accordance with equation 5, as follow:

$$\delta_x = \frac{C_d \times \delta_{xe}}{I_e} \leq \delta_a \qquad \textbf{(Eq. 5)}$$

h_{sx}= story height, in mm.
C_d = the deflection amplification factor.
δ_{xe} = the deflection determined by an elastic analysis.
I_e = the importance factor.
δ_a= allowable story drift, according to table 12.12-1 from ASCE/SEI 7-10

As defined in earlier, BRBFs must satisfy check for designing story drifts as recommended in ASCE/SEI 7-10. Check for satisfying the allowable story drifts for four story BRBFs are shown in table 7 and for eight story in table 8, (the deflection amplification factor, C_d, for BRBs is equal to 5 according to ASCE/SEI 7-10.

Table 7. Control of BRBFs story drifts in four-story retrofitted building

Story	***Story height (mm)*** h_s	***Elastic story displacement*** $\delta_{xe}(mm)$	***Story drift (mm)*** Δ_e	***design Story Drift (mm)*** $\Delta = C_d \times \Delta_e$	***Allowable Story Drift (mm)***
4	3200	13.77	2.35	11.75	64
3	3200	11.42	3.52	17.6	64
2	3200	7.9	3.89	19.45	64
1	3200	4.01	4.01	20.05	64

Table 8. Control of story drifts in eight-story BRBFs building

Story	Story Height (mm) h_s	Elastic Story Displacement (mm) δ_{xe}	Story Drift (mm) Δ_e	Design Story Drift (mm) $\Delta = C_d \times \Delta_e$	Allowable Story Drift (mm)
8	3200	53.80	3.54	17.7	64
7	3200	50.26	5.08	25.4	64
6	3200	45.18	6.53	32.65	64
5	3200	38.65	7.44	37.2	64
4	3200	31.21	7.58	37.9	64
3	3200	23.63	7.81	39.05	64
2	3200	15.82	7.94	39.7	64
1	3200	7.88	7.88	39.4	64

7. Findings and results:

After calculation of story drifts for four and eight story BRB, it is observed that both systems have story drifts less than allowable story drift. Elastic story displacement in eight story BRB is larger than four story and obviously design story drift of eight story BRB is larger too. Comparison of design story drift in four and eight story BRBR buildings are shown in Figure 6 and it's observed that stiffness of four story BRB is more therefore, in low to relatively moderate earthquake four story BRB may undergo less damage specially in secondary (non-structural) elements, like in-fills or in general, elements like mechanical and electrical instruments which are sensitive to story drift.

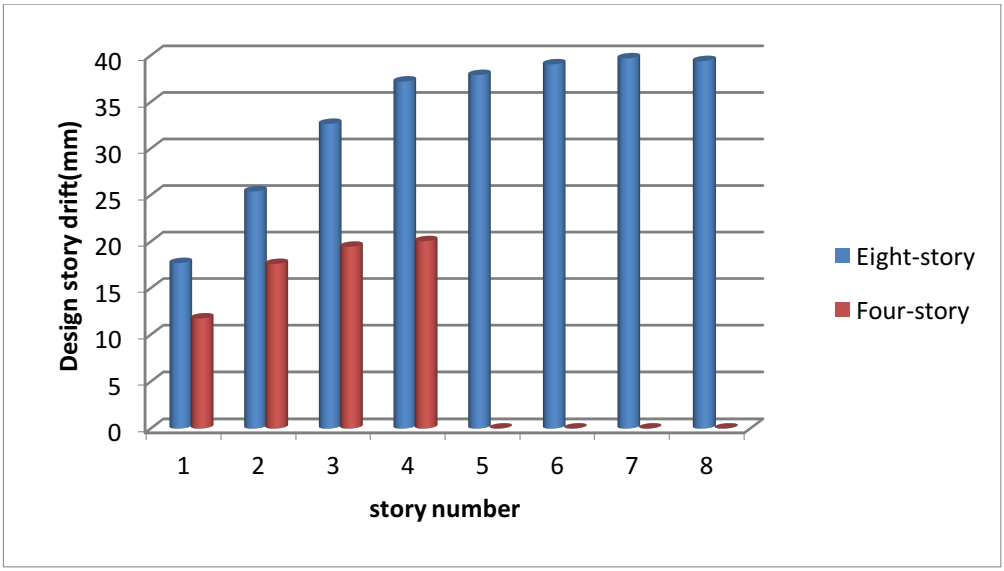

Figure 6. Comparison of four and eight story design story drift

8. Nonlinear static analysis of BRBF

8.1 Determination of target displacement of four and eight story BRBF

Target displacements are calculated manually and compare with results of software that extract from SAP2000; details of calculation are shown in tables 9 to 12.

Table 9. Target displacement parameters of four story BRBF in X-direction4

W (kN)	C_0	C_1	C_2	C_m	R
15548.3	1.25	1.0761	1.0107	0.9	2.8723
a	V_y (kN)	S_a	T_e (Sec)	$\delta_t(mm)$	$1.5\delta_t(mm)$
60	4694.28	0.9625	0.64	133.3308	199.9962

Table 10. Target displacement parameters of four story BRBF in Y-direction4

W (kN)	C_0	C_1	C_2	C_m	R
15548.3	1.25	1.0772	1.0109	0.9	2.8966
a	V_y (kN)	S_a	T_e (Sec)	$\delta_t(mm)$	$1.5\delta_t(mm)$
60	4656.14	0.9625	0.64	133.4898	200.2347

Table 11. Target displacement parameters of eight story BRBF in X-direction

W (kN)	C_0	C_1	C_2	C_m	R
31625.51	1.3	1.031438	1.0048	0.96	3.0480
a	V_y (kN)	S_a	T_e (Sec)	δ_t (mm)	$1.5\delta_t$ (mm)
60	6900.87	0.73828	1.042	268.6488	402.9731

Table 12. Target displacement parameters of eight story BRBF in Y-direction

W (kN)	C_0	C_1	C_2	C_m	R
31625.51	1.3	1.032549	1.005176	0.96	3.1190
a	V_y (kN)	S_a	T_e (Sec)	δ_t (mm)	$1.5\delta_t$ (mm)
60	6739.87	0.73828	1.042	269.0237	403.5356

8.2 Capacity curve of four and eight story BRBFs under pushover analysis

Capacity curves of the BRBF buildings under vertical distribution that are proportional to the building first mode of vibration are computed and they are shown in figures 7 and 8.

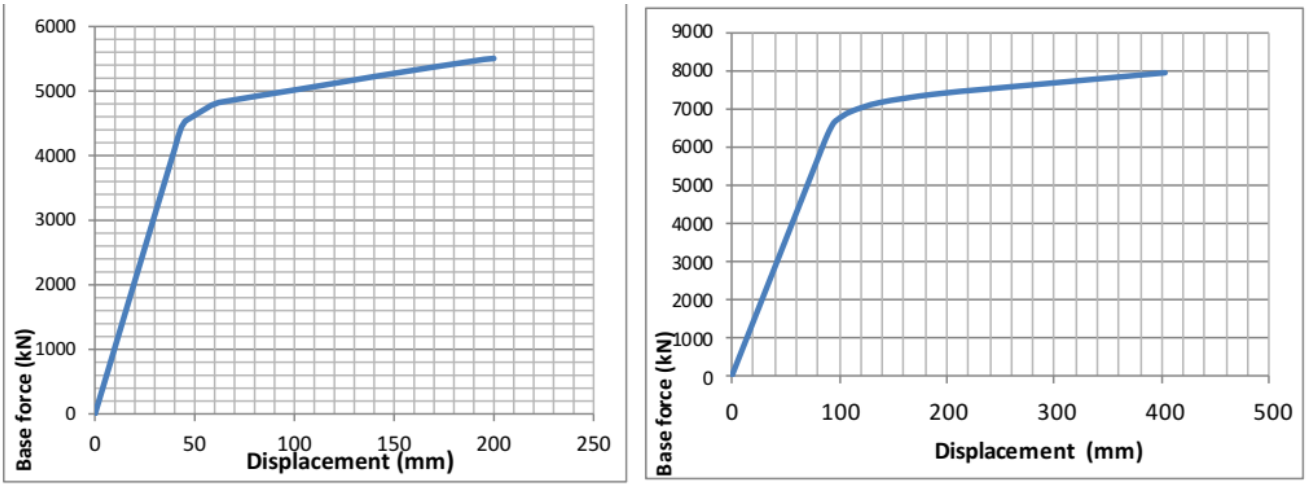

Figure 7. Capacity curve of four (left) and eight story (right) BRBFs building in X-direction (kN-mm)

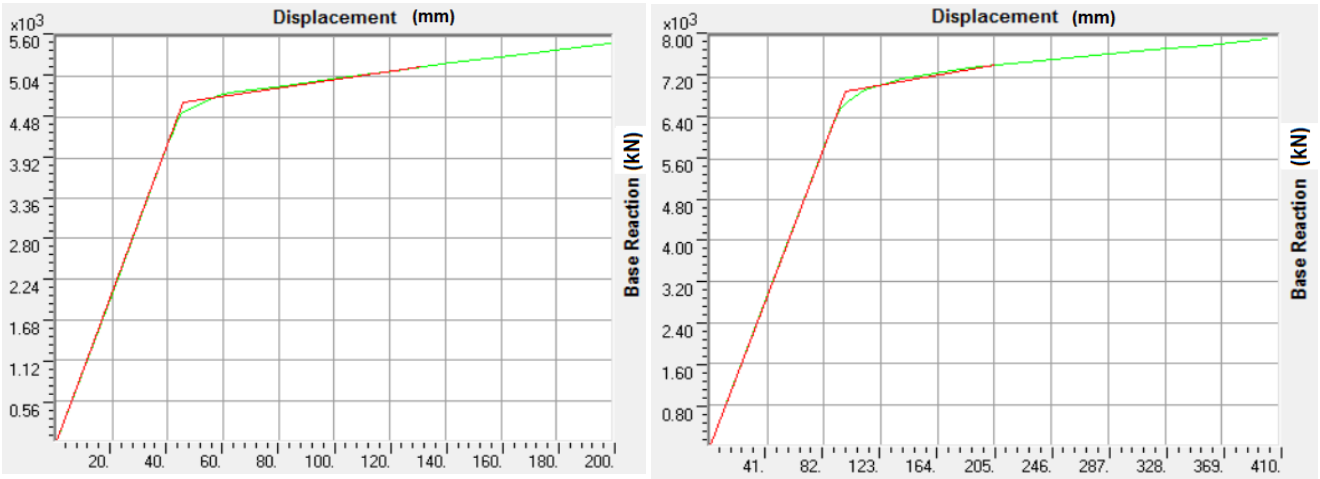

Figure 8. Adjustment of pushover with standard curve in X-direction for BRBFs four-story (left) and eight-story (right) buildings (kN-mm)

8.3 Hinge formation sequence in four story BRBFs

After performing nonlinear static analysis for four-story retrofitted building with BRBs, sequence of hinges that are formed in the structure can be observed in tables 13 and figure 9. As it is shown from following figures, plastic hinges are formed in braces only and there is not any hinges in columns of this system and it is because of very good manner of dissipation of seismic energy in BRBFs.

In X-direction (table 13), the first hinge is formed from (B to IO) limit at step 3 with displacement equals to 41.60 mm. At step 6, we have three hinges from (B to IO) limit and four hinges from (IO to LS) limit, increasing in number of hinges that are formed from (IO to LS) limit continue from step 6 with four hinges to step 12 with eight hinges. Around target displacement (133.33 mm) in step 11, eight hinges are formed from (IO to LS) limit and it shows that the performance of structure is acceptable according to our desire performance level (LRO) of ASCE 41-06. At 1.5 times of target displacement (199.99 mm) at step 12, we have two hinges from (B to IO)

limit plus six hinges from (IO to LS) limit and it shows even in 1.5 times of target displacement performance of structure is good and dangerous plastic hinges are not formed yet.

Table 13. Hinges formation sequence of BRBFs retrofitted building in X-direction4

Step	Displacement	Base Force	AtoB	BtoIO	IOtoLS	LStoCP	CPtoC	CtoD	DtoE	BeyondE	Total
	mm	kN									
0	0	0	233	0	0	0	0	0	0	0	233
1	19.945087	2054.536	233	0	0	0	0	0	0	0	233
2	39.944087	4109.079	233	0	0	0	0	0	0	0	233
3	41.608413	4280.059	232	1	0	0	0	0	0	0	233
4	43.400615	4443.3	230	3	0	0	0	0	0	0	233
5	45.145349	4534.042	229	4	0	0	0	0	0	0	233
6	58.442411	4778.863	226	3	4	0	0	0	0	0	233
7	62.087373	4823.134	225	4	4	0	0	0	0	0	233
8	82.086373	4925.301	225	0	8	0	0	0	0	0	233
9	102.085373	5027.478	225	0	8	0	0	0	0	0	233
10	122.084373	5129.666	225	0	8	0	0	0	0	0	233
11	142.083373	5231.909	225	0	8	0	0	0	0	0	233
12	168.002752	5362.447	223	2	8	0	0	0	0	0	233
13	195.023777	5489.167	221	3	5	4	0	0	0	0	233
14	199.936087	5503.876	221	2	6	4	0	0	0	0	233

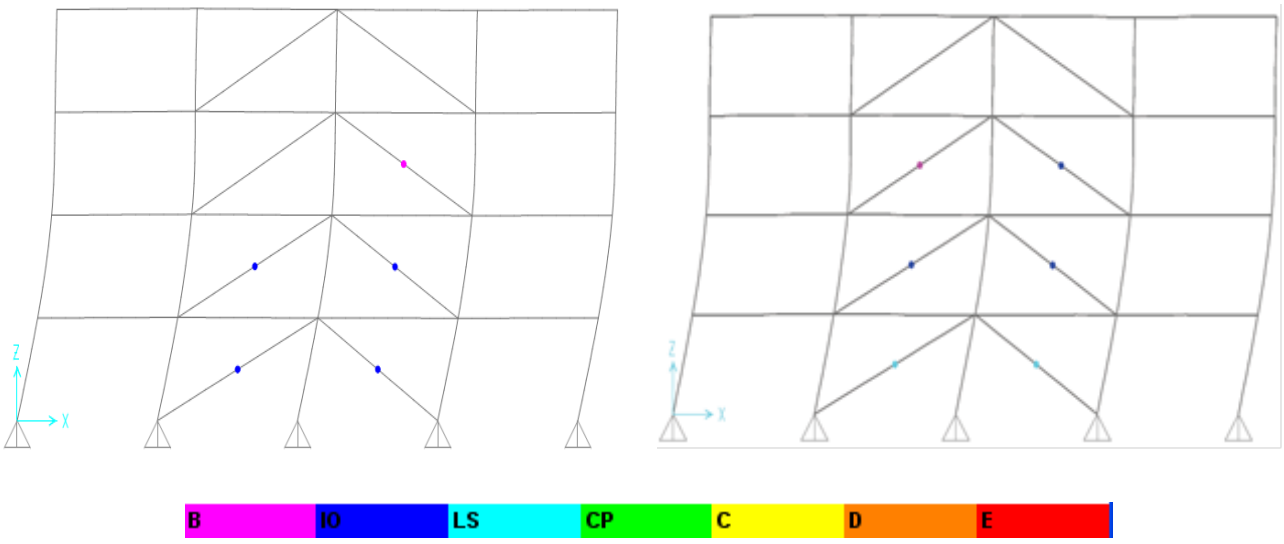

Figure 9. *Hinges formation of four story BRBFs building in X-direction at step 12 with displacement equals to 168 mm (left) and step 13 with displacement equals to 195.02 mm (right)*

8.4 Hinge formation sequence in eight story BRBFs

After performing nonlinear static analysis of eight-story retrofitted building with BRBFs, sequence of hinges that are formed in the structure can be observed in tables 14 plus figure 10.

In X-direction (see table 14), the first plastic hinge from (B to IO) limit is formed in step 3 at displacement equals to 86.88 mm. Around target displacement (268.64 mm) at step 10, we have twenty hinges from (IO to LS) limit and it shows that performance of retrofitted building is acceptable and in light to moderate earthquakes

performance of structure is good according to ASCE 41-06. At 1.5 times of target displacement (402.94 mm) at step 13, We have one hinges from (B to IO) limit and eighteen hinges from (IO to LS) limit plus two hinges from (LS to CP) limit and it shows that performance of retrofitted building even in 1.5 times of target displacement is also acceptable and it is almost reliable even in sever earthquakes.

Table 14. Hinges formation sequence of eight story BRBFs retrofitted building in X-direction8story

Step	Displacement	Base Force	AtoB	BtoIO	IOtoLS	LStoCP	CPtoC	CtoD	DtoE	BeyondE	Total
	mm	kN									
0	0	0	464	0	0	0	0	0	0	0	464
1	40.248561	2864.759	464	0	0	0	0	0	0	0	464
2	80.545561	5729.516	464	0	0	0	0	0	0	0	464
3	86.886364	6180.291	463	1	0	0	0	0	0	0	464
4	93.513037	6569.012	458	6	0	0	0	0	0	0	464
5	98.274293	6711.741	455	7	2	0	0	0	0	0	464
6	111.459276	6929.503	451	5	8	0	0	0	0	0	464
7	137.898712	7158.634	448	3	13	0	0	0	0	0	464
8	186.314889	7370.419	445	3	16	0	0	0	0	0	464
9	237.212127	7511.729	444	0	20	0	0	0	0	0	464
10	277.509127	7615.391	444	0	20	0	0	0	0	0	464
11	317.806127	7719.064	444	0	20	0	0	0	0	0	464
12	358.103127	7822.782	444	0	20	0	0	0	0	0	464
13	402.921561	7937.283	443	1	18	2	0	0	0	0	464

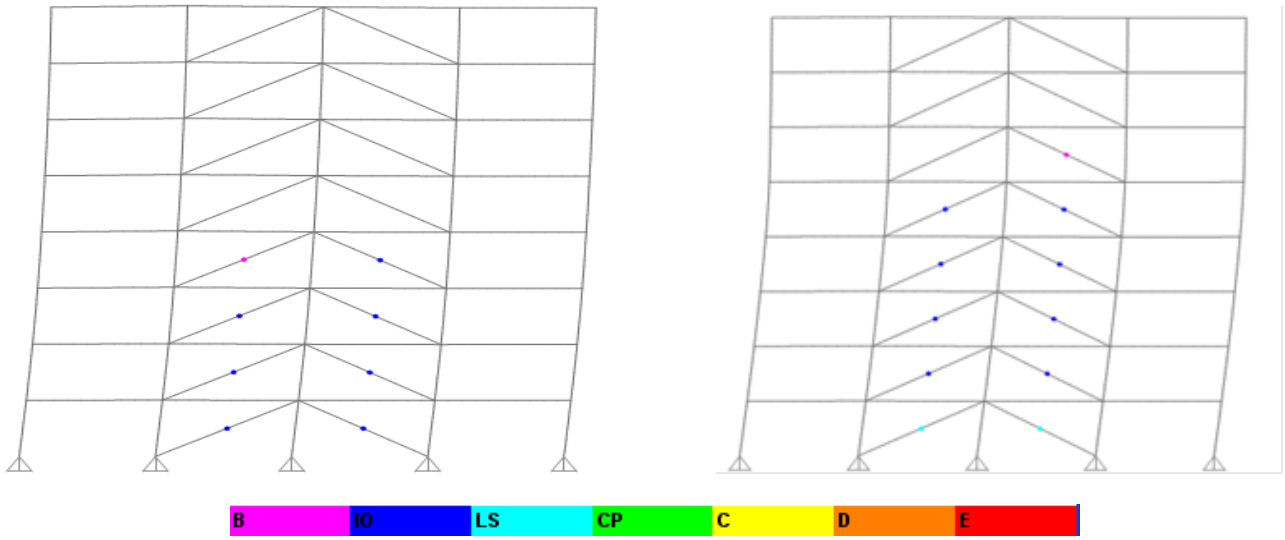

Figure 10. *Hinges formation of BRBFs building in X-direction at step 7 with displacement equals to 137.89 mm (left) and step 13 with displacement equals to 402.92 mm (right)*

9. Discussion

It is observed that in X-direction the first plastic hinge in eight-story BRBF system occurs at displacement equals to 86.60 mm where in four-story BRBF systems at almost same displacement we have eight hinges from (IO to LS) limit and the first plastic hinges occurs at displacement equals to 41.60 mm.

Target displacement in eight story building is equal to 268.64 mm with base force of 7615.40 (kN) that 20 hinges from (IO to LS) are formed but in four story structure with same displacement, it's passed the CP limit and structure is probable to collapse, target displacement in four story structure is equal to 133.33 mm with base force of 5150 (kN), so it shows that energy dissipation in eight story structure is more and displacement and base force that eight story structure is able to tolerate is almost 2 times of four story BRB. At 1.5 time of target displacement also response for eight story structure is better.

Figure 11 shows the stiffness of eight story BRBF is lesser than four-story. We can see this fact by compare the effective stiffness, K_e, of both systems in pushover curves too (figure 7 and 8). As it is seen the K_e for four-story BRBF systems is equals to 103 (kN/mm) and K_e for eight-story BRBF systems is equals to 71.21 (kN/mm) so for BRBF with increasing height, effective stiffness will decrease so we can see that ductility is increased too.

According to figure 11, the initial stiffness of four-story building retrofitted with BRBF is also more than eight-story and as the result four-story buildings may suffer less damage in low to moderate earthquakes if story drifts be a measurement of damage to the building.

So consequently structure's response for eight story structure is better than four story and it's recommended to use of BRBF for high raise building to get best of it. BRBF shows its best seismic performance in high raise building, (after target displacement) and confronting with moderate to severe earthquake (in moderate to high seismicity regions). It's mainly because of, with increasing height it gets more ductile and it will increase energy dissipation. Also from economical aspect, use of BRB is rather expensive in comparison with other braces so it's better to use of other braces system like SCBF for retrofitting of low raise building in low to moderate seismicity regions and use of BRB for retrofitting high raise building in high seismicity regions (Farizani et al., 2015).

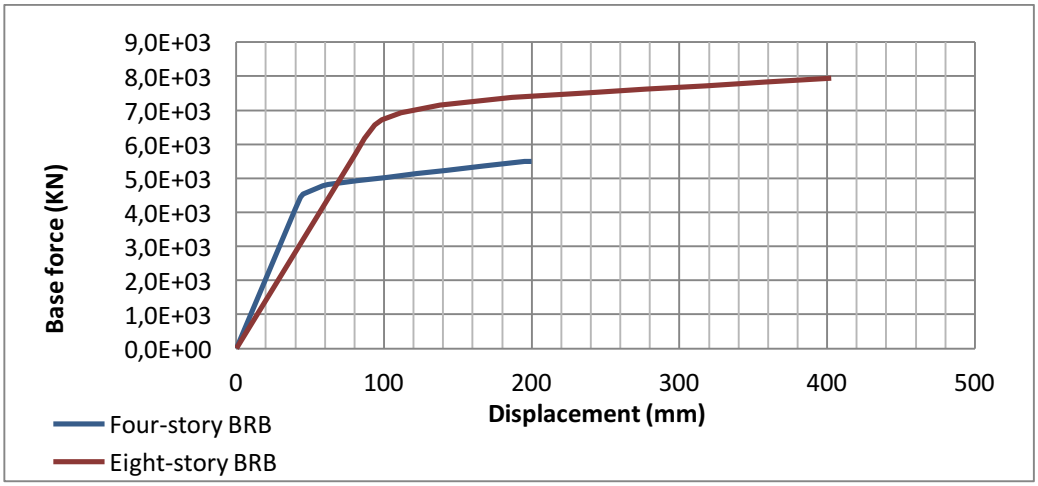

Figure 11. Compare of capacity curves for eight-story and four-story BRBF

10. Conclusions

I. Initial stiffness of four story building is more than eight story and as the result buildings with four story BRB may suffer less damage in low to moderate earthquakes if story drifts be a measurement of damage to the building.
II. Effective stiffness in four story building is larger than eight story and four story BRB may undergo less lateral displacements than eight story BRBF so Damage to nonstructural element is eight story is more.
III. Drift in eight story retrofitted building is more that four-story retrofitted buildings.
IV. The ductility and energy dissipation of eight story BRB is more than four story buildings.
V. With increasing height, effective stiffness will decrease so we can see that ductility is increased too.
VI. It's recommended to use of BRB for retrofitting of high raise buildings in relatively moderate to high seismicity regions.

References:

American institute of steel construction (AISC), 2010, "Seismic provisions for structural steel buildings", Chicago, USA.

American society of civil engineers (ASCE 41-06), 2007, "Seismic rehabilitation of existing buildings", Boston, USA.

American society of civil engineers (ASCE/SEI 7-10), 2010, "Minimum design loads for buildings and other structure", Boston, USA.

Aniello, M., and Della Corte, G., and Mazzolani, F., 2008, "Buckling- Restrained braces an experimental study ", Steel tips, Italy.

Bozorgnia, Y., and Bertero, V., 2004, "Earthquake Engineering from Engineering Seismology to Performance-Based Engineering", CRC press, chapter 16.

Bruneau, M., 2005, "Seismic retrofit of steel structure", Multidisciplinary Center for Earthquake Engineering Research, Buffalo, NY, USA,

Central public works department, Indian institute of technology-MADRAS., 2007, "Handbook on Seismic Retrofit of Building", chapter 1.

Deulkar, W., and patil, H., 2010, "Buckling restrained braces for vibration control of building", India.

Di Sarno, L., and Elnashai, A. S., 2004, "Bracing system for seismic retrofit of steel frames", 13th World conference on Earthquake Engineering, B.C., Canada.

Farizani, S., and Kazemi, MT., 2015, "Retrofitting of existing steel frames using ductile bracing systems", conference of science and engineering, Dubai.

Fuqua, B. W., 2009, "Buckling Restrained Braced frames as a seismic force resisting system", Kansas state university, Kansas.

Garcia, J., and Teran-Gilmore, A., 2010, "Seismic Performance of Existing Steel Buildings Retrofitted with Buckling-Restrained Braces", ECEE, Mexico.

Hussain, S., Benschoten, P., Satari, M., and Lin, S. (2005). Buckling Restrained Braced Frame (BRBF) Structures: Analysis, Design and Approvals Issues, Nippon Steel News, 333.

Merrell, M. Y., 2007, "Design of ductile braced frames", Brigham Young university.

Parry Brown, A., and Aiken, I., and Jeff Jafarzadeh, F., 2001, "Buckling Restrained Braces Provide the Key to the Seismic Retrofit of the Wallace F. Bennett Federal Building", USA.

Permanent Committee for Revising the Iranian Code of Practice for Seismic Resistant Design of Buildings (Standard 2800), 1988, "Iranian code of practice for Seismic resistant design of buildings", 1st edition.

Permanent Committee for Revising the Iranian Code of Practice for Seismic Resistant Design of Buildings (Standard 2800), 2007, "Iranian code of practice for Seismic resistant design of buildings", BHRC Publication No. S – 465, 3rd edition.

Prinz, S., 2007, "Effect of beam splicing on seismic response of buckling restrained braced frames", Birgham Young Univresity.

Sabelli, R., and Lopez, W., 2004,"Design of Buckling-Restrained Braced Frames", San Francisco, CA.

Sabelli, S., and mahin, S., and Chunho Chang., 2003, "Seismic Demands on Steel Braced Frame Buildings with Buckling-Restrained Braces".

Uang, C.M., Bruneau, M., Whittaker, A. S., and K.C. Tsai, 2001, "Seismic Design of Steel Structures", Chapter 9.

ASIAN INSTITUTE OF RESEARCH
Connecting Scholars Worldwide

The Asian Institute of Research
Engineering and Technology Quarterly Reviews
Vol.2, No.1, 2019: 16-23
ISSN 2622-9374

Analysis of Relationship Between Ground Water Resources and Spatial Planning in Bali, Indonesia

Ngakan Made Anom Wiryasa[1], Ngakan Ketut Acwin Dwijendra[2]

[1] Department of Civil Engineering, Udayana University, Bali, Indonesia
[2] Department of Architecture Engineering, Udayana University, Bali, Indonesia.

Corresponding Email: acwin@unud.ac.id

Abstract
Earth is the only planet in the solar system that has life. Almost 71% of the earth's surface is covered by water and all life on Earth is highly dependent on the presence of water. Conflicts of interest between life and water resources in space occur because of various interests. The purposes of this study is to investigate the potential and utilization of the Bali Ground Water Basin (CAT); and to analyze the strategy and policy directions in spatial planning of Ground Water Basin (CAT) in Bali Province, Indonesia. This research is conducted in Bali Province area, using data collecting technique is observation, literature study, and while data processing technique analyzed by analytic induction and comparative description. The findings of the study are ground water potential in Ground Water Basin (CAT) in Bali Province area is 1,577 Million M3/year (unconfined), 21 Million M3/year (confined) and ground water utilization of 8.4% or 134` M3/year. The strategy and policy direction can be formulated is to synchronize and harmonize between the organization of spatial planning, drilling permits and ground water monitoring.

Key Words: CAT (Ground Water Basin), Spatial Planning, Water Resources, Strategy and Policy Directions

1. Introduction

Water is a very important element for life, Earth is the only planet in the Solar System that has life (Parker, 2007). All life on Earth is highly dependent on water and according to Matthews (2005) nearly 71% of Earth's surface is covered by water in form of liquid, solid (ice), and water vapor/gas. Hydrological cycle is the journey of water from the sea, air, and land, this hydrological cycle is called water spatial plan. On land, water is the source of life.

Population growth will affect the increasing needs of primary and secondary human needs both in the economic, social, and environmental dimensions. This will result in uncontrolled changes in land use, increased utilization or use of water, which will affect the decrease in environmental carrying capacity. Population and industrial growth will affect the land use, which in turn change the land space. Changes that occur in land spatial planning will also affect the hydrological process (water spatial planning)

The final hydrological process is the flow of water back into the sea, it also seeps into the soil and is accommodated in the Basin of Ground water. Bali Province has eight Ground Water Basins, both local and cross-district. The most extensive ground water basin is the Denpasar-Tabanan Ground Water Basin covering

nearly seven districts/cities. The research was conducted at the Denpasar-Tabanan Ground Water Basin covering the central part of Bali Province. The objectives to be achieved in this research are: (i) to analyze the potential and utilization of ground water in the central part of Bali Province; (ii) harmonization of water and land spatial planning in the central part of Bali Province.

2. Literature Review

Hydrological Cycle

The journey of water naturally always flows from the higher to the lower places and also flows both on the ground and below the soil surface. In accordance with the location and environmental conditions, water can change its shape. At 0˚C the water changes into ice; at a temperature of 100˚C, the water turns into gas (water vapor) and at a certain temperature, it will return to water. The water movement follows a hydrological cycle (Figure 1).

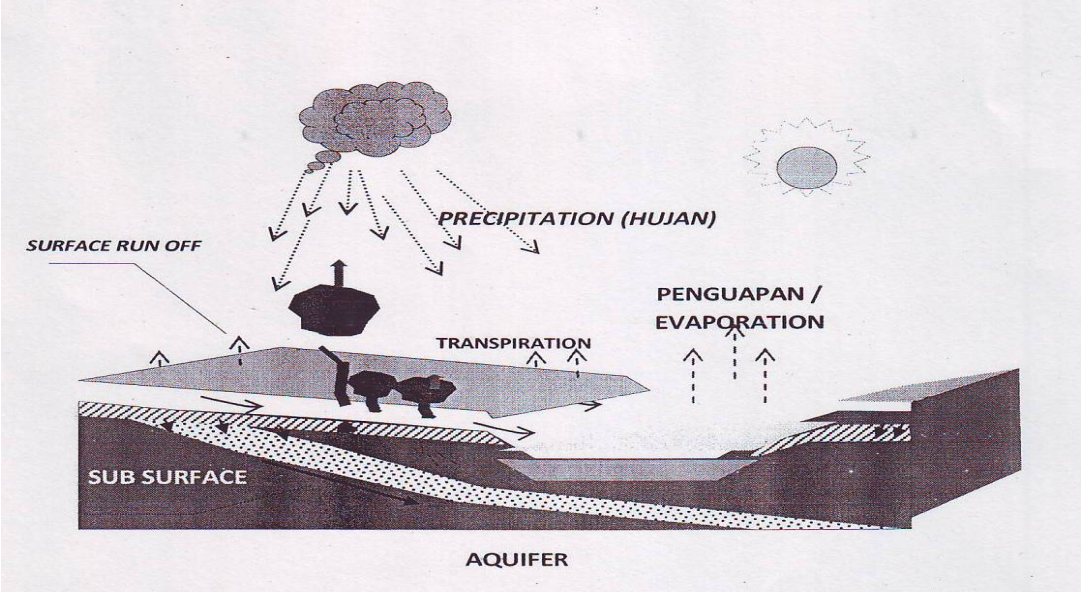

Figure 1. Hydrological Cycle
Source: Zoning Map of Ground Water Use, Bali Province (Public Works Office, 2014).

The Hydrological Cycle can be explained as follows: (1) Evaporation: occurs in areas that contain lots of water such as seas, lakes, rivers, reservoirs, lakes and others. Evaporation occurs because of the effects of sunlight; (2) Evapotranspiration: consists of two types of water flow i.e. evaporation and transpiration. Transpiration is the absorption of water by plant roots that are utilized for the plant's living needs. Because of the influence of sunlight there is evaporation. These two streams of water, which are absorption by plant roots and evaporation refer to evapotranspiration; (3) Rain Water: the water vapor caused by evaporation and evapotraspiration in the air will move. The process of condensing water vapor (cloud) into rainwater is called precipitation. The water vapor moves in the air and due to the difference in air temperature, the water vapor changes to a temperature below the freezing point then the moisture will turn into ice grains. Grains of water and ice grains due to the influence of gravity will fall down as rain. Rainwater is the main source of water either flowing in the soil surface or absorbing to the ground; (4) Rainwater Flow: (a) Run-off: is a flow above the ground level, flows from high to lower and empties into the ocean; (b) River flows: surface water will flow into catchment areas or often called watersheds, which then flow into the river system and last empties into the ocean; (c) Interflow: the water in the vadose zone (Fig. 2.2) then flows into the network system of rivers, reservoirs, lakes, and others; (d) Base Flow: ground water flow that fills the network system of rivers, reservoirs, lakes, etc.; (e) Run-out flow: ground water that flows directly into the ocean; (f) Infiltration: surface water not only flows on the surface but some are absorbed into the soil. Water that seeps into the soil refers to infiltration; (g) Capillaries: water that

seeps into the soil and returns to soil moisture; and (h) Percolation: water derived from soil moisture in the vadose zone area that replenishes ground water flow.

Sub-Surface Water Formation

Basically ground water conditions are divided into two (Driscoll, 1987: in Kodoatie and Sjarief, 2010) as shown in Figure 2. Such as: (1) Vadoze Zone (Soil Water, Intermediate Zone Water adn Capillary Water); (2) Phreatic Zone adn (3) The two above zones are described in Fig. 2. In ground water zones, much of the ground water is used for agricultural purposes. Water will disappear in the ground water zone due to transpiration, evaporation and percolation. Capillarity power will fill the spaces between particles to full, then water will flow due to the force of gravity. Zone under ground water zone is middle zone, in this zone water will move down and some have retained. Capillary pipe is located in the zone below the middle zone, where water flows upward due to capillary force. Ground water is the boundary between the ground water zone with the capillary pipe, the ground water level provides a reference or approximation of ground water level.

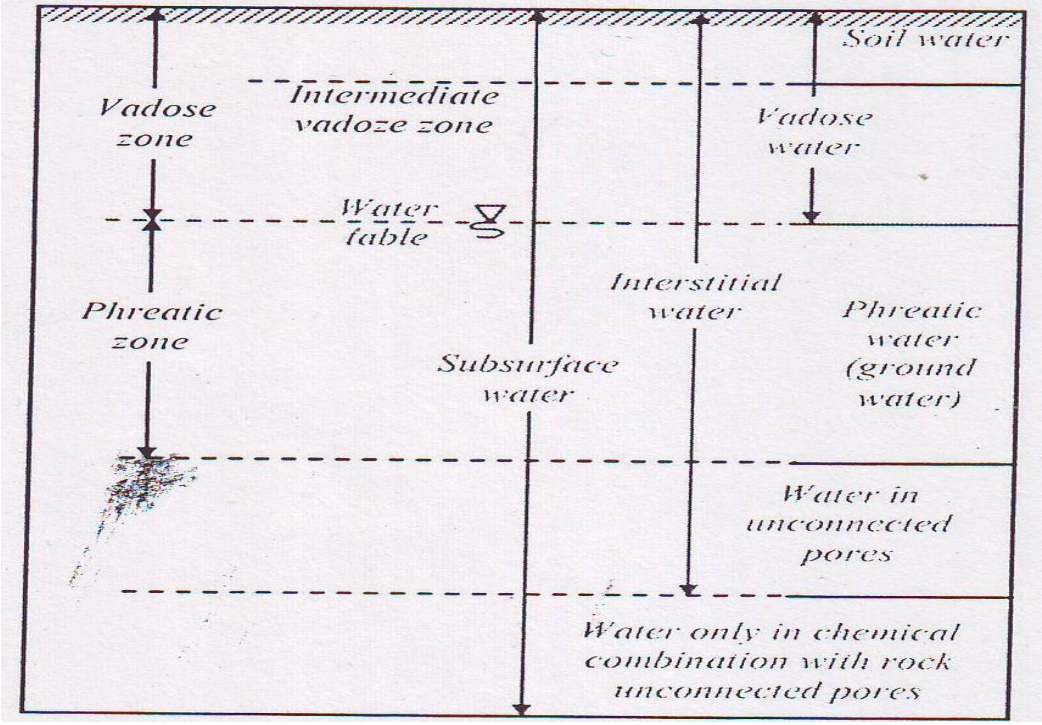

Figure 2. Sub surface water formation
Source: Kodoatie and Sjarief (2010).

Definition of Ground Water

Definition of ground water according to Government Regulation of the Republic of Indonesia Number 43 Year 2008 regarding Ground Water is water contained in a layer of soil or rocks located below the soil surface. Ground water or Phreatic Water which is the area that is restricted at the top is the water table and the lower limit is the initial boundary of water in unconnected pores. Soil Water is the starting area from the ground level to the beginning of the intermediate vadose zone.

3. Research Methods

Observations made to obtain data are empirical studies that are useful for measuring natural phenomena and/or real or grounded experiences. Empirical approach is done to gain knowledge through direct and indirect observation and also focus group discussion, which is then analyzed quantitatively and/or qualitatively. Quantitative analysis can also be transformed into qualitative by describing the existing data.

The study refers to the empirical approach because the research instrument tends to be designed more qualitatively to obtain data and information. This study tends to be "qualitative-verifying" in which the "triangulation-strategy" in obtaining data remains open. One of the qualitative-verifying qualities is the effort to reveal the facts behind the apparent data.

4. Results and Discussion

Potential and Water Utilization at Ground Water Basins of Denpasar-Tabanan

Based on the Government Regulation Number 43 Year 2008, it is stipulated that Ground Water Basins have hydrogeological boundaries that can be controlled by ground water hydraulic conditions. While the hydrological boundary is the physical boundary of the ground water management area that is limited by permeable and impermeable rocks, the limits of ground water separation, the slope of the rock layers, folds, and fractures. In addition, the water basin should also have an auxiliary area and a ground water release area in a ground water formation system. The ground water additive area is a ground water protected area which in principle ground water in the area is not to be utilized. While the release area is the ground water area to be utilized. The water basin must also have an aquifer system with a confined or unconfined impermeable layer underneath it.

The potential of ground water basin is highly dependent on the recharge area, which in the land spatial planning is designated as a strategic area that serves as a conservation. Based on Decree of the President of the Republic of Indonesia Number 26 Year 2011 concerning Stipulation of ground water basins in Bali Province, where in the decision, Bali Province consists of 8 ground water basins. The ground water basins are: (i) across district-ground water basins, which consist of: Denpasar-Tabanan; Singaraja; Negara; Gilimanuk, Tejakula and (ii) the local ones (within one district) consisting of: Amlapura; Nusa Penida; and Nusa Dua.

Ground water Basin in Bali Province covers an area of 4,382.33 km² or 77.75% of Bali Province area. The potential for unconfined ground water is 1,577 million m³/year, while the potential for confined ground water is 21 million m³/year. From the above data, it can be seen that the Province of Bali has 77.75% of the ground water potential (according to Table 1), while the small amount or 22.25% (non-water basin area) does not have the ground water potential.

Ground water basin of Denpasar-Tabanan is located in the central part of Bali Province. It is the largest ground water basin covering 47.46% of all existing ground water basin covering seven districts/cities. Ground water basin of covers Tabanan, Bangli, Karangasem, Klungkung, Gianyar, Badung and Denpasar districts. In the north bordering Abiansemal and Nyelati, Ambengan in the south and Sanur in the southeast, while in the east bordering Paksebali and Gubug in the west. (See Figure 3).

The ground water basin of Denpasar-Tabanan has shallow ground water potential in unconfined aquifers of 894 million m³/year, while the potential for confined aquifer has a potential of 8 million m³/year (Table 1). The height of the topography of this basin is 0-2.000 m above sea level, with rainfall of 1,000-3,500 mm/year. This basin has a flow pattern as a trellis river flow, i.e. flow in the direction of the slope.

Table 1. Potential of ground water at ground water basins in Bali Province

Num.	Ground water basin	Size (Ha)	Precipitation (mm)	Unconfined (million m3/tahun)	Confined (million m3/year)
1	Denpasar-Tabanan	208.000	1000-3500	894	8
2	Gilimanuk	13.130	1000-1500	30	1
3	Negara	41.850	1500-2000	73	4
4	Singaraja	50.520	1000-2500	215	3
5	Tejakula	75.050	500-2000	188	3
6	Amlapura	19.982	1000-2000	60	2
7	Nusa Dua	9.911	1500-2000	38	
8	Nusa Penida	19.790	500-1000	79	
	Total	438.233		1.577	21
	% of Bali area	77,75			

Source: Ministry of Energy and Mineral Resources, 2005

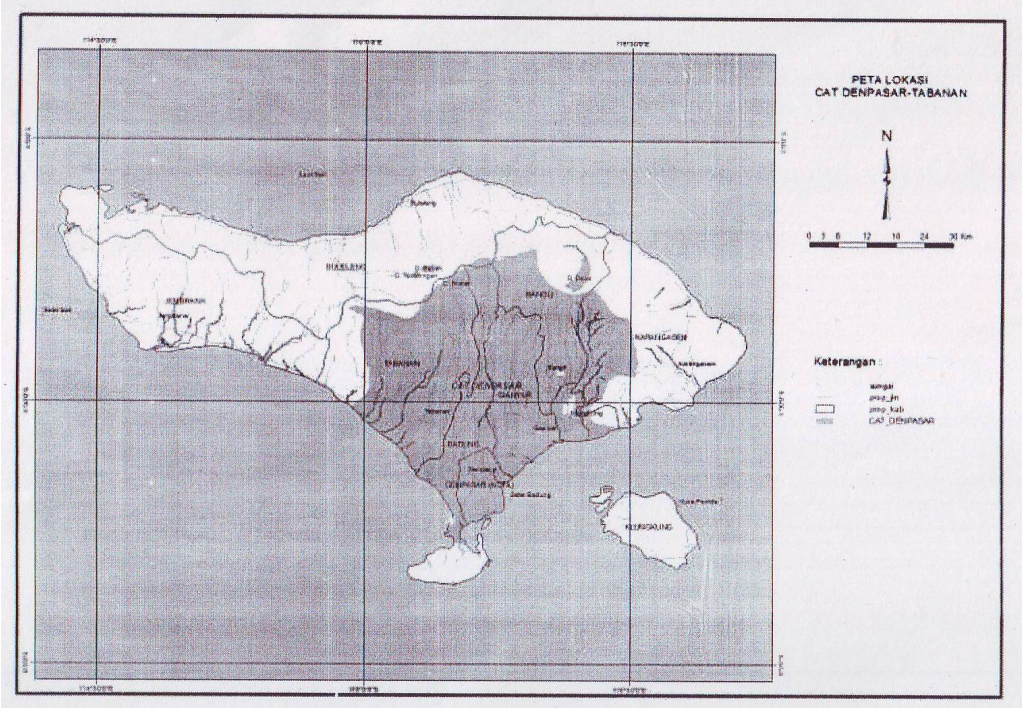

Figure 3. Ground water basins of Denpasar-Tabanan
Source: Map of Ground Water Utilization Zone (2014)

The main lithology of this check is coastal and lake sediments that function as an aquifer with a depth of 60-210 m (local subsurface). The sediment is gravel, sand and gravel with medium soluble, while the rock is volcanic rock group of Lesong-Pohen-Sanghyang, rocks of Mount Batukau, Mount Agung, and volcano group of Buyan-Beratan and Batur.

Emerging springs on Ground water Basin of Denpasar and Tabanan amounted to 425 units with the largest flow of 500 L/sec. and the discharge of 14512.50 L/sec. (See Figure 4 and Table 2). From the analysis, the utilization of ground water taken from 188 drills and 441 deep wells for both household and industrial needs. Total ground water usage is 134 million m³/year (8.40% of ground water basin of Bali Province) or 15% of ground water basin of Denpasar-Tabanan.

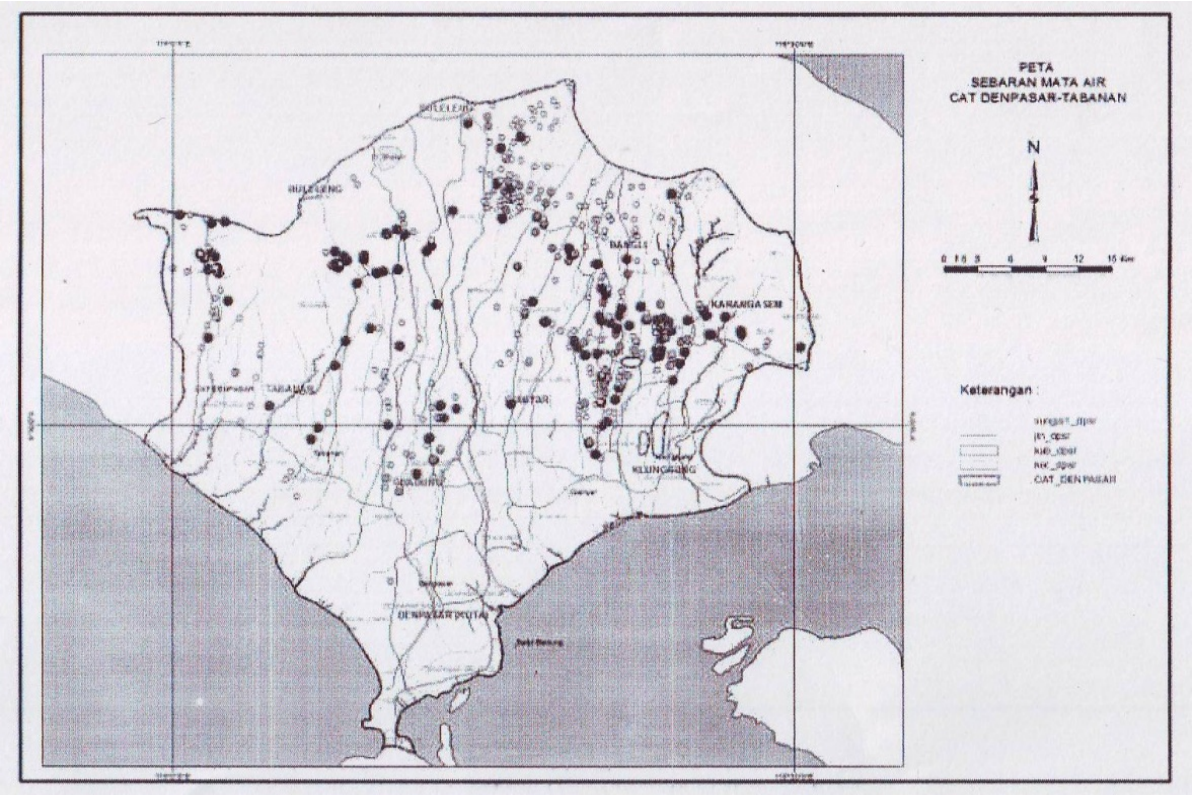

Figure 4. Ground water usage of ground water basins of Denpasar-Tabanan
Source: Map of Ground Water Utilization Zone (2014)

Table 2. Average Potency of Spring on Ground water Basin of Denpasar-Tabanan

Num.	Debit (L/sec)	Average Debit (L/sec)	Number of spring	Total (L/sec)
1	5,0	5,00	253	1.265,00
2	5,0-10,0	7,50	59	442,50
3	10,0-25,0	17,50	56	980,00
4	25,0-50,0	37,50	26	975,00
5	50,0-100,0	75,00	19	1.425,00
6	100,0-250,0	175,00	6	7.050,00
7	250,0-500,0	375,00	5	1.875,00
8	500,0	500,00	1	500,00
		Total	425	14.512,50

Source: Analysis (2015)

Harmonization of Spatial Planning

Each law uses different terminologies with different meanings too. To find the relevance of the differences in those terminologies, it will be compared between Law Number 7 of 2004 on Water Resources (PSDA) and Law Number 26 of 2007 on Spatial Planning, as per Table 3.

Table 3. Relevance of Law Number 7 of 2004 with Law Number 26 of 2007

No.	Law Number 7 of 2004	Law Number 26 of 2007
1	Conservation of water resources	Protected areas
2	Water resources management pattern of the river basin	Regional Spatial Plan (National, Province, and District/City)
3	Technical boundaries are Watersheds, Ground water Basins, River Basins	Administrative boundaries (National, Province, and District/City)

From Table 3 it can be concluded that Law Number 7 of 2004 emphasizes the river area which is the responsibility of the local river area (vertical institution), while Law Number 26 of 2007 emphasizes the administrative area which is the responsibility of the regional head. In the Spatial Planning as stipulated in Bali Provincial Regulation Number 16 of 2009 covers protected areas and cultivation areas. Protected areas include areas that protect their subordinate areas (protected forest areas and water catchment areas). The catchment area covers all forest areas and upstream watershed areas in Bali Province.

The determination of the Ground water Basin in Bali Province is based on Presidential Decree Number 26 of 2011 with the recent discharge compared to Regional Regulation No. 16 of 2009. Therefore, the regulation of the Regional Regulation has not regulated in detail about the Ground water Basin. For that we need further detailed arrangement of Ground water Basin.

5. Conclusions and Recommendation

Based on the research results, it can be concluded:

1. Ground water basin of Denpasar-Tabanan is located in the central part of Bali Province and it is an inter-district ground water basin. It is the largest ground water basin covering seven districts/cities : Tabanan, Bangli, Karangasem, Klungkung, Gianyar, Badung and City of Denpasar. In the north bordering Abiansemal and Nyelati, Ambengan in the south and Sanur in the southeast, while in the east bordering Paksebali and Gubug in the west.
2. The ground water basin of Denpasar-Tabanan has shallow ground water potential in unconfined aquifers of 894 million m^3/year, while the potential for confined aquifer has a potential of 8 million m^3/year (Table 1). The height of the topography of this basin is 0-2.000 m above sea level, with rainfall of 1,000-3,500 mm/year. This basin has a flow pattern as a trellis river flow, i.e. flow in the direction of the slope;
3. Dependence on the ground water usage mainly for both household and industrial or commercial needs. The total ground water usage is 134 million m^3/year (8.40% of ground water basin of Bali Province) or 15% of ground water basin of Denpasar-Tabanan. The ground water usage is taken from 188 drills and 441 deep wells.
4. It needs harmonization between Law Number 7 of 2011 on Water Resources and Law Number 26 of 2007 on Spatial Planning along with all its derivatives that concerns about Ground water Basins in Bali Province

Some recommendation and suggestion can be formulated as below:

1. Although the use of ground water in terms of percentage is still small in number (conclusion 3), ground water levels have decreased due to drilling density and different ground water productivity levels. It is therefore necessary to draw attention to areas prone to decreasing ground water levels and periodically control the decrease of ground water levels;
2. There should be restrictions on drilling permits, especially areas where drilling density is high enough, especially that may affect the decrease of ground water level.

Acknowledgments

Acknowledgments to those who have supported the writing of this paper arr the Faculty of Engineering Udayana University for the support of research grants and Local Planning Board and Public Works Department for providing official data and interviews.

References

Acemoglu, D. (2003). *Root Causes: A Historical Approach to Assessing the Role of Institutions in Economic Development*. Finance and Development, 40(2), 27-30.

Aldershot (UK)and Vermont (USA). Alston, L., & Joseph, P. F. (1996). *The Economics and Politcs of Institutional Change*. In L. J. Alston, T. Eggertsson, & D. C. North. (Eds.), Emperical Studies in Institutional Change. Cambridge University Press. Cambridge.

Bali Provincial Regulation No. 16 Year 2009 on Spatial Planning of Bali Province

Decree of the President of the Republic of Indonesia Number 26 Year 2011 on the

Government Regulation Number 43 Year 2008 on Ground Water
Ground water Basins in the Province of Bali
Hodgson, G. (1998). The Approach of Institutional Economics. *Journal of Economic Literature,* 36(1), 166-192. Ikhsan, M. (2000). Reforms and Economic Development. Journal of Democracy and Human Right, 1(2), 30-58. Kasper, W., & Manfred, E.S. (1998). Institutional Economics: Social Order and Public Policy. Edward Elgar. Law of the Republic of Indonesia Number 26 Year 2007 on Spatial Planning.
Institutional Economics (Vol. 2). Edward Elgar. Aldershot (UK) dan Vermont (USA). Yustika, A. E. (2008). *Institutional Economics, Definition, Theory and Strategy*. Bayumedia Publishing, Jl.Puncak Yamin No. 20, Malang.
Kodoatie dan Sjarief, 2010, *Tata Ruang Air*. Andi Yogyakarta Publishing
Law of the Republic of Indonesia No. 26 Year 2007 on Spatial Planning
Law of the Republic of Indonesia Number 7 Year 2008 on Water Resources
Matthews, Rupert, 2005. *Planet Bumi, Topik Paling Seru*. Translation by Darmaring Tyas Wulandari. Jakarta: Erlangga
Muslion, E. J. B. (2008). *Paradigm Changes in National Development Planning Documents*. Jakarta: BP Pusaka.
Ngakan Made Anom Wiryasa & Ngakan Ketut Acwin Dwijendra (2017). Institutional Structure Models in Implementation of Spatial Planning. *Journal of Sustainable Development; Vol. 10, No. 4; 2017 ISSN 1913-9063 E-ISSN 1913-9071.* Published by Canadian Center of Science and Education.
Parker, Steve, 2007. *Tata Surya – Just the Facts*. Translated by Soni Astranto, S. Si. Erlangga for Kids, Erlangga Publishing.
Prassad, B. C. (2003). Institutional Economics and Economic Development: The Theory of Property Right Economic Development, Good Governance and the Environment. *International Journal of Social Economics*, 30, 1341-1353. https://doi.org/10.1108/03068290310474120
Rustiadi, E., & Wafda, R. (2007). *Problems of Spatial Planning and Land and Agrarian Reform in Indonesia.* Paper presented at the Anniversary Faculty of Economics and Management IPB April 25, 2007.
Rustiadi, E., Sefulhakim, S., & Panuju, D. R. (2011). *Planning and Regional Development*. Jakarta: Crestpent Press dan Yayasan Pustaka Obor Indonesia.
Rustiadi, E., Sefulhakim, S., dan Panuju, DR. 2011. *Perencanaan dan Pengembangan Wilayah*, Crespent Press and Yayasan Pustaka Obor Indonesia, Jakarta
Sutami. (1977). *Regional science in relation to the Policy Analysis and Planning in Indonesia*. Direktorat Penyelidikan Masalah Bangunan, Direktorat Jenderal Cipta Karya, Departemen Pekerjaan Umum dan Tenaga Listrik, Bandung.
Widiastuti, Syamsul Alam Paturusi & Ngakan Ketut Acwin Dwijendra. (2017). Cultural Value Transformation in Traditional Market Spatial Planning in City of Denpasar, Gianyar and Klungkung – Bali, Indonesia. *Journal of Sustainable Development; Vol. 10, No. 4; 2017 ISSN 1913-9063 E-ISSN 1913-9071.* Published by Canadian Center of Science and Education.
Williamson, O. E. (1998). *The Institions of Governance. The American Journal Review,* 88(2), 75-79. Witte, E. E. (1998). Institutional Economics as Seen by an Institutional Economist. In W. J. Samuels (Ed.),
Wiryasa, Anom, 2014. *Analisis Kelembagaan dalam Pelaksanaan Penataan Ruang Wilayah Provinsi Bali* (Dissertation).

ASIAN INSTITUTE OF RESEARCH
Connecting Scholars Worldwide

The Asian Institute of Research
Engineering and Technology Quarterly Reviews
Vol.2, No.1, 2019: 24-37
ISSN 2622-9374

Design and Construction of a Domestic Solar Cooker

Augustine U. Iwuoha[1], Martins B. Ogunedo[2]

[1] Department of Mechanical Engineering, Imo State University, Owerri
[2] Department of Mechanical Engineering, Imo State University, Owerri

Corresponding Author: Martins B. Ogunedo. Email: briggsogunedo@gmail.com

Abstract
Over the years, increase in energy demand has stirred up research interest aimed at harnessing the abundant energy from the sun to meet human's energy needs. One of such needs is feeding, and this is achieved through cooking. Most of the conventional cooking methods affect the ecological system negatively. Hence, the study aimed to design and construct a solar cooker. The solar cooker is made up of four main parts viz: the pot, the parabolic reflective dish, the bracket and the dish stand with its base. The selection of materials for the construction of the solar cooker is governed by material properties, local availability, the service condition and cost. The quantity of heat needed for cooking a 2.5 kg of beans, for 120 minutes and the lowest solar insolation value of Owerri city recorded in December as 33.19 MJ/m2/day were used as the criteria for the dish sizing to ensure effective performance all year round. As a result, the area of the solar dish was constructed to be 3.6 m2 with a diameter of 2.15 m and a focal length of 1.0 m. Results of the performance evaluation carried out on the solar cooker showed that at a solar insolation value of 412.15 W/m2, the cooking time for 2.5kg each of beans, rice, yam, and boiling of 2.5kg of water were 120, 93, 67, and 13 minutes respectively. The efficiency of the unit is relatively stable within slight changes in solar insolation; a 6% change in the solar intensity would only affect the efficiency of the solar cooker by 0.7%.The study noted that solar insolation value plays a major role in the performance of the solar cooker because increase in the solar insolation value increases the heating rate, thereby reducing the cooking time. This suggests that in areas of the country with more hours of sun light and higher solar insolation, the use of concentrated solar panels for cooking is a viable option during day time.

Key Words: Solar insolation (Owerri), Solar cooker, 2.5 kg of Beans, Efficiency

Introduction

Solar technologies are designed to harness the renewable energy from the sun to meet human energy needs. These technologies could either be passive or active depending on the way they capture, convert and distribute sunlight. Passive solar technologies involve systems that do not require moving parts to harness solar energy, rather depend on the orientation, geometry, and external elements/factors to efficiently control the heat it receives from the sun. Examples of passive solar technology include orienting a building to the sun, and adjustment of the windows so as to balance the energy requirements of the building in both summer and winter seasons. Active solar techniques involve the movement of photons, electrons or fluid to convert the trapped solar energy to useful forms [1]. They include the use of photovoltaic systems, concentrated solar power and solar water heating to harness the energy. Photovoltaic systems harness solar energy for the production of electricity; concentrated solar power systems focus beams of reflected sun rays on an area to generate working fluid in steam turbines. Concentrated solar panels (CSP) could also be used for water heating and domestic cooking. When CSPs are used in this form, the system could be called a solar cooker. Solar cooker is a device that cooks using only sun energy in the form of solar heat, thus could save a significant amount of conventional fuel usage

currently. Solar cooking is one of the simplest, safest, clean, environment friendly, and most convenient way to cook without consuming conventional fuels or heating up the kitchen. A major concern of today is the rapidly depleting non-renewable natural sources of energy due to increasing energy needs. For instance, in the rural areas of Nigeria, the use of firewood to cater for the cooking needs of families has led to trees been felled indiscriminately. This action exposes those areas to deforestation and increased rate of erosion. A domesticated application of this CSP technology would alleviate these attendant consequences of deforestation. Hence, this study aims at the design and construction of a domestic solar cooker as an alternative to cookers that use non-renewable sources of energy.

Solar Cooker Description

The cooker consists of four main parts viz: the pot, the parabolic reflective dish, the bracket and the dish stand with its base. The cooking pot together with the pot holder and the parabolic dish are mounted on the bracket, which is supported by the dish stand and the base. The parabolic dish is fixed to the bracket with a tilting mechanism to enable manual tracking of the sun. A silver-coated glass mirror is used to obtain a reflective surface for the parabolic dish. In order to maintain the curvature of the parabola, the mirror was cut into pieces of 25.4 mm × 25.4 mm chips. These mirror chips were glued onto the surface of the parabolic dish. The choice of the pot is of primary importance, it is painted black; a black surface absorbs all radiation that falls on it but reflects none[2]. The heat radiation that was reflected by the mirror is absorbed by the black plate placed at the focal point of the parabolic dish where the cooking takes place.

Material Selection

The selection of materials for the construction of the solar cooker is governed by material properties, local availability, suitability for the service condition and cost. The following materials were used to construct the solar cooker: Mild Steel, Silver polished mirror, Aluminium. Table 1 gives a summary of the materials selected for the various components of the solar cooker.

Table 1: Material Selection

S/N	Component Parts	Material Used	Reasons
1	Parabolic dish, Bracket, Dish stand, and Base.	Mild steel	Ductile and malleable. High tensile strength. Ease in welding.
2	Reflector	Glass mirror	High optical reflectance/heat transmittance.
3	Pot (Absorber plate)	Aluminium	Ductile and malleable. High resistance to corrosion. Good conductor of heat and food hygiene friendly.

Component Description and Design

The Parabolic Dish

The parabolic dish collects solar radiation over a large area and concentrates it onto a smaller area usually the focal point, where the pot containing the food is located. To develop sufficient quantity of heat required to meet the design requirements , the solar insolation of the environment was considered. Solar insolation is the amount of electromagnetic energy (solar radiation) incident on the surface of the earth. The solar insolation is the amount of sunlight incident on a square meter of an environment per day. This knowledge was used to determine the size of solar collector required and the energy output.

Solar Dish Sizing

The solar cooker is required to cook beans meal of 2.5 kg by mass at a maximum cooking time of 120 minutes. The temperature at which beans would be cooked and deemed fit to be served is 102 ^{o}C [4]. Equation 1 gives the relation used to determine the quantity of heat needed to cook the beans.

$$Q = M_b C_b(\Theta_f - \Theta_i) + M_w C_w(\Theta_f - \Theta_i) + M_v L_v \quad (1)$$

where:

Mass of beans, (M_b)	2.5 kg
Mass of water,(M_w)	6.25 kg
Mass of water vapourized, (M_v)	3.5 kg
Latent heat of vapourization, L_v	2260 kJ/kg
Specific heat capacity of beans,(C_b)	3.68 kJ/kg ^{o}C
Specific heat capacity of water,(C_w)	4.186 kJ/kg ^{o}C
Initial temperature of the mixture,(Θ_i)	28^{o}C
Final temperature of the mixture,(Θ_f)	102^{o}C

Substituting the values, we get:

$$Q = (2.5\times3.68\times74) + (6.25\times4.186\times74) + (3.5\times2260) = 10526 \text{ kJ}$$

To achieve this quantity of heat, the solar dish area is determined using the lowest mean value of Owerri solar insolation recorded as 33.19 MJ/m^2/day [3]. This solar insolation value of 33.19 MJ/m^2/day implies that 406.59 J of solar energy falls on a square meter surface in Owerri per second or 1 m^2 of Owerri receives 406.59 W of solar power. The solar power needed to generate a heat of 10526 kJ in 120 minutes is therefore 1462.06 W. To determine the area, A_s required to trap 10526kJ of heat, Equation 2 is employed.

$$A_s = \frac{Required\ solar\ power\ (W)}{Solar\ insolation\ (W/m^2)} \quad (2)$$

$$A_s = \frac{1462.06}{406.59} = 3.6\ m^2$$

The diameter (D) corresponding to the cross sectional area of the solar cooker dish is determined using Equation 3.

$$D = \sqrt{\frac{4A_s}{\pi}} \quad (3)$$

$$D = \sqrt{\frac{4\times3.6}{\pi}} = 2.14\ m$$

The radiations incident on the dish are reflected (converged) to a focal point f and this is where the cooking pot would be located. The focal point (f) is determined with Equation 4.

$$f = \frac{D^2}{16h} \quad (4)$$

Where D = diameter of dish, and h = height of dish.

Based on the geometry of the dish, a dish height, h of 0.28 m is selected.

$$f = \frac{D^2}{16h} = \frac{2.14^2}{16\times0.28} = 1.0\ m$$

The orthographic drawing of the parabolic dish is shown in figure 1.

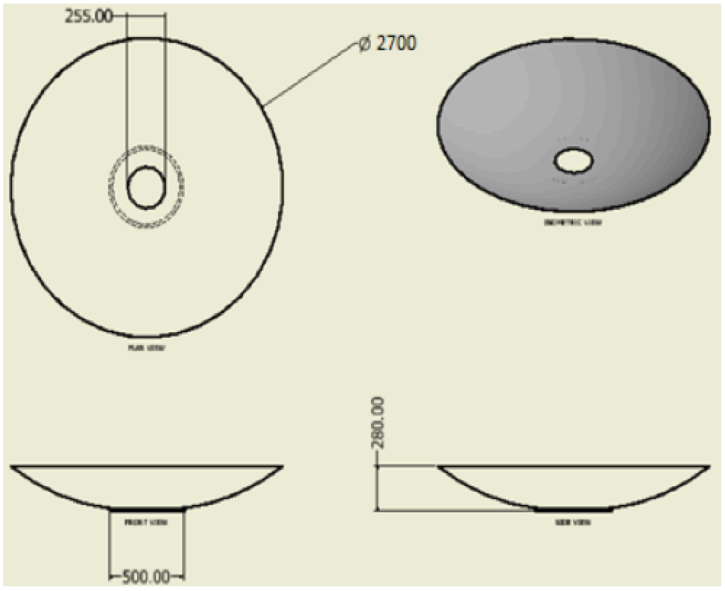

Figure 1: Orthographic projection of the parabolic dish.

According to [3], the monthly mean extra-terrestrial solar radiation on horizontal surface in Owerri varies from January to December. The lowest mean value is recorded in December; 33.19 MJ/m^2/day. This value was chosen in sizing the solar dish to ensure effective performance all year round.

Bracket

The bracket provides the means of hinging the dish on the stand so that it could be tilted freely towards the direction of the sun, to enhance manual sun tracking. Figure 2 shows the orthographic drawing of the bracket.

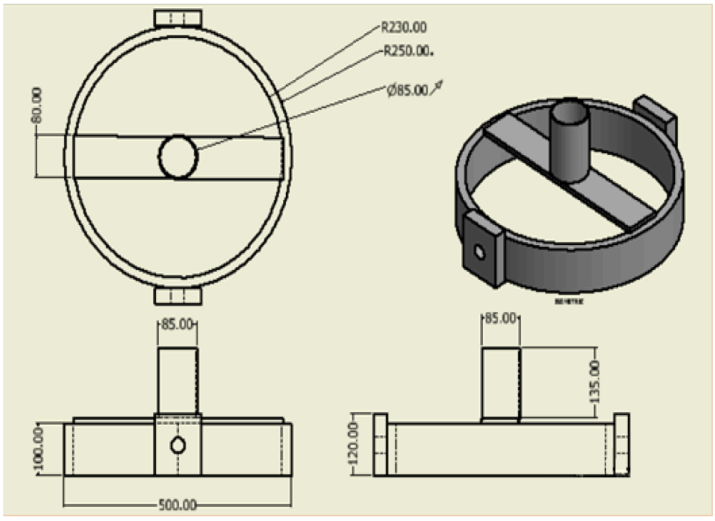

Figure 2: Orthographic projection of the bracket.

Dish stand

The dish stand provides support for the dish and connects it to the base. It is welded rigidly to the base, it is designed to have a total length of 625 mm with a diameter of 90 mm. The length of the stand is designed to withstand the given load without failure. The stand is treated as a column under load.
According to Euler, the critical buckling load is given by Equation 5:

$$W_{cr} = \frac{C\pi^2 EI}{{L_e}^2} \quad (5)$$

C = Constant, representing the end conditions of thr column or end fixity coefficient = 4 when both ends are fixed [5].
E = Modulus of ridgidity of the colum material
$I =$ Moment of inertia of the cross section.
L = equivalent length of the shaft.

But, for a column with both ends hinged the equivalent length (L) is equal to $l/2$ (Khurmi and Gupta, 2010). Therefore, from equation (6)

$$l/2 = \sqrt{\frac{\pi^2 EI}{W_{cr}}} \quad (6)$$

Where $W_{cr} = W$ =the crippling load which is taken as the load applied on the shaft.
The total load applied on the shaftW_{cr} is given by Equation 7:

$$W = M_d + M_p + M_{ps} + M_{fw} \quad (7)$$

Where,
$M_d =$ mass of dish, $M_p =$ mass of pot, $M_{ps} =$ mass of pot stand, $M_{fw} =$ Mass of food and water

Calculating the masses;

For mass of dish, M_d

$$\text{density} = \frac{\text{mass}}{\text{volume}}$$

Therefore, $\text{mass} = \text{density} \times \text{volume}$

But volume of a parabola,

$$v = \frac{\pi}{2} h {r_o}^2 - {r_i}^2$$

Where thickness of the dish = 1mm
$r_o =$ outer radius of the dish $= 0.915\text{m}$
$r_i =$ inner radius of the dish $= 0.915\text{m} - 1\times10^{-3}\text{m} = 0.914\text{m}$

$$v = \frac{3.142}{2} \times 0.28 \times 0.915^2 - 0.914^2$$

$$v = 8.045\times10^{-4}\text{m}^3$$

Density of mild steel = 7850 kg/m^3[6]
Therefore mass of the dish $= 7850\times8.045\times10^{-4} = 6.32\text{kg}$
Weight of dish $= 6.32\times9.81 = 61.95\text{N}$
For mass of the pot stand, M_{ps}
$\text{mass} = \text{density}\times\text{volume}$
volume of the shaft $= A\times L$
$L =$ length of the pot stand $= 750\text{mm}$
where $A =$ area of the shaft $\frac{\pi {d_o}^2 - {d_i}^2}{4}$
$d_o =$ outer diameter of the shaft (m) $= 30\text{mm}$

d_i = inner diameter of the shaft = 20mm

Therefore,

$$A = \frac{3.142\times0.03^2 - 0.02^2}{4} = 3.9275\times10^{-4}m^2$$

volume $= 0.750\times3.9275\times10^{-4} = 2.945\times10^{-4}m^3$

mass of the pot stand $= 7850\times2.945\times10^{-4} = 2.31kg$

weight of the pot stand $= 2.31\times9.81 = 22.6N$

For mass of the pot,M_p

Mass of pot = 1.8 kg, therefore weight of pot = 1.8 × 9.81

For mass of food and water, M_{fw}

Mass of food measured on scale 2.5kg and mass of water used in cooking= 6.5kg.

Therefore total mass= $2.5 + 6.25 = 8.75kg$

Weight $8.75\times9.81 = 85.83N$

Total weight/load on the shaft,

$$W = (61.95 + 22.6 + 17.66 + 85.83)N = 188.13N$$

$$\text{Recall from } l/2 = \sqrt{\frac{\pi^2 EI}{W}}$$

E = 200 GPa [6]

$$I = \text{moment of inertia of the cross section} = \frac{\pi(D^4 - d^4)}{64}$$

Where,

D = outer diameter of the shaft = 90mm

d = inner diameter of the shaft = 80mm

$$I = \frac{3.142\times(0.09^4 - 0.08^4)}{64}$$

$I = 1.21\times10^{-6}m^4$

Substituting the values from W_{cr}, E and I into equation (5); we get:

$$l = 2\left[\sqrt{\frac{3.142^2\times 200\times10^6 \times1.21\times10^{-6}}{188.13N}}\right]$$

$$l = 4.0m$$

This implies that the shaft will buckle under the applied load if the length is 4.0m; every other length below this is safe. Hence, 0.625m was chosen to enable for easy removal of the pot from the dish and to suit a wide range of operator heights.

Buckling analysis was run on the chosen length to ensure that the weight it carries does not exceed the critical buckling load limit of the dish stand material. From Equation 5, we get the critical buckling load of the dish stand to be:

$$W_{cr} = \frac{4\times3.142^2\times200\times10^9\times1.21\times10^{-6}}{0.625^2} = 24.46\ MN$$

Also, the crushing stress the dish stand is subjected to as a result of the weight it carries is given as:

$$\sigma_{cr} = \frac{W}{A}$$

But $A = \text{area of the cross section} = \frac{\pi D^2 - d^2}{4}$ where,

D = Outer diameter of the shaft = 90 mm

d = inner diameter of the shaft = 80 mm

$$A = \frac{3.142\times(0.09^2 - 0.08^2)}{4} = 1.335\times10^{-3}m^2$$

Therefore, the crippling stress of the column/dish stand is $\sigma_{cr} = \frac{188.13}{1.335\times10^{-3}} = 140.92$ kPa

Since W <<<W_s, and the value of the dish stand crippling stress is less than the crushing stress of mild steel (300 MPa [5]) the choice of 0.625m for the dish stand is safe and would not buckle under the weight of the dish and pot. The orthographic drawing of the dish stand is shown in figure 3.

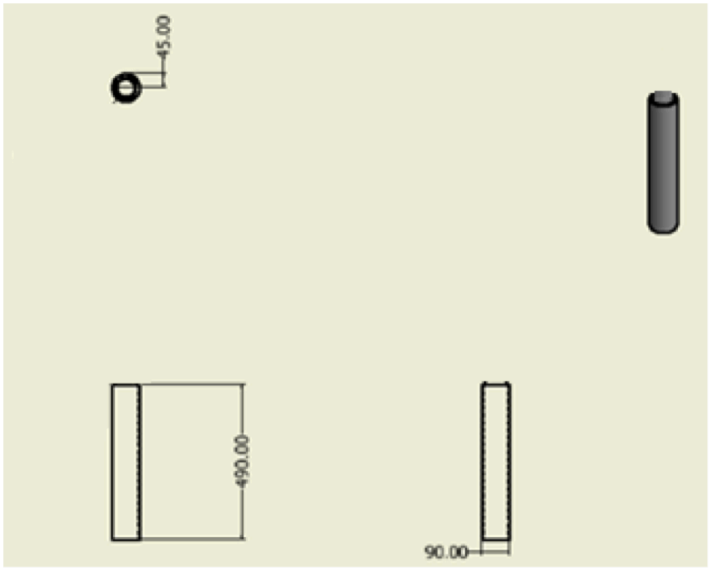

Figure 3: Orthographic view of the dish stand.

Base

A 9 mm thick mild steel angle iron was used for the base. The base carries and supports the components of the solar cooker. A square base of 700 mm was constructed.

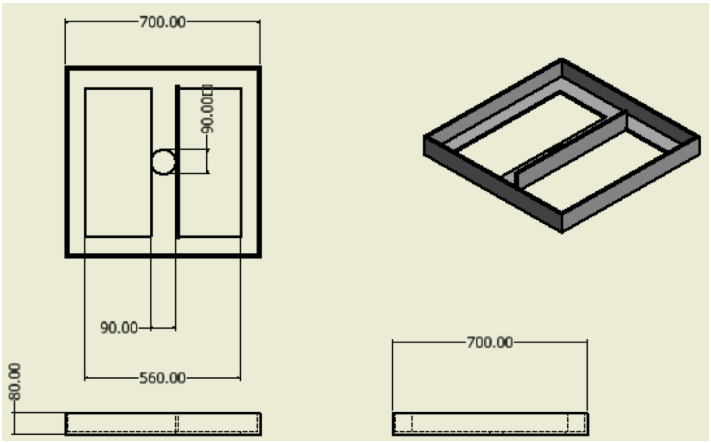

Figure 4: Orthographic view of the solar cooker base.

Figures 5a and 5b show the 3D model and the product prototype of the solar cooker respectively.

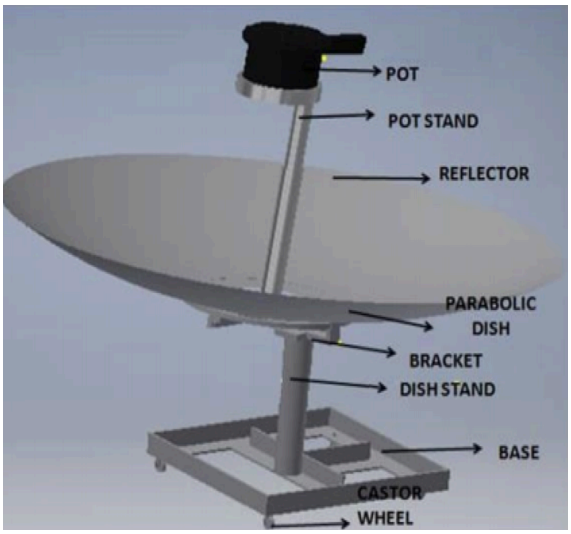

Figure 5a: 3D model of the domestic solar cooker.

Figure 5b: Product prototype of the domestic solar cooker.

Heat Losses

Heat Lost by Conduction

Equation 8 gives the heat loss by conduction,

$$Q = \frac{KA}{x}(\theta_f - \theta_i) \qquad (8)$$

Where

$K =$ Coefficient of thermal conductivity for mild steel $= 48.5\ W/m^2{}^\circ C$ [7]

The temperature of the pot is assumed to be in thermal equilibrium with the mixture

$x =$ thickness of the pot $= 2mm$

And $A =$ surface area of the pot $= 2\pi(R^2 - r^2) + 2\pi(R - r)h$

where, $R =$ Outer radius of the pot $= 0.120m$, $d =$ inner radius of the pot $= 0.11965m$, $h =$ height of the pot $= 0.165m$

Therefore,

$A = 2\times3.142\times(0.120^2 - 0.11965^2) + 2\times3.142(0.120 - 0.11965)\ \times0.165 = 8.90\times10^{-4}$

Therefore

$$Q = \frac{48.5\times8.90\times10^{-4}\times74}{2\times10^{-3}} = 1597J = 1.59kJ$$

Heat Lost by Convection

Equation (9) gives the heat lost by convection.

$$Q = H_C A\,(\theta_f - \theta_i) \qquad (9)$$

$H_C =$ Convection heat transfer coefficient

$= 28.5\ W/m^2{}^\circ C$

$Q = 28.5\times8.90\times10^{-4}\times74 = 1.8770J$

Heat Lost by Radiation

The heat lost by radiation is expressed in Equation 10 as:

$$Q = \sigma AT^4 \qquad (10)$$

Where T= temperature of the solar cooker which is also assumed to be in thermal equilibrium with the mixture= $273 + 102 = 375$ K
σ =stefan boltzman contsant given as 5.67×10^{-8}
A= area of the solar cooker
$Q = 5.67\times10^{-8}\times2.86\times375^4 = 3206.8\,J = 3.2\,kJ$

Heat loss as shown graphically in figure 6 is greatest by radiation, followed by conduction and convection.

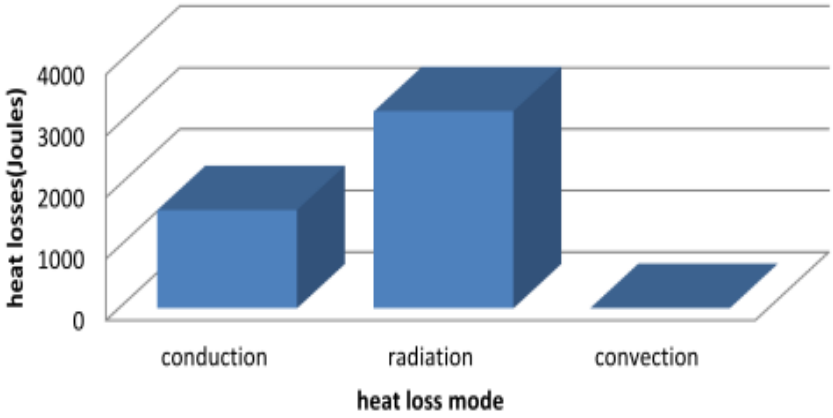

Figure 6: Heat losses across the solar cooker.

Performance Evaluation

After construction, the solar cooker was positioned in an open air space away from any form of sunlight hindrance/obstruction. The ambient temperature and solar insolation for each day when the performance test was carried out were measured using a thermometer and a solarimeter. 2.5kg of beans and 6.5 kg of water was placed in the pot. The probe of a digital thermometer was inserted in the pot in order to make contact with the food, enabling the cooking temperature to be recorded. The pot was then placed on the solar cooker pot stand for cooking to commence. The start time for cooking was recorded. Cooking temperature was monitored through the digital thermometer and changes in temperature values were recorded against corresponding changes in time. The monitoring time interval was 10 minutes, however, in cases where changes in temperature became gradual as the meal was about to get done, minute-by-minute recording of the corresponding cooking temperature was carried out. Therefore, from the start of the gradual change, a 2 minutes interval check was carried out in order to end the test just when the meal is done. The time at which this occurs is recorded as end time for cooking. The difference between the start and end time of cooking is recorded as the cooking time. Table 2 gives information on the variation of cooking temperature with respect to cooking time for the days the test was carried out.

Table 2: Observed values of cooking time against cooking temperature

Cooking Time (mins)	Cooking Temperature (°C)				
	Day 1	Day 2	Day 3	Day 4	Day 5
0	28.34	28.31	28.33	28.32	28.38
10	36.56	40.43	40.67	43.02	40.45
20	46.56	52.67	52.32	55.78	52.51
30	56.34	63.32	63.45	65.42	62.08
40	66.67	74.56	73.90	78.71	75.59
50	76.89	81.47	79.56	83.17	79.31
60	86.21	91.87	83.98	90.30	88.56
70	90.34	92.43	89.92	95.07	92.78
80	93.77	93.75	94.67	98.59	96.53
90	94.34	94.66	98.53	100.72	98.93
110	96.67	95.12	100.78	102.01	100.05
115	98.89	97.19	102.56	102.03	101.01
116	100.01	100.45	102.55		102.61
118	101.34	102.64			102.64
120	102.39	102.62			
122	102.41				

Table 2 shows that the beans meal was cooked at an average temperature of 102.45°C and the temperature varies with increase in time. The cooking curves in figure 7 reveal that day 4 has the highest heating gradient than all the other days. This is also corroborated in Table 2 as it seen that it took a lesser time for the meal to cook in day 4 as compared to values obtained in other days.

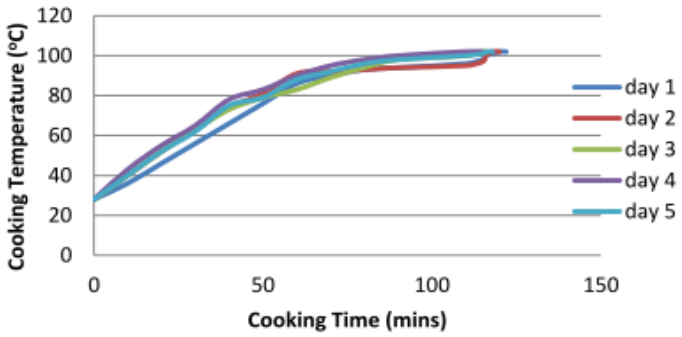

Figure 7: Graph of cooking temperature versus cooking time.

These observations can be explained with the information captured in Table 3. From the Table, it can be deduced that the solar insolation has an influence on the cooking time. This assertion is graphically illustrated in figure 8.

Table 3: Recorded values of ambient temperature, solar insolation and cooking time for various test days.

Test Day	Ambient Temperature (°C)	Solar Insolation (W/m²)	Cooking Time (mins)
Day 1	33.29	406.59	122

Day 2	29.28	412.15	120
Day 3	29.37	428.82	116
Day 4	30.28	431.25	115
Day 5	31.02	418.75	118

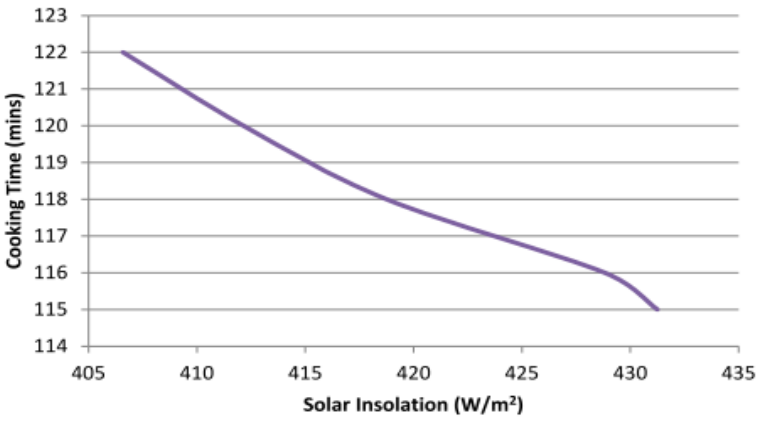

Figure 8: Graph of cooking time versus solar insolation

Figure 8 reveals that increase in the solar insolation would invariably, decrease the cooking time. This is expected because increase in solar intensity implies an increase in the amount of solar energy radiated to the pot, hence, an increase in the heating rate, and reduction in cooking time. Table 3 also shows that the differences between the cooking time for the various days is within a range of 1 to 7 minutes, corresponding to the variations obtained in values for solar insolation for the various days. In other words, slight variations observed in the solar insolation values are responsible for the slight differences in the cooking time for the various days.

Area Concentration Ratio

The area concentration ratio is the ratio of the area of the aperture to that of the receiver. The area of the aperture is determined by the area of the reflected light on the pot base. Equation 11 expresses the concentration area.

$$Area\ concentration\ ratio\ C_A = \frac{Area\ of\ aperture\ (A_p)}{Area\ of\ reciver\ (A_r)} \quad (11)$$

$$C_A = \frac{0.02}{3.6} = 0.005$$

Efficiency of the Solar Cooker

The efficiency of the system was evaluated using equation 12.

$$\eta = \frac{Q_{out}}{Q_{in}} = \frac{Q}{I_b A t} \quad (12)$$

Where:
Q_{out} = Q = Quantity of heat needed to cook the beans meal (J).
I_b = Solar insolation (W/m^2).
A = Cross sectional area of parabolic dish (m^2).
t = Cooking time (sec).
Table 4 shows the efficiency of the system for the days the test was carried out.

Table 4: Efficiency of the solar cooker for various test days.

Test Day	Ambient Temperature (°C)	Solar Insolation (W/m^2)	Efficiency (η)
Day 1	33.29	406.59	0.987
Day 2	29.28	412.15	0.990
Day 3	29.37	428.82	0.984
Day 4	30.28	431.25	0.987
Day 5	31.02	418.75	0.991

From Table 4, it can be deduced that the solar cooker is stable in its operation since its highest percentage change in value is 0.7%.This implies that a 6% change in the solar intensity would only affect the efficiency of the solar cooker by 0.7%

Table 5 shows the result on the performance evaluation carried out for various food substances such as2.5kg of beans, 2.5 kg of rice,1.8kg of yam and 1 kg of water. The quantity of heat needed to cook each meal was calculated and thecooking timeof the meal was recorded.

Table 5: Cooking time for various meals using solar cooker.

S/N	Recorded Solar Insolation (W/m^2)	Temperature (°C)	Meal	Quantity of Heat (kJ)	Cooking Time (Mins)
1	412.15	29	Beans	10526	120
2	412.15	29	Rice	3260.85	93
3	412.15	29	Yam	3618.64	67
4	412.15	29	Water	302.4	13 (Boiling Time)

The various meals cooked on the solar cooker was also cooked using different cooking medium like gas cooker, kerosene stove, firewood and comparisons were made.

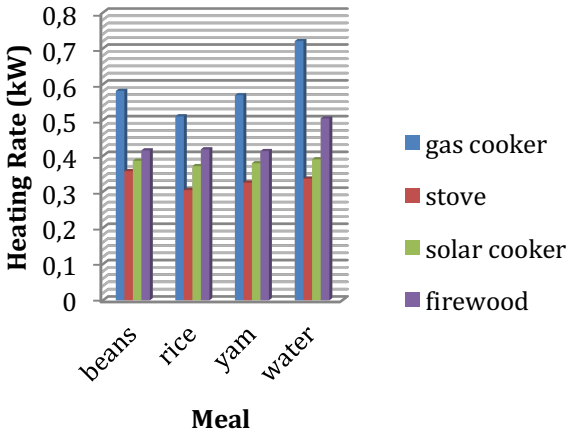

Figure 9: Graph showing the heating rate for various cooking medium

Figure 9 shows the comparison of the heating rate of the various cooking medium for rice, yam, beans and water.

From the four cooking medium, gas cooker has the highest heating rate and kerosene stove is the lowest. For firewood and solar cooker there's a slight difference in the heating rates, this suggests that on days when the

solar intensity would be higher or in areas where there is higher solar intensity, there's a possibility that the heating rate of the solar cooker will be higher than that of the firewood.

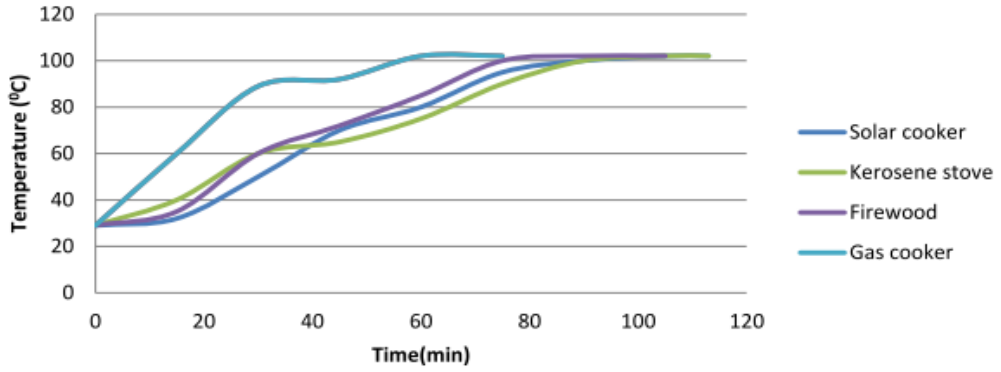

Figure 10: The variation of temperature against cooking time across the various cooking medium for beans

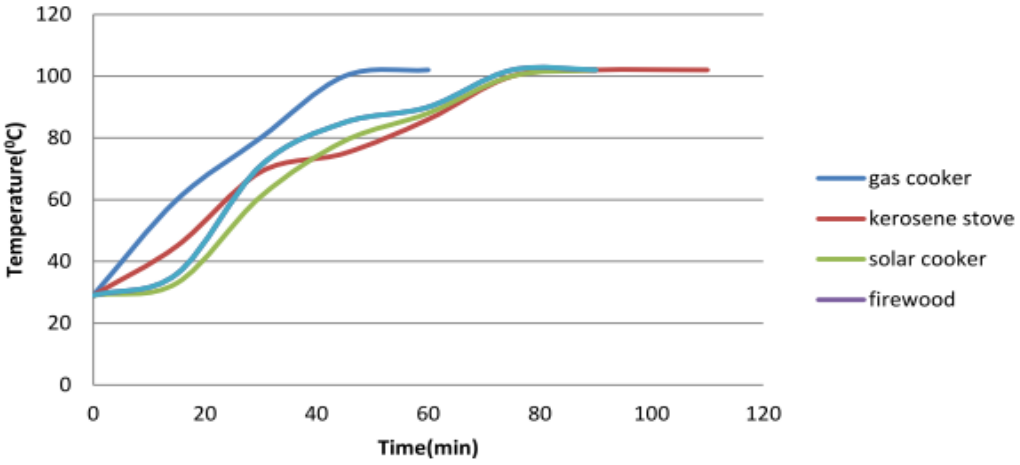

Figure 11: Variation of temperature against cooking time across different cooking medium for rice

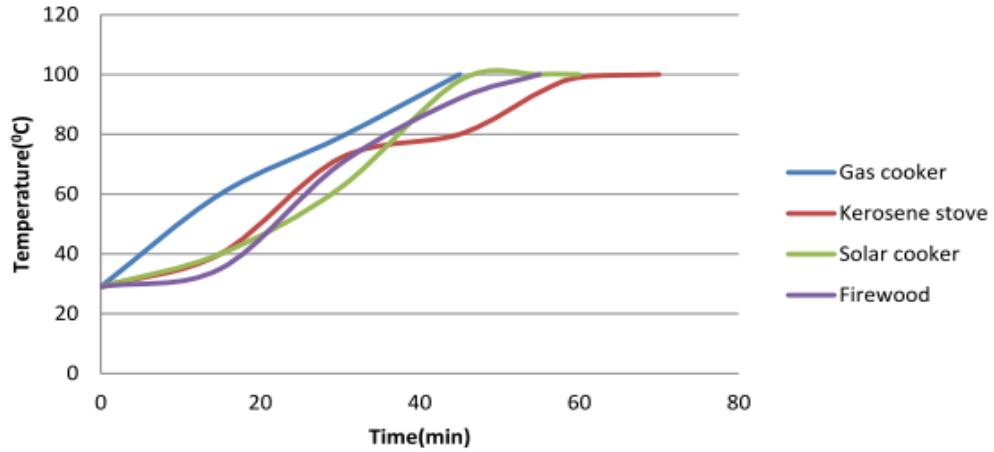

Figure 12: variation of temperature against cooking time across different cooking medium for yam

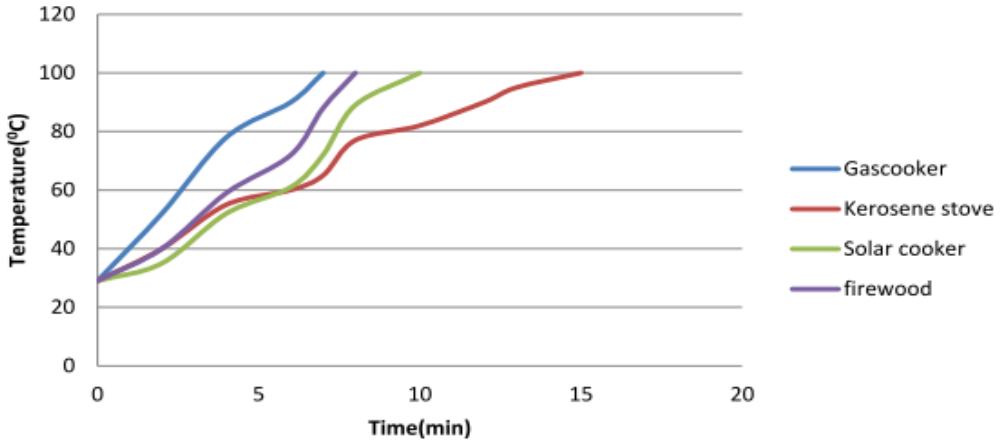

Figure 13: Variation of temperature against cooking time across different cooking medium for water.

Figures 10 to 13 show the variation of temperature against cooking time for beans, rice, yam and water across the various cooking medium. For all the meals, gas cooker and firewood take a shorter time than the solar cooker and the kerosene stove takes a longer time.

The firewood is slightly faster than the solar cooker because firewood undergoes uncontrolled combustion and solar insolation was not at its peak at the time of the year when the experiments were carried out. This suggests that in areas of the country with more hours of sun light and higher solar insolation, the use of CSP for cooking is a viable option.

Conclusion

The realization of this work provides potentially convenient alternative to conventional domestic ways of cooking; with their attendant negative effects on the environment – deforestation, erosion, emission of greenhouse gases. The test performance results obtained from the prototype of the solar cooker met the design requirements – the average cooking temperature of the beans was 102.45 ˚C compared with 102 ˚C from literature. The thermal efficiency was high and remained relatively stable within slight changes in the solar intensity. Places with higher solar insolation values would lead to portable designs and decreased cooking time exposure. A number of improved steps need to be taken in future designs and constructions of this particular case to minimize heat losses, maximize overall thermal efficiency and reduce component sizes.

References

1. http://www.solar-for-energy.com/active-solar-energy.html. Accessed 21/5/2018
2. Siegel R. and Howell J. R. 2002. Thermal Radiation Heat Transfer. Volume 1. 4 edition. Taylor and Francis.
3. Augustine, C and Nnabuchi, M.N. 2000. Analysis of some metrological data of some selected cities in the eastern and southern zone of Nigeria. *African Journal of Environmental Science and Technology.* 4 (2), 92 – 99.
4. Ihekoronye, A. I. and Ngoddy, P. O. 1985. Integrated Food Science and Technology for the Tropics, Macmillian Publishers, London.
5. Khurmi, R. S. and Gupta, J. K. 2010. A Textbook of Machine Design. Eurasia Publishing House (Pvt) Ltd., New Delhi India.
6. www.matweb.com/densityof mildsteel.html. Accessed 23/5/2018
7. www.farm.net/-mason/materials/thermal_conductivity.html. Accessed 21/5/2018

ASIAN INSTITUTE OF RESEARCH
Connecting Scholars Worldwide

The Asian Institute of Research
Engineering and Technology Quarterly Reviews
Vol.2, No.1, 2019: 38-54
ISSN 2622-9374

Concrete Specification and Methods of Quality Testing

Khalid Abdel Naser Abdel Rahim[1]

[1] Researcher in Department of Civil Engineering, University of Coimbra, Coimbra, Portugal

Corresponding Author: Khalid Abdel Naser Abdel Rahim, Department of Civil Engineering, University of Coimbra, Coimbra 3030-788, Portugal. Tel: +351 960021678. E-mail: khalid.ar@outlook.com

Abstract
This manuscript is about the concrete specification. The concrete specification testing is a process by which different tests are carried out such as compressive strength, carbonation depth, ASTM rapid chloride permeability, NDT chloride and initial surface absorption test (ISAT-10) to determine the quality and performance of the concrete in terms of strength, carbonation depth, chloride permeability and surface absorption.

Key Words: Concrete Specification, Quality Testing, Compressive Strength, Carbonation Depth, ASTM Rapid Chloride Permeability, NDT Chloride, ISAT-10.

1. INTRODUCTION

1.1. Scope of work

The BS EN 206/ BS 8500 – Part 1: 2006 Method of specifying and guidance for the specifier (The British Standards Institution BSI, 2006), is set to provide the specifier with five approaches for designing concrete and aids in the determination of the appropriate concrete. This includes method of specifying the concrete.

The concrete specification testing in the structures lab consisted of five tests compressive strength, carbonation depth, ASTM rapid chloride permeability, NDT chloride and initial surface absorption test (ISAT-10). The testing was carried out on concrete specimens with different concrete mixes. The concrete mixes were 100% gravel, 100% recycled aggregate, 30% fly ash and 10% silica fume. In addition, each concrete mix had three specimens with different w/c ratios of 0.45, 0.60 and 0.75 as requested and with reference to (Halliday, 2010).

In the first section of this report, the material used, such as gravel, recycled aggregate, fly ash and silica fume will be described briefly in terms of their influence on carbonation, chloride attack and resistance. In addition, the methods for each test will be described briefly. The mix proportions that were obtained in lab 1: mix design and fresh properties of concrete for each group will be introduced in this report. Moreover, the engineering and durability properties results for each test that was obtained in the lab will be illustrated and discussed. Additionally, the appropriate mix designs for a reinforced concrete bridge deck over a river under carbonated environment, chloride environment and both will be presented and discussed. The design life for bridge deck is 50 years with a cover depth of 50mm. Finally, a conclusion to which of the concrete mix with w/c ratio is more suitable to be used for bridge deck under carbonated environment, chloride environment and both.

1.2. Aims of the paper

The main objectives of the manuscript are:

- Achieve a better understanding of concrete specification.
- Obtain a greater in-depth knowledge of concrete specification testing methods and tests carried out in the concrete structures lab.
- Become familiar with designing concrete using BS EN 206/ BS 8500.

2. MATERIALS USED

2.1. Gravel

Gravel is considered to be a coarse aggregate. The coarse aggregate sizes that were used in lab 1 concrete mixing vary from 5 to 10mm and 10 to 20mm with an absorption value of 1.0%. Generally, gravel maintains good compactability and finishability. It is believed that a good finishability means less cracks and voids appearing on concrete surface after curing. According to (Jackson et al., 1980), this indicates that the diffusion of chloride and carbon ions through concrete will be minimized, therefore, the concrete resistivity will be better.

2.2. Recycled aggregate

Recycled aggregate (RA) is considered to be cheaper than natural aggregates and good as far as the environmental issues are concerned. They consist mainly from recycled destruction remains with high amount of masonry. The recycled aggregates tend to reduce the quality of concrete in relation with natural aggregates. Moreover, recycled aggregates has high rate of water absorption and reduces the workability of concrete (Dhir et al., 1998). Since recycled aggregates reduce the concrete quality in terms of strength, it is assumed that a concrete with a large amount of RA will have low resistivity against carbon and chloride ions.

2.3. Fly ash

Fly ash is considered to be very high fine material. It combines with lime in the water to produce cementitious mix. The particles of fly ash has plain surface and are spherical in shape. In addition, the size and shape of fly ash particles are extremely alike to that of dispersed air bubbles. This provides air entrainment inhibition in cases where the carbon content is high. Also fly ash improves the fresh properties of concrete such as, reducing permeability, bleeding and segregation. Additionally, it has lots of advantages in fresh and hardened properties, such as, maintaining better cohesion, plasticity. Furthermore, it improves workability, durability and increases concrete strength. Moreover, the characteristics of fly ash give it an advantage in terms of reducing the water requirement in concrete mix. Thus, the reduction of water in concrete at a specific w/c ratio improves the quality of concrete in terms of strength. It is known that the strength of concrete is sufficient when considering the resistivity rate of concrete against carbonation and chloride attacks. As the concrete is higher in strength this means a harder concrete and more resistivity against the penetration of carbon or chloride ions in reference to (Day et al., 2006).

2.4. Silica fume

Silica fume is a new material in the construction industry. It is considered to be extremely fine material. Additionally, it consists mainly from pure silicon dioxide approximately 90% or more. Moreover, it is very small in terms of size between 0.03 to 0.3 μm and has greater surface area than fly ash. According to Day, 2006 "… Silica fume in concrete maintains high strength and provides a previously unattainable level of low permeability…" In addition, silica fume reduces water content and gives concrete good surface finishability, which means no existence of cracks. Moreover, the low electrical conductivity of concrete which contains silica fume maintains resistance to corrosion of reinforcement. Therefore, these factors give more protection against the penetration of chloride and carbon ion from environment.

3. TESTING METHODS

3.1. Compressive strength

The test was carried out in accordance to (The British Standards Institution BSI, 2002) BS EN 12390-3:2002 – Testing hardened concrete – Part 3: Compressive strength of test specimens. As shown in figure 1 the compression testing machine that has been used for functioning the test. The compression testing machine applies pressure on the concrete cube until it brakes and failure of specimen is noticed. After that the maximum sustained load is converted to a numerical reading and recorded. From the maximum sustained load the compressive strength of cube is calculated in N/mm².

The testing was carried out on 100mm concrete specimens. After the concrete was mix and cast it was then air-cured in concrete lab for 24 hours. Then it was immersed in water tank with a fixed temperature of 20ºC ± 2ºC. The specimen was then kept in the water tank for testing after 7 and 28 days. Before operating the testing, the cubes were cleaned with a dump cloth to remove any existing material on concrete surface. The next step was adjusting the cube in compression testing machine so that the load is applied equally on the cube surfaces. Each cube was then loaded to failure at a rate of 0.2-0.4 N/mm². The load was then applied until the cube breaks. After that the reading of maximum load was recorded in N. Subsequently, the compressive strength was calculated using the following equation 1.

Compressive strength (N/mm²) = Maximum load (N) / Surface area under test (mm²) (1)

Figure 1. Apparatus of compression testing machine.

3.2. Carbonation depth

The test was carried out in accordance to (University of Dundee, Department of Civil Engineering, 1995) CEN/TC51/WG12/TG5: draft 1995 – Measurement of hardened concrete carbonation depth (Modified by university of Dundee, 1998). The test works by measuring the carbonate depth of a concrete after applying indicator solution and calculating the mean value of readings.

The testing was carried out on 100mm concrete specimens. After the concrete was mix and cast it was then air-cured in concrete lab for 24 hours and kept for another 7 days in air. Then it was situated in exposure chamber for 4 weeks. Then the specimen was chopped in to two equal parts using special equipment for these purposes. The surface was then cleaned to remove the existence of dust. The next step was spraying the specimen surface

with indicator solution which consists from 1% phenolphthalein in 70% ethyl alcohol. After that the carbonation depth was measured at four sides. The readings were then recorded and the mean value of the readings was determined.

3.3. ASTM rapid chloride permeability

The test was carried out with respect to the (American Society for testing and materials ASTM, 1997) American standard ASTM C 1202 – 97 / AASHTO T 277-831 Method: Rapid chloride permeability test. The test gives a quick indication of the concrete resistivity against the penetration of chloride ions by determining the electrical conductance of concrete, according to (Feldman et al., 1994). Figure 2 below illustrates the dimension of specimen for ASTM rapid chloride permeability test. While figure 3 demonstrates the microprocessor RCPT testing machine.

Figure 2. Shows the dimension of specimen for ASTM rapid chloride permeability test.

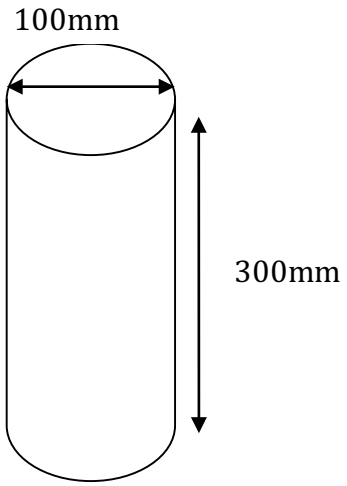

Figure 3. Microprocessor RCPT testing machine.

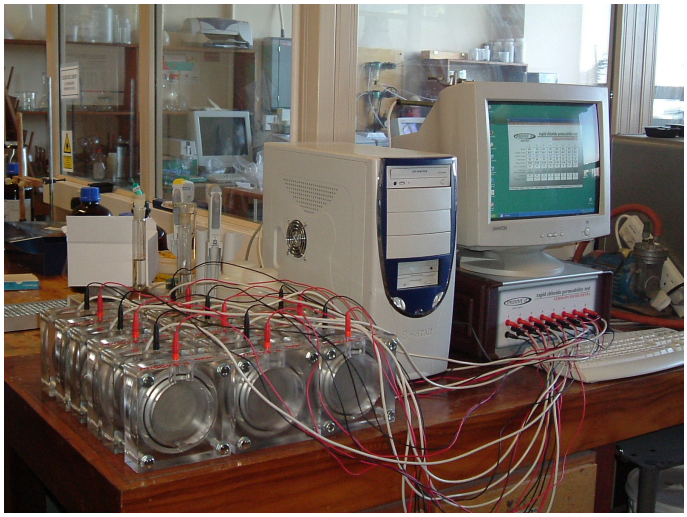

3.4. NDT Chloride

The test was carried out in accordance to (Nordic Council of Ministers, 1999) NT build 492 Nordtest method UDC 691.32/691.53/691.54 (Approved 1999 – 11) – Concrete mortar and cement-based repair materials: Chloride migration coefficient from non-steady-state migration experiments. The chloride ions from external atmosphere penetrate the specimen as an external electrical potential is operated axially. After approximately 24 hours the specimen is split equally and a solution of silver nitrate is spread on one of the sections. After 15

minutes a white silver colour appears on the split surface. This is due to the penetration of chloride which leads to the precipitation of solution. Then the coefficient of the chloride migration can be calculated from depth of penetration. Figure 4 presents the dimensions of NDT chloride test specimen.

Figure 4. Shows the dimension of specimen for NDT chloride test.

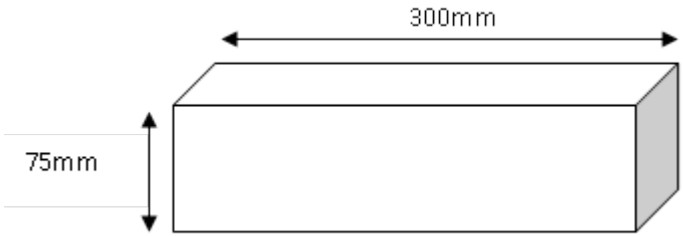

3.5. Initial surface absorption test (ISAT – 10)

The test was carried out with respect to (The British Standards Institution BSI, 1996) BS 1881: Part 208: 1996 – Recommendations for the determination of the initial surface absorption of concrete. Initial surface absorption test is used to measure the surface absorption of the external part of concrete and flow of water rate in concrete specimen Neville (1996, pp.488). The fill of reservoir with water and opening the tape after the adjustment of the apparatus initiates the water in reservoir to flow throw the rubber tube. After the water in rubber tube reaches concrete surface, time will be measured for 9 minutes. When the tape is closed after 9 minutes, the reading of the distance water moved in concrete surface along the capillary tube in 1 minute and 2 minutes is recorded and the ISAT value in ml/m^2/s (x10^{-2}) is calculated.

4. MIX PROPORTIONS AND FRESH PROPERTIES

4.1. Mix proportions

Table 1 to 4 illustrates the mix proportions that has been used in lab 1 mixing concrete for 100% gravel, 100% recycled aggregate, 30% fly ash and 10% silica fume with reference to the research carried out by (Abdel Rahim et al., 2019).

Table 1. Mix proportions for 100% Gravel.

MIX, w/c ratio	MIX PROPORTIONS, kg/m³								
	CEM I	FA	SF	Water	RA		AGGREGATES		
					5/10	10/20	0/5	5/10	10/20
100% GRAVEL									
0.45	400	-	-	180	-	-	660	380	750
0.6	300	-	-	180	-	-	720	390	790
0.75	240	-	-	180	-	-	820	380	755
Particle density, kg/m³	3150	2250	2000	1000	2400		2600	2600	2600

Table 2. Mix proportions for 100% Recycled aggregate.

MIX, w/c ratio	MIX PROPORTIONS, kg/m³								
	CEM I	FA	SF	Water	RA		AGGREGATES		
					5/10	10/20	0/5	5/10	10/20
100% RA									

0.45	400	-	-	180	350	710	600	-	-
0.6	300	-	-	180	360	730	670	-	-
0.75	240	-	-	180	345	695	780	-	-
Particle density, kg/m³	3150	2250	2000	1000	2400		2600	2600	2600

Table 3. Mix proportions for 30% Fly ash.

MIX, w/c ratio	MIX PROPORTIONS, kg/m³								
	CEM I	FA	SF	Water	RA		AGGREGATES		
					5/10	10/20	0/5	5/10	10/20
30% FA									
0.36	355	150	-	180	-	-	560	380	755
0.47	265	115	-	180	-	-	690	375	755
0.59	215	90	-	180	-	-	740	385	770
Particle density, kg/m³	3150	2250	2000	1000	2400		2600	2600	2600

Table 4. Mix proportions for 10% Silica fume.

MIX, w/c ratio	MIX PROPORTIONS, kg/m³								
	CEM I	FA	SF	Water	RA		AGGREGATES		
					5/10	10/20	0/5	5/10	10/20
10% SF									
0.45	360	-	40	180	-	-	595	370	735
0.6	270	-	30	180	-	-	685	375	740
0.75	215	-	25	180	-	-	785	360	715
Particle density, kg/m³	3150	2250	2000	1000	2400		2600	2600	2600

4.2. Fresh properties

Table 5 to 8 illustrates the fresh properties that was obtained in lab 1 mixing concrete for 100% gravel, 100% recycled aggregate, 30% fly ash and 10% silica fume.

Table 5. Fresh concrete properties for 100% Gravel.

PROPERTY	W/C RATIO		
	0.45	0.6	0.75
Slump, mm	35	55	35
Plastic Density, kg/m³	2405	2385	2365
Bleeding	None	None	None
Segregation	None	None	None
Cohesiveness	Good	Good/fair	Good
Compactability	Fair	Good	Good
Finishability	Fair	Good	Good

General Observation - Good mixes generally and cement-rich pastes.

Table 6. Fresh concrete properties for 100% Recycled aggregate.

PROPERTY	W/C RATIO		
	0.45	0.6	0.75
Slump, mm	185 (Collapse)	195 (Collapse)	195 (Collapse)
PlasticDensity, kg/m³	2390	2375	2340
Bleeding	Slight	Slight	Slight
Segregation	Slight	Slight	Slight

Cohesiveness	Poor	Poor	Poor
Compactability	Good	Good	Good
Finishability	Good	Good	Good

General Observation - Absorption value probably too high for this RA, therefore more water in mix causing high slumps. Moreover, the density of this RA was probably more than 2400kg/m³ assumed in design stage, approximately 2550kg/m³.

Table 7. Fresh concrete properties for 30% Fly ash.

PROPERTY	W/C RATIO		
	0.37	0.45	0.6
Slump, mm	85	Collapse	190 Collapse
Plastic Density, kg/m³	2470	2455	2470
Bleeding	None	Slight	Slight
Segregation	None	None	Slight
Cohesiveness	Good	Poor	Poor
Compactability	Good	Good	Good
Finishability	Good	Good	Good
General Observation	Cement-rich mix	Too much SP	Too much SP

Table 8. Fresh concrete properties for 10% Silica fume.

PROPERTY	W/C RATIO		
	0.45	0.60	0.75
Slump, mm	95	80	75
Plastic Density, kg/m³	2410	2375	2380
Bleeding	None	None	None
Segregation	None	None	None
Cohesiveness	Good	Good	Good
Compactability	Good	Good	Good
Finishability	Good	Good	Good

5. RESULTS AND DISCUSSION

5.1. Engineering and durability properties (All Results)

Table 9 to 12 illustrates the concrete specification results that was obtained in lab 4 for concrete mixes of 100% gravel, 100% recycled aggregate, 30% fly ash and 10% silica fume (Abdel Rahim, 2019).

Table 9. Concrete specification results for 100% Gravel.

w/c	28 day strength	Carbonation depth	ASTM Chloride	NDT Chloride	ISAT-10
	N/mm²	28days, mm	Coulombs	mm	ml/m^2/s (x10^{-2})
0.45	57.5	6	5469	19.3	43.3
0.6	40.0	9	6667	24.8	39.6
0.75	27.0	14	6689	43.4	52.3

The compressive strength results for 100% gravel concrete mix was 57.5 N/mm^2, 40 N/mm^2, 27 N/mm^2 for 0.45, 0.60 and 0.75 w/c ratio respectively. Moreover, the carbonation depth after 28 days was 6mm, 9mm and 14mm with respect to a 0.45, 0.60 and 0.75 w/c ratio. Furthermore, the ASTM chloride results were 5469, 6667 and 6689 coulombs for w/c ratios of 0.45, 0.60 and 0.75. In addition, the NDT results illustrated an increase in value

as w/c ratio increases. The results were 19.3mm, 24.8mm and 43.3mm for 0.45, 0.60 and 0.75 w/c ratios. Finally, the initial surface absorption results showed no relation with each other since the ISAT value increase from a w/c ratio 0.45 to 0.60 and decrease from w/c ratio 0.60 to 0.75. The results were 43.3 ml/m^2/s × 10^2 for 0.45 w/c ratio, 39.6 ml/m^2/s × 10^2 for 0.60 w/c ratio and 52.3 ml/m^2/s × 10^2 for 0.75 w/c ratio.

The above results indicate that as the w/c ratio increases the 28 day compressive strength decreases. It is known that a high compressive strength means fewer voids, pores in the concrete and more resistivity against chloride and carbon ions. Generally speaking, more compressive strength indicates better durability. On the other hand, an increase in w/c ratio increases carbonation depth, ASTM chloride, NDT chloride. In addition, it is believed that the w/c ratio has a major influence on all tests. To proof this mix of 0.45 w/c ratio had the highest compressive strength and lowest carbonation depth than other w/c ratios. Thus, the 0.45 w/c ratio had the best concrete quality in terms of strength and lowest penetration of carbon and chloride ions. As far as the permeability is concerned the lower the ISAT value the better. Alternatively, high ISAT means more pores in the concrete which results in more absorption of water. Though the highest ISAT – 10 value was for the 0.75 w/c ratio, the results showed a moderated for 0.45 w/c ratio concrete mix. Generally, gravel has provided the mix with strength since it is more functional in giving strength than recycled aggregates.

Table 10. Concrete specification results for 100% Recycled Aggregate.

w/c	28 day strength	Carbonation depth	ASTM Chloride	NDT Chloride	ISAT-10
	N/mm²	28days, mm	coulombs	mm	ml/m^2/s (x10^{-2})
0.45	43.0	5	6055	2.5	43.3
0.6	25.0	9	4969	26.4	50.5
0.75	17.0	12	7704	36.6	57.7

The compressive strength results for 100% recycled aggregate concrete mix was 43 N/mm^2, 25 N/mm^2, 17 N/mm^2 for 0.45, 0.60 and 0.75 w/c ratio respectively. Moreover, the carbonation depth after 28 days was 5mm, 9mm and 12mm with respect to a 0.45, 0.60 and 0.75 w/c ratio. Furthermore, the ASTM chloride results were 6055, 4969 and 7704 coulombs for w/c ratios of 0.45, 0.60 and 0.75. In addition, the NDT results illustrated an increase in value as w/c ratio increases. The results were 2.5mm, 26.4mm and 36.6mm for 0.45, 0.60 and 0.75 w/c ratios. Finally, the initial surface absorption results showed an increase with the increase in w/c ratio. The results were 43.3 ml/m^2/s × 10^2 for 0.45 w/c ratio, 50.5 ml/m^2/s × 10^2 for 0.60 w/c ratio and 57.7 ml/m^2/s × 10^2 for 0.75 w/c ratio.

According to the results obtained, the 0.45 w/c ratio mix for 100% recycled aggregate is the most durable. (Glanville, 1995) has mentioned that "the usual primary requirement of a good concrete in its hardened state is compressive strength" Though it has the lowest ISAT value and moderated results for ASTM chloride, it is still good in quality with the highest compressive strength and lowest in carbonation depth and NDT chloride. Furthermore, the NDT chloride result for 0.45 w/c ratio might be wrong due to its very low value and having no relation with the others. As can be seen from the results recycled aggregate provided the mix with more resistivity against carbonation if compared with other mixes.

Table 11. Concrete specification results for 30% Fly Ash.

w/c	28 day strength	Carbonation depth	ASTM Chloride	NDT Chloride	ISAT-10
	N/mm²	28days, mm	Coulombs	mm	ml/m^2/s (x10^{-2})
0.36	59.0	6	2624	23.0	38.2
0.47	37.5	11	-	28.0	45.4
0.59	25.0	23	3240	31.2	60.7

The compressive strength results for 30% fly ash concrete mix was 59 N/mm^2, 37.5 N/mm^2 and 25 N/mm^2 for 0.36, 0.47 and 0.59 w/c ratio respectively. Moreover, the carbonation depth after 28 days was 6mm, 11mm and 23mm with respect to a 0.36, 0.47 and 0.59 w/c ratio. Furthermore, the ASTM chloride results were 2624 and 3240 coulombs for w/c ratios of 0.36 and 0.59. In addition, the NDT results illustrated an increase in value as w/c ratio increases. The results were 23mm, 28mm and 31.2mm for 0.36, 0.47 and 0.59 w/c ratios. Finally, the initial surface absorption results showed an increase with the increase in w/c ratio. The results were 38.2 ml/m^2/s $\times$ 10^2 for 0.36 w/c ratio, 45.4 ml/m^2/s $\times$ 10^2 for 0.47 w/c ratio and 60.7 ml/m^2/s $\times$ 10^2 for 0.59 w/c ratio.

The fly ash demonstrated the worst result among all the other mixes. Though it provided high strength, it still had the highest ISAT results. In addition, fly ash had greatest chloride and carbonation penetration value when evaluated with other mixes. This might be due to less amount of calcium hydroxide. Thus, fly ash did not give sufficient durability property to the concrete. The mix could have been improved by reducing the percentage of fly ash in the mix, approximately between 6 to 10% with respect to the British Standards BS 8500.

Table 12. Concrete specification results for 10% Silica Fume.

w/c	28 day strength	Carbonation depth	ASTM Chloride	NDT Chloride	ISAT-10
	N/mm²	28days, mm	Coulombs	mm	ml/m^2/s (x10^{-2})
0.45	62.0	5.5	1600	9.9	19.2
0.6	49.0	12	2501	18.5	30.6
0.75	33.0	19	4780	30.8	33.0

The compressive strength results for 10% silica fume concrete mix was 62 N/mm^2, 49 N/mm^2 and 33 N/mm^2 for 0.45, 0.60 and 0.75 w/c ratio respectively. Moreover, the carbonation depth after 28 days was 5.5mm, 12mm and 19mm with respect to a 0.45, 0.60 and 0.75 w/c ratio. Furthermore, the ASTM chloride results were 1600, 2501 and 4780 coulombs for w/c ratios of 0.45, 0.60 and 0.75. In addition, the NDT results illustrated an increase in value as w/c ratio increases. The results were 9.9mm, 18.5mm and 30.8mm for 0.45, 0.60 and 0.75 w/c ratios. Finally, the initial surface absorption results showed an increase with the increase in w/c ratio. The results were 19.2 ml/m^2/s $\times$ 10^2 for 0.45 w/c ratio, 30.6 ml/m^2/s $\times$ 10^2 for 0.60 w/c ratio and 33 ml/m^2/s $\times$ 10^2 for 0.75 w/c ratio.

The results demonstrated the most reliable in terms of durability comparing with other concrete mixes. Silica fume is known for producing a denser concrete, by which it did fully established its properties in this concrete mix. In addition, the results for 10% silica fume had the highest strength, lowest carbonation depth, chloride penetration and ISAT values among all other mixes. In the author point of view, the best concrete mix to be used in the concrete design for bridge deck under both carbonation and chloride atmospheres is 10% silica fume with a 0.45 w/c ratio. This was decided due to the high compressive strength and low carbonation depth, chloride penetration and initial surface absorption. Additionally, these properties demonstrated good durable concrete for that mix.

6. APPROPRIATE MIX DESIGNS

Design requirements are to design concrete for a bridge deck below tidal zone as shown in figure 5 with a minimum cover of 50mm and 50 years design life. The designs was carried out with accordance to BS EN 206-1, BS 8500.

Figure 5. Shows tidal zone of the bridge.

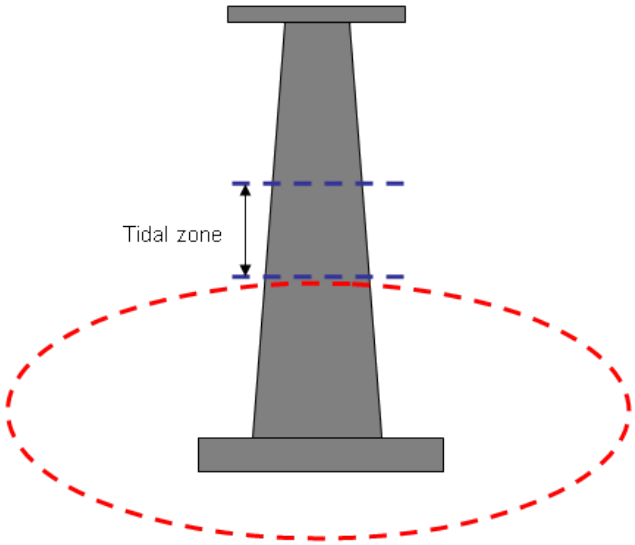

6.1. Carbonated environment

- Step 1 Choosing exposure class
- From Table A.1 Exposure classes
  Choose **XC3 and XC4** (Moderate humidity or cyclic wet and dry) illustrated in table 13 of this report.

- Step 2 Finding compressive strength class
- From Table A.4 Compressive strength class
  Form XC3 and XC4 (Moderate humidity or cyclic wet and dry) ~ choose XC3 (Moderate humidity) the minimum strength is **C25/30** with a maximum w/c ratio of 0.65 and minimum cement content is 260 kg/m^3. The following is shown in table 14.

Table 13. Exposure class Table A.1 from BS8500-1.

Table A.1 **Exposure classes**

Class designation	Class description	Informative examples applicable in the United Kingdom
No risk of corrosion or attack (X0 class)		
X0	For concrete without reinforcement or embedded metal: all exposures except where there is freeze-thaw, abrasion or chemical attack For concrete with reinforcement or embedded metal: very dry	Unreinforced concrete surfaces inside structures Unreinforced concrete completely buried in soil classed as AC-1 and with a hydraulic gradient not greater than 5 Unreinforced concrete permanently submerged in non-aggressive water Unreinforced concrete surfaces in cyclic wet and dry conditions not subject to abrasion, freezing or chemical attack Reinforced concrete surfaces exposed to very dry conditions
Corrosion induced by carbonation (XC classes) [A] *(where concrete containing reinforcement or other embedded metal is exposed to air and moisture)*		
XC1	Dry or permanently wet	Reinforced and prestressed concrete surfaces inside enclosed structures except areas of structures with high humidity Reinforced and prestressed concrete surfaces permanently submerged in non-aggressive water
XC2	Wet, rarely dry	Reinforced and prestressed concrete completely buried in soil classed as AC-1 and with a hydraulic gradient not greater than 5[B]
XC3 and XC4	Moderate humidity or cyclic wet and dry	External reinforced and prestressed concrete surfaces sheltered from, or exposed to, direct rain Reinforced and prestressed concrete surfaces subject to high humidity (e.g. poorly ventilated bathrooms, kitchens) Reinforced and prestressed concrete surfaces exposed to alternate wetting and drying Interior concrete surfaces of pedestrian subways not subject to de-icing salts, voided superstructures or cellular abutments Reinforced or prestressed concrete beneath waterproofing

Table 14. Compressive strength class Table A.4 from BS8500-1.

Table A.4 Durability [A] recommendations for reinforced or prestressed elements with an intended working life of at least 50 years

Nominal cover [B]	Compressive strength class where recommended, maximum water-cement ratio and minimum cement or combination content for normal-weight concrete [C] with 20 mm maximum aggregate size [D]								Cement/combination types
mm	15 + Δc	20 + Δc	25 + Δc	30 + Δc	35 + Δc	40 + Δc	45 + Δc	50 + Δc	
Corrosion induced by carbonation (XC exposure classes)									
XC1	C20/25 0.70 240	C20/25 0.70 240	C20/25 0.70 240	C20/25 0.70 240	C20/25 0.70 240	C20/25 0.70 240	C20/25 0.70 240	C20/25 0.70 240	All in Table A.6
XC2	—	—	C25/30 0.65 260	C25/30 0.65 260	C25/30 0.65 260	C25/30 0.65 260	C25/30 0.65 260	C25/30 0.65 260	All in Table A.6
XC3/4	—	C40/50 0.45 340	C30/37 0.55 300	C28/35 0.60 280	C25/30 0.65 260	C25/30 0.65 260	C25/30 0.65 260	C25/30 0.65 260	All in Table A.6 except IVB-V
	—	—	C40/50 0.45 340	C30/37 0.55 300	C28/35 0.60 280	C25/30 0.65 260	C25/30 0.65 260	C25/30 0.65 260	IVB-V
Corrosion induced by chlorides (XS from sea water, XD other than sea water) *Also adequate for any associated carbonation induced corrosion (XC)*									
XD1	—	—	C40/50 0.45 360	C32/40 0.55 320	C28/35 0.60 300	C28/35 0.60 300	C28/35 0.60 300	C28/35 0.60 300	All in Table A.6
XS1	—	—	—	C45/55 [E] 0.35 [F] 380	C35/45 [E] 0.45 360	C32/40 [E] 0.50 340	C32/40 [E] 0.50 340	C32/40 [E] 0.50 340	CEM I, IIA, IIB-S, SRPC
	—	—	—	C40/50 [E] 0.35 [F] 380	C32/40 [E] 0.45 360	C28/35 0.50 340	C25/30 0.55 320	C25/30 0.55 320	IIB-V, IIIA
	—	—	—	C32/40 [E] 0.40 380	C25/30 0.50 340	C25/30 0.50 340	C25/30 0.55 320	C25/30 0.55 320	IIIB
	—	—	—	C32/40 [E] 0.40 380	C28/35 0.50 340	C25/30 0.50 340	C25/30 0.55 320	C25/30 0.55 320	IVB-V
XD2 or XS2	—	—	—	C40/50 [E] 0.40 380	C32/40 [E] 0.50 340	C28/35 0.55 320	C28/35 0.55 320	C28/35 0.55 320	CEM I, IIA, IIB-S, SRPC
	—	—	—	C35/45 [E] 0.40 380	C28/35 0.50 340	C25/30 0.55 320	C25/30 0.55 320	C25/30 0.55 320	IIB-V, IIIA
	—	—	—	C32/40 [E] 0.40 380	C25/30 0.50 340	C20/25 0.55 320	C20/25 0.55 320	C20/25 0.55 320	IIIB, IVB-V

- Step 3 Determining the w/c ratio for compressive strength

Graph 1. w/c Ratio vs. Compressive strength for carbonate environment.

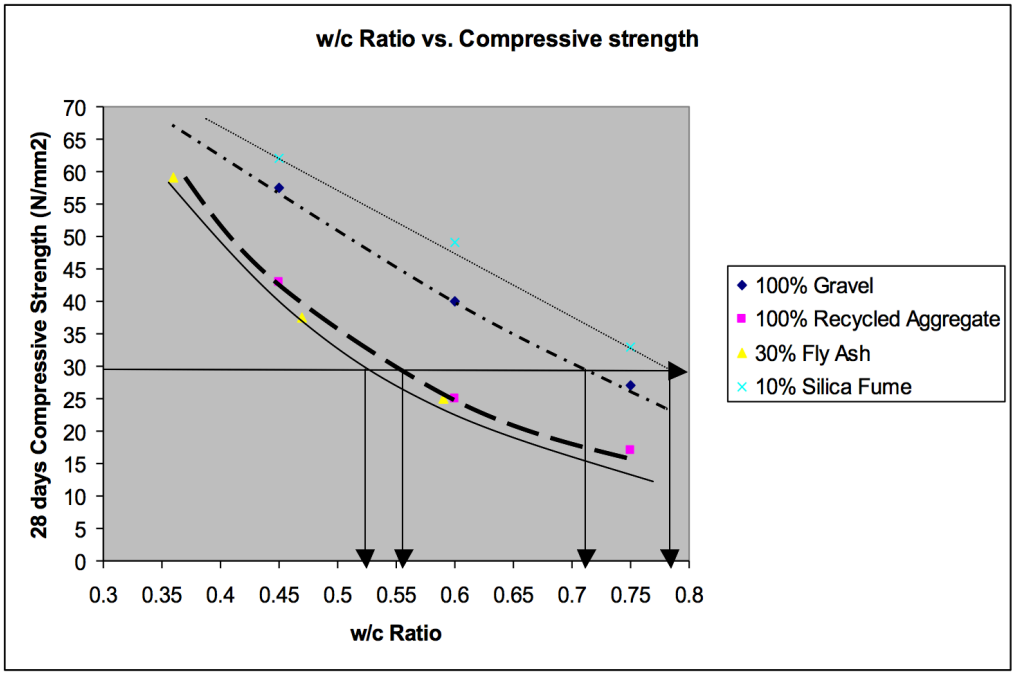

The w/c ratios for 30 N/mm^2 target strength are as follow:

- 100% Gravel = 0.71 w/c ratio
- 100% Recycled aggregate = 0.56 w/c ratio
- 30% Fly ash = 0.52 w/c ratio
- 10% Silica fume = 0.78 w/c ratio

Graph 2. w/c Ratio vs. Carbonation depth.

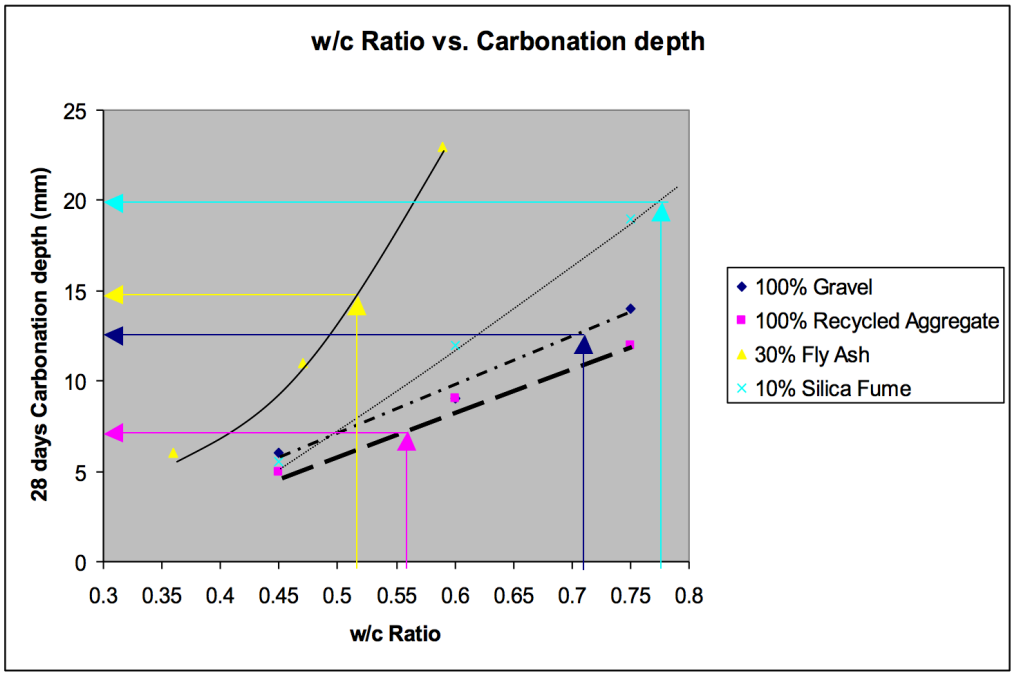

Graph 3. w/c Ratio vs. ISAT - 10.

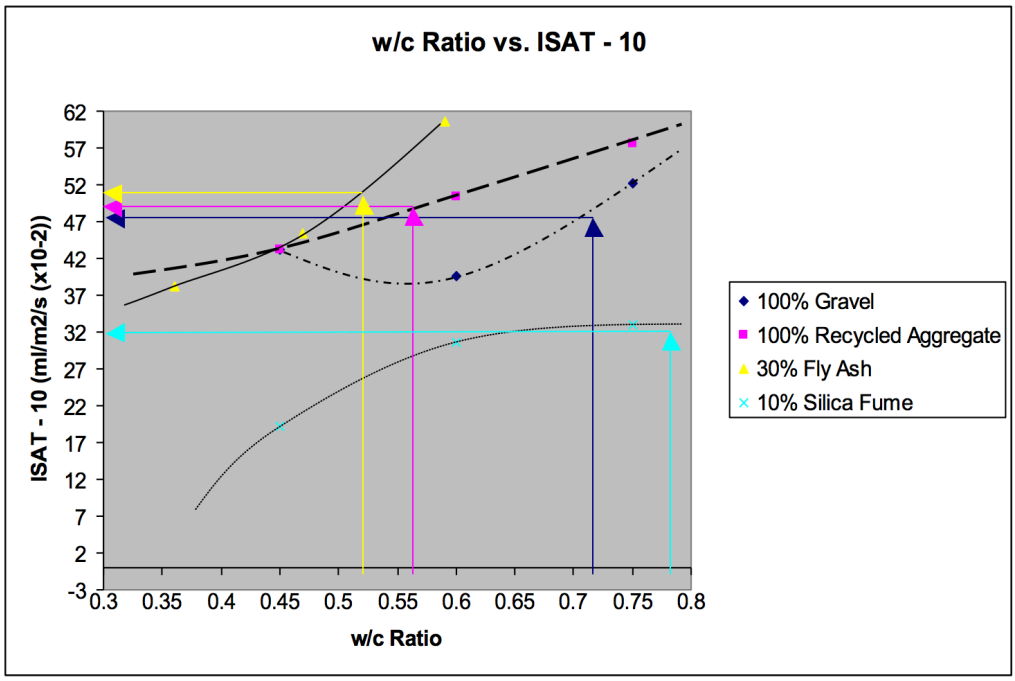

Therefore, for 30% fly ash choose the composition IIB-V with 21% Portland cement to 35% fly ash and comprises cement and combination types CEM II/B-V, CIIB-V. Moreover, for 10% silica fume choose the composition IIA with 6% to 10% fly ash and comprises cement and combination types CEM II/A-V, CIIA-V, CEM II/A-D. In accordance to the results presented in graphical illustration Graphs 1 to 3 for the w/c ratio vs. compressive strength, carbonation depth and ISAT-10 respectively.

6.2. Chloride environment (Not from sea water)

- Step 1 Choosing exposure class

- From Table A.1 Exposure classes
  Choose **XD1** (Moderate humidity) illustrated in table 13 of this report.

- Step 2 Finding compressive strength class

- From Table A.4 Compressive strength class
  For XD1 the minimum strength is **C28/35** with a maximum w/c ratio of 0.65 and minimum cement content is 300 kg/m^3. The selection is shown in table 15.
- Identifying cement combinations:
  From Table A.6 Cement and combination types
  For XD1 the minimum strength is **C28/35** with a maximum w/c ratio of 0.60 and minimum cement content is 300 kg/m^3 for CEM I (Gravel and recycled aggregate), IIA (Silica fume) and IIB-V (Fly ash). The selection is shown in table 16.

Table 15. Compressive strength class Table A.4 from BS8500-1.

			0.45 340	0.55 300	0.60 280	0.65 260	0.65 260	0.65 260	
Corrosion induced by chlorides (XS from sea water, XD other than sea water)									
Also adequate for any associated carbonation induced corrosion (XC)									
XD1	–	–	C40/50 0.45 360	C32/40 0.55 320	C28/35 0.60 300	C28/35 0.60 300	C28/35 0.60 300	C28/35 0.60 300	All in Table A.6
XS1	–	–	–	C45/55[k] 0.35[f] 380	C35/45[k] 0.45 360	C32/40[k] 0.50 340	C32/40[k] 0.50 340	C32/40[k] 0.50 340	CEM I, IIA, IIB-S, SRPC
	–	–	–	C40/50[l] 0.35[f] 380	C32/40[l] 0.45 360	C28/35 0.50 340	C25/30 0.55 320	C25/30 0.55 320	IIB-V, IIIA
	–	–	–	C32/40[l] 0.40 380	C25/30 0.50 340	C25/30 0.50 340	C25/30 0.55 320	C25/30 0.55 320	IIIB
	–	–	–	C32/40[l] 0.40 380	C28/35 0.50 340	C25/30 0.50 340	C25/30 0.55 320	C25/30 0.55 320	IVB-V
XD2 or XS2	–	–	–	C40/50[l] 0.40 380	C32/40[l] 0.50 340	C28/35 0.55 320	C28/35 0.55 320	C28/35 0.55 320	CEM I, IIA, IIB-S, SRPC
	–	–	–	C35/45[k] 0.40 380	C28/35 0.50 340	C25/30 0.55 320	C25/30 0.55 320	C25/30 0.55 320	IIB-V, IIIA
	–	–	–	C32/40[k] 0.40 380	C25/30 0.50 340	C20/25 0.55 320	C20/25 0.55 320	C20/25 0.55 320	IIIB, IVB-V

- Step 3 Determining the w/c ratio for compressive strength

Graph 4. w/c Ratio vs. compressive strength for chloride environment.

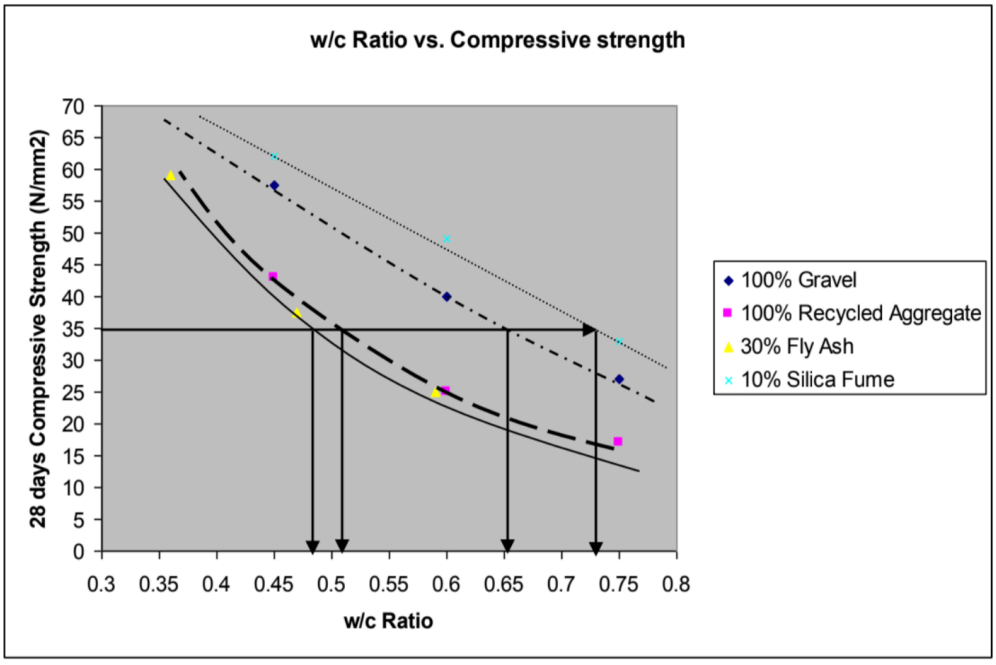

The w/c ratios for 35 N/mm^2 target strength are as follow:

- 100% Gravel = 0.65 w/c ratio
- 100% Recycled aggregate = 0.51 w/c ratio
- 30% Fly ash = 0.48 w/c ratio
- 10% Silica fume = 0.73 w/c ratio
  - Step 4 Determining the chloride results for each w/c ratio

Graph 5. w/c Ratio vs. ASTM Chloride for chloride environment.

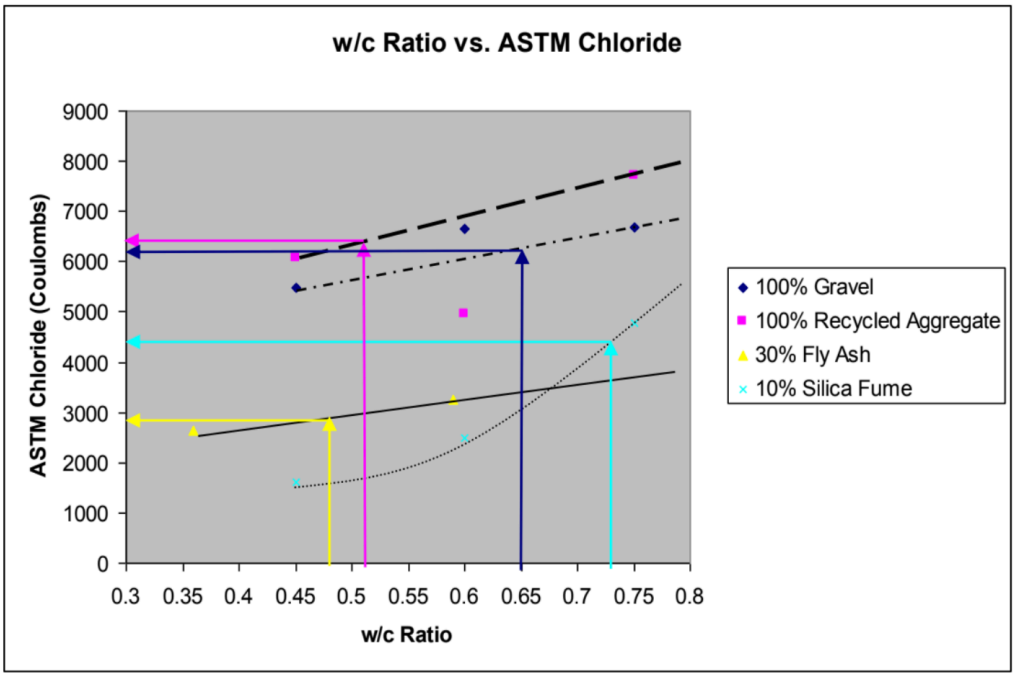

Graph 6. w/c Ratio vs. NDT Chloride for chloride environment.

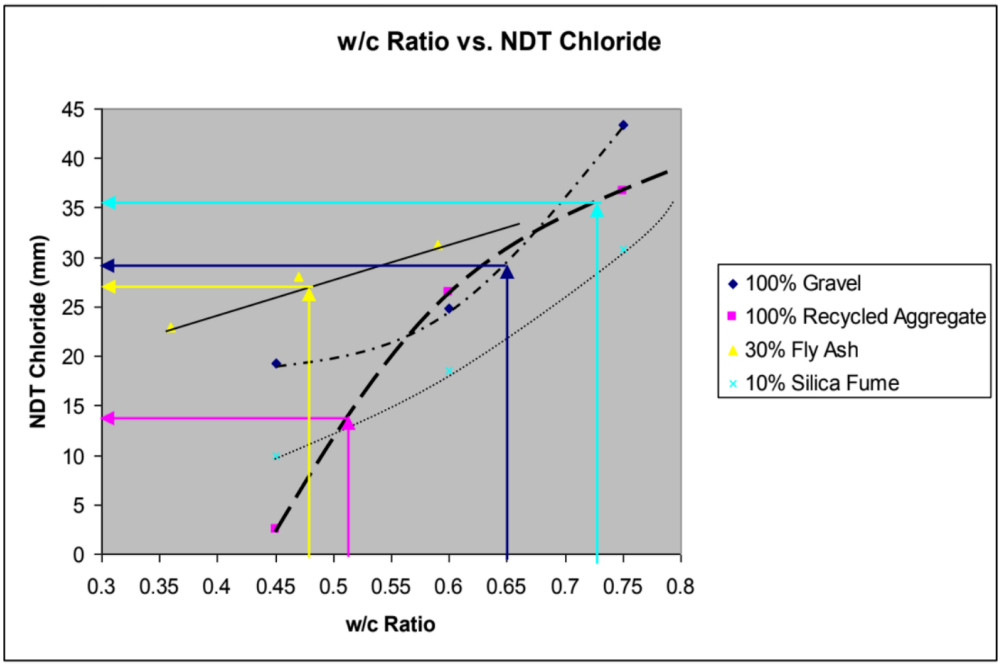

Since XD3 is more aggressive than XD4 it has been decided to choose XD3 with 30% fly ash choose the composition IIB-V with 21% Portland cement to 35% fly ash and comprises cement and combination types CEM II/B-V, CIIB-V. Moreover, for 10% silica fume choose the composition IIA with 6% to 10% fly ash and comprises cement and combination types CEM II/A-V, CIIA-V, CEM II/A-D, as shown in Graphs 4 to 6.

Table 16. A record of the concrete design results.

Test description	100% Gravel = 0.71 w/c Ratio	100% Recycled Aggregate = 0.56 w/c Ratio	30% Fly Ash = 0.52 w/c Ratio	10% Silica Fume = 0.78 w/c Ratio
Cement Content (kg/m^3)	280	355	375	245
Carbonation Depth (mm)	13	7.5	15	20
ASTM Chloride (coulombs)	6200	6500	2900	4400
NDT Chloride (mm)	29	13	26	35
ISAT – 10 ($ml/m^2/s$ ($x10^{-2}$)	47	50	51	32

6.3. Both

The concrete design for carbonated environment was **XC3 and XC4** (Moderate humidity or cyclic wet and dry) and minimum strength of **C28/35**. Moreover, the chosen concrete design for chloride environment was **XD1** and minimum strength of **C25/30** (from table A.1). The observed results has been demonstrated in table 17 below.

Table 17. Concrete designs under carbonation, chloride environments and both.

Description	XC3 and XC4 Carbonation	XD1 Chloride	Chosen for both (XD1)
Maximum w/c Ratio	0.65	0.60	0.60
Minimum compressive strength	C25/30	C28/35	C28/35
Minimum cement content (kg/m^3)	260	300	300

Thus, the chosen concrete design for bridge deck under both carbonation and chloride environments is XD1 (Moderate humidity) with a minimum w/c ratio of 0.60, minimum compressive strength C28/35 and minimum cement content of 300 kg/m^3.

For 30% fly ash chooses the composition IIB-V with 21% Portland cement to 35% fly ash and comprises cement and combination types CEM II/B-V, CIIB-V. Moreover, for 10% silica fume choose the composition IIA with 6% to 10% fly ash and comprises cement and combination types CEM II/A-V, CIIA-V, CEM II/A-D.

7, CONCLUSION

The concrete specification lab was set to determine the compressive strength, carbonation depth, chloride penetration and initial surface absorption values for 100% gravel, 100% recycled aggregate, 30% fly ash and 10% silica fume concrete mixes and compare them in terms of engineering and durability of concrete. It was observed that the w/c ratio had a great influence on all the test results. Hence a decrease in w/c ratio maintains a better concrete by increase the compressive strength and durability.

The results for 10% silica fume demonstrated the highest strength, lowest carbonation depth, chloride penetration and ISAT values among all other mixes. Thus, it is considered to be essential to be used for concrete design with durable property. Additionally, the best concrete mix to be considered in the concrete design for

bridge deck under both carbonation and chloride atmospheres is 10% silica fume with a 0.45 w/c ratio. On the other hand, the results for 30% fly ash were the most unsatisfactory compared with other mixes. This is due to the highest carbonation depth and chloride penetration results. According to concrete specification tests results the following was concluded:

- Durability of concrete is an important aspect of good quality concrete and should be taken in to consideration when designing concrete.
- Silica fume produces denser concrete and increase compressive strength.
- Gravel is more functional in giving concrete strength than recycled aggregates.
- Recycled aggregate mix provided the concrete with more resistivity against carbonation when compared with other mixes.
- Fly ash had the greatest chloride and carbonation penetration.
- Higher compressive strength means better concrete durability.
- Lower carbonation depth indicates greater concrete durability and vies versa.
- Lower ASTM and NDT chloride results in higher concrete durability.
- Lower initial surface absorption illustrates good concrete in terms of durability.

The concrete design for bridge deck was carried out in three stages depending on the environment. The chosen concrete design was10% silica fume and the composition IIA with 6% to 10% fly ash and comprises cement and combination types CEM II/A-V, CIIA-V, CEM II/A-D.

References

Abdel Rahim, K. A. N. et al., (2019), *Experimental study on the mix design and fresh properties of concrete*, Volume 3, Issue 1, pp. 30-36, ISSN 2208-6404, Australian Journal of Science and Technology, Melbourne Scientific Publishers, Victoria, Australia. Available online [http://www.aujst.com/vol-3-1/04-AJST-70_REV.pdf].

American Society for Testing and Materials (ASTM), (1997), ASTM C1202 – 97 / AASHTO T 277-831 *Standard test method for electrical indication of concrete's ability to resist chloride ion penetration - Method: Rapid chloride permeability test*, American Society for Testing and Materials (ASTM), USA.

Day, K., et al. (2006), *Concrete mix design, quality control and specification*, Oxon, Taylor & Francis.

Dhir, R. et al., (1998), *Use of recycled concrete aggregate*, Concrete Technology Unit, University of Dundee, Dundee, Thomas Trelford.

Feldman et al., (1994), *Investigation of rapid chloride permeability test*, ACI Materials journal, technical paper, title no. 91-M23, Available online [http://www.concrete.org/tempComDocs/-24728/91-M23.pdf].

Glanville, J. et al., (1995), *Predication of concrete durability*, The Geological Society, London, E & FN Spon.

Halliday, J. et al., (2010), *Assessment of concrete structures, Summary of the test methods to be used in labs*, University of Dundee, Dundee.

Halliday, J. et al., (2010), *Assessing Quality and Durability of Concrete. Lecture 4 tutorial Notes Concrete Specification*, University of Dundee, Dundee.

Jackson, N. et al., (1980), *Civil engineering materials*, London, Macmillan.

Nordic Council of Ministers, (1999), *NT build 492 Nordtest method UDC 691.32/691.53/691.54 (Approved 1999 – 11) – Concrete mortar and cement-based repair materials: Chloride migration coefficient from non-steady-state migration experiments*, Nordic Council of Ministers, Nordtest, Finland.

The British Standards Institution (BSI), (1996), BSI - BS 1881-208 *Testing concrete - Part 208: Recommendations for the determination of the initial surface absorption of concrete,* The British Standards Institution (BSI), London.

The British Standards Institution (BSI), (2006), BSI - BS EN 206/ BS 8500, *Concrete - Part 1: Method of specifying and guidance for the specifier*, The British Standards Institution (BSI), London.

The British Standards Institution (BSI), (2002), BSI - BS EN 12390-3:2002, *Testing hardened concrete – Part 3: Compressive strength of test specimens*, The British Standards Institution (BSI), London.

University of Dundee, Department of Civil Engineering, (1995), CEN/TC51/WG12/TG5: draft 1995, *Measurement of hardened concrete carbonation depth (Modified by University of Dundee, 1998)*, University of Dundee, 1995, Dundee.

ACKNOWLEDGEMENT: I would like to thank my family, my mother, my father and my brothers for their moral support. Many thanks to Dr. Judith Halliday a senior lecturer at the University of Dundee and to all the staff of the Department of Civil Engineering in the University of Dundee for their technical support for providing the testing materials and for making the concrete structures laboratory available for conducting this experimental investigation.

ASIAN INSTITUTE OF RESEARCH
Connecting Scholars Worldwide

The Asian Institute of Research
Engineering and Technology Quarterly Reviews
Vol.2, No.1, 2019: 55-61
ISSN 2622-9374

Rainwater Harvesting for Drinking Water in Bali, Indonesia

I Nyoman Norken[1], I Ketut Suputra[2], Ida Bagus Ngurah Purbawijaya[3], Ida Bagus Putu Adnyana[4]

[1] Department of Civil Engineering, Faculty of Engineering, Udayana University

Abstract
The water source on the island of Bali, Indonesia, tends to be uneven and depends on geographical and climatological factors. In the remote area at Kubu Subdistrict, Karangasem Regency experiences with very limited water supply, due to the absence of water sources and lack of water services from the piping system. In such conditions, people harvest rainwater and then collect it with cubang (water reservoir) to meet their daily drinking water needs. This study aims to find out how effective the cubang that has been made by the community to meet drinking water needs and how ideal cubang model for the community should be made so that water needs can be fulfilled throughout the year. The results showed that cubang which had been built less effectively to meet drinking water needs, which was caused by the age of the cubang which had reached 20 years old, even more, most of them had already leaked, the size of cubangs varied greatly with the volume of water collected was not sufficient with needs all the time. Water collected in a cubang, harvested through the roof of a house is only able to meet water needs for 4 months a year, the rest for 8 months, the community buys water from tank trucks. To meet water requirements every year, a new cubang model is needed and equipped with a roof as a rainwater harvester. For cubang in leaked conditions can be repaired with ferrocement layers to function properly and last longer.

Key Words: Drinking Water, Rainwater Harvesting, Cubang, Effectiveness, Kubu Subdistrict, Bali

1. Introduction

The island of Bali, Indonesia, which is very well known as a world tourist destination in the world, however, the availability of water resources is uneven and depends on geographical and climatological factors. In the southern part of the island, there tends to be greater availability compared to the northern part. This is directly related to the existing rainfall, and the southern part tends to have higher rainfall than the northern part. One of the areas that have a very limited water supply due to low rainfall is Kubu Subdistrict, Karangasem Regency, Bali Province (JICA, 2006). The low coverage of drinking water services from the piping system causes people in the area to be more likely to meet water needs by harvesting rainwater and to accommodate rainwater in a water reservoir called "*cubang*." According to Geredeg (2011) in the Medium-Term Development Plan of Karangasem Regency 2010-2015, in Karangasem Regency, there are around 9000 *cubangs* scattered in various places including in Kubu Subdistrict. Beritabali.com (2016) describes that residents of Kubu Subdistrict are still in need of *cubang* because in this area until now they have not received drinking water services through piping systems from Government Water Company (PDAM), and in the future, it is expected that the government can provide *cubang* in each household. This research was focused on Kubu Subdistrict, which is one of the sub-districts with dry land and it is very difficult to reach by drinking water supply with piping systems because this area is mostly very remote. This research is expected to be able to identify the current *cubang* conditions and to provide solutions for people, especially those who live in rural areas, to get a *cubang* model that is effective and is able to meet drinking water needs throughout the year.

2. Methodology

This research was conducted in 2018 and using qualitative and quantitative descriptive methods. As many as 3 household *cubang*s were taken as samples in each village and a total of 27 samples from 9 villages in Kubu Subdistrict. The samples were selected using the principle of purposive sampling, which was chosen in such a way that has the criteria of a remote place and has very little chance of being reached by drinking water with a piping system. The data were collected through interviews and by observing the existing *cubangs*. The types of data collected include number of family members; education; socio-economic conditions; water use from a *cubang*; size, construction, and utilization of *cubang* water; age and condition of *cubang*; the reliability of available *cubang* water; catchment area for rainwater harvesting. In addition, rainfall data were also collected for 10 years. That data analysis was done qualitatively and quantitatively and is expected to provide answers and recommendations for the current *cubang* conditions and reliability, as well as recommendations for improvement; making *cubang* model designs that are effective in accordance with local rainfall conditions in order to be able to meet drinking water needs throughout the year.

3. Results and Discussion

1) Description of the study area
   Kubu is one of the sub-districts in Karangasem Regency, geographically located around $115^0$25'20 "and $115^0$36'50" East Longitude and around $8^0$13'20 "and $8^0$17'10 'South Latitude and has an area of 234.71 km², and is dry land. Kubu Subdistrict consists of 9 (nine) villages, including Dukuh Village, Tulamben Village, Kubu Village, Batu Ringgit Village, Sukadana Village, Tianyar Village, Tianyar Tengah Village, Tianyar Barat Village and Ban Village (Fig 1). The climate in the study area is not much different from the climate in general in Karangasem Regency, which is a tropical climate, influenced by two types of seasons: the dry season (April-October) and the rainy season (November - March). The daytime air temperature is around 29^0C and at night around 26^0C with humidity reaching 70-80% during the day. The annual average rainfall is 1461.96 mm / year in Kubu Station and 1173.08 mm / year at Tianyar Station, and the annual average rainfall from both stations was obtained at 1317.52 mm/year. Kubu Subdistrict is very pronounced as a very dry area, because inexperience to low rainfall, there is no indication that there are rivers that flow water throughout the year which can be used as a source of raw water for drinking water supply. According to information from the Director of the Government Water Company (PDAM) of Karangasem Regency, the current service coverage of PDAM for Kubu Subdistrict has only reached 18.69% of the total population. The people who get drinking water services from the PDAM are only people who live around the main highway of Karangasem-Singaraja. In addition, there are village water supply services (PAM Desa) which cover services as much as 27.86% of the total population. Communities living on highlands and far from the highway, practically only rely on household *cubang* besides buying water distributed by tank trucks.

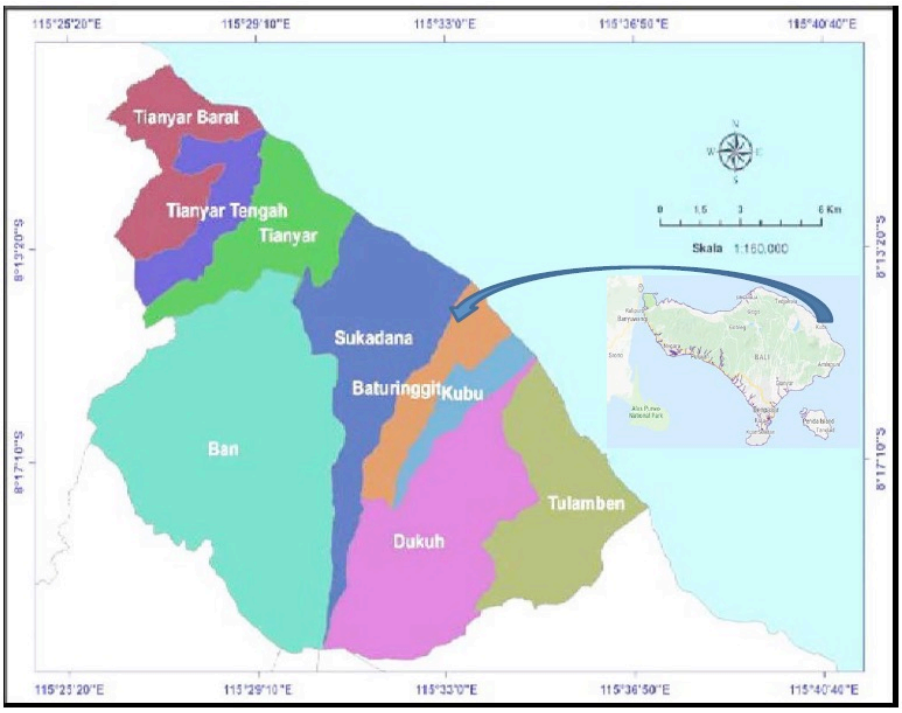

Figure 1. Map of Kubu Subdistrict in Bali.
(Source: Kubu Subdistrict in Numbers, 2017)

2) Socio-economic counseling

The socio-economic conditions of the respondents indicated that the majority of their livelihoods were farmers and also as breeders, with income below IDR 1,000,000 (USD 70) and even less than IDR 500,000 (USD 35) per month. Besides being a farmer, a small percentage of respondents also work as employees earning more than IDR 1,000,000 (USD 70). The family size of the majority of respondents (55.5%) is as many as 4 people or less (2 or 3 people per family), while the remaining 44.5% the number of family members varies from 5 to the largest reaching 10 people. Based on the existing socio-economic conditions, it is felt that the economic conditions of most people are very heavy and still have not reached a decent standard of living. In addition, there is a scarcity of drinking water sources as a daily necessity, forcing them to buy water from 1-4 tanks each month with prices varying from IDR 100,000 (USD 7) to IDR 150,000 (USD 10.5) per tank.

3) Current *cubang* conditions

The limited availability of access to drinking water forces a large number of people in Kubu Subdistrict to harvest rainwater through the roof of a house and to be accommodated in a *cubang*. Interview with respondents indicated that, each household had at least 1 (one) *cubang*, only a few families had more than one *cubang* (having 2 *cubangs* even one respondent had 4 *cubangs*) with very varied capacities, ranging from 5.16 m^3 to almost 120 m^3, but if overall, 74% of the *cubang* volume built is less than or equal to 40 m^3, only 26% of the volume is greater than 40 m^3. There are 2 types of *cubang* cross-section, round and rectangular, but the size of *cubang* is very varied. *Cubang* which has a round cross-section shape with diameters varying from 2 meters to 4 meters with depths varying from 2 meters to 6 meters, as well as *cubang* with rectangular or square cross-section shapes with varying sizes 1.6 x 1.6 m^2 up to 5 x 5 m^2 with depth varies from 0.8 meters to 3.9 meters (as shown in Fig 2). Most of the *cubang* age (78%) is more than 10 years, even more than 20 years, only 6 respondents (22%) with the age of 5 years or less. *Cubang* conditions that have been more than 10 years generally have leaked, but those in good condition are the result of repairs by coating with a kind of leak-proof paint, the repairs carried out are only temporary. The *cubang* material is made of stones, using only a small amount of material from the concrete blocks. In addition, the *cubang* built is located underground; especially those made of stones, while the ones built from the concrete blocks are built on the ground (Fig 2a and Fig 2b).

a. *Cubang* made of stone. b. *Cubang* made of blocks. c. Roof as a rainwater harvester

Figure 2. *Cubang* made of stones and blocks and the roof as rainwater harvester.
(Source: Survey results)

Furthermore, the interview results indicate that the catchment area for harvesting rainwater is mostly less than 50 m^2 using the roof of a residential house, then the rainwater harvested from the roof of the house is channeled using plastic gutters into the *cubang*, as shown in Figure 2 c. The water in *cubang* is only to fulfill the needs for 4 (four) months or only in the rainy season, the rest for 8 (eight) months they buy water from the water provider. The amount of water purchased by respondents varies from 1 to 2 tanks each month. Each tank contains 5 m^3 at an average price of IDR 120,000 (USD 8.27) per tank and can be more or less depending on the distance of the respondent's residence from the location of the available water source.

Cubang which has been built at this time is ineffective and unreliable as a reservoir of rainwater harvested, because some are in a leaky condition or only good after being repaired, besides the existence of *cubang* is unable to provide water throughout the year because most respondents buy water from tank trucks throughout the dry season, even the duration of buying water reaches 8 (eight) months in a year (from April to November).

4) *Cubang* models are needed because a *cubang* which was built independently by the community turned out to be ineffective and reliable to meet the needs of drinking water and livestock throughout the year, a design was needed that was based on water requirements and the amount of rainwater that could be utilized. There are several things that need to be taken into consideration in making the design of *cubang*s to be effective and reliable enough to meet water requirements throughout the year, including:
   a) Water requirements
      For water needs, according to the standard of the Directorate of Cipta Karya, it is 60 liters/person/ day (Mediatataruang.com, 2016). Water needs for livestock are assumed that every livestock (cattle or pig) requires as much as 5 liters of water/livestock/ day.
   b) Number of family members
      The number of family members according to the results of interviews with respondents is dominated by families with a number of family members of 2; 4 and 5 people per family, with the consumption for families with 2 members raising 1 livestock, while for families with 4 or 5 members raising 2 cattle (cows or pigs).
   c) Rainfall and catchment area
      The annual average rainfall for Kubu District is 1317.52 mm. The amount of rainfall is used to determine the roof area of the building that is used as the area of rainwater catchment/rainwater harvesting according to the amount of water needed for each *cubang* model. Furthermore, based on the

average annual rainfall the catchment area needs to be calculated to meet water needs throughout the year.

The calculation results of various *cubang* models, water requirements, and required catchment area are presented in Table 1, assuming that each *cubang* model is closed with a roof to reduce the amount of free water evaporation and is used as a catchment area for rainwater harvesting, while the lack of roofing still uses the existing ones. To drain rainwater from the roof of a house or *cubang* roof, a gutter from a plastic pipe is used. For *cubang* placement, it is placed in such a way near the house to facilitate the flow of water harvested from the roof of the house and water from *cubang*. After going through interviews and in-depth discussions with building structure experts (Made Sukrawa Ph.D.), *cubang* construction is suggested being made of sturdy reinforced concrete structures to prevent construction failure due to earthquakes, cracks and being able to have a lifetime of 50 years or more.

Table 1. *Cubang* model designs for various family sizes

No	Description	Unit	Family *Cubang* Model		
			For 2 persons and 1 livestock	For 4 persons and 2 livestock	For 5 persons and 2 livestock
1	Family size	Persons	2	4	5
2	Drinking water needs	l/person/day	60	60	60
3	Drinking water needs	l/family/day	120	240	300
4	Water needs for livestock	l/day	5	10	10
5	Water needs for 1 year	m^3	45.625	91.25	113.15
6	Water loss	%	10	10	10
7	Total of water needs for 1 year	m^3	50	100	124
8	Amount and size of *cubang*	Amount x length x width x height (m)	2x4x3.2x2	2x5x5x2	2x5.6x5.6x2
9	Average annual rainfall	mm	1317.52	1317.52	1317.52
10	Need for water catchment	m^2	38	76	94
11	Water loss assumption	%	20	20	20
12	Catchment area needed	m^2	46	91	113
13	Catchment area from *cubang* roof	m^2	36	66	66
14	Area of the additional catchment from the house roof	m^2	10	25	47

Source: Analysis results

5) Repair of existing *cubang*

In addition to making a *cubang* model that fits the water needs, the *cubang* can also be repaired from leaks to function properly and last longer. The results of the interview with Dr. Nyoman Pujianiki recommend repairing *cubang* using ferrocement. Ferrocement is a type of thin reinforced concrete wall made from cement mortar which is reinforced with continuous chicken wire/wire (chicken mesh) and a tight layer and relatively small wire size. The technical fixes can be done as follows:

a) Material for repairs

To repair *cubang* which is leaking using ferrocement with the basic material is Portland Cement (PC) Type 1, fine sand that passes the No. 8 filter or diameter 2.36 mm, chicken wire/wire mesh (chickenmesh) with small diameter, 5 cm concrete nails, and material addition to additives as leak-proof.

b) How to repair

Mix mortar or stir PC with sand, 1 PC with 2 sand (1PC: 2 sand) with a volume proportion, with cement water factor 0.35-0.5. Mortar is added with additives to strengthen mortar and leak resistance. Chicken wire/wire mesh is installed on the inner wall of the *cubang* surface by nailing it using 5cm long concrete

nails which function to hold the woven wire on the *cubang* wall. The distance of woven wire from *cubang* wall is 2 cm. Furthermore, the mortar added with the additive plastered on the wall and the *cubang* base which has been fitted with chicken wire with a thickness of 4 cm.

6) *Cubang* Modelling and Repair Costs
   a) The cost of making a *cubang* model
   To make a *cubang* model according to the type needed based on the material and artisan prices in 2018, it is: Type 1 costs IDR 44,600,000 (USD 3075); type 2 for IDR 66,100,000 (USD 4,558); and Type 3 of IDR 74,700,000 (USD 5,150).
   c) The cost of repairing *cubang*
   The cost needed to repair the *cubang* that has been built to function properly is IDR 219,718 (USD 15.1) for each ferrocement m^2. For example, for *cubang* with a diameter of 3 meters and in 3 meters, a cost of IDR 7,800,000 (USD 538) is required.

4. Conclusions and suggestions

The conclusions and suggestions of the study can be summarised as follow:

Conclusions

Access to drinking water supply through the PDAM in Kubu Subdistrict is still very low (18.69% of the total population), most people rely on rainwater harvested and stored in water tanks (*cubang*) for drinking water (drinking, cooking, washing, and bathing) and water requirements for livestock. The volume/capacity of *cubang* built by the community is very varied, most of which have been built for quite a long time (20 years) and are in a leaky condition or only in good condition after being repaired. The amount of water stored in *cubang* is not enough to meet water needs for one year, only available for 4 months and for 8 months buying water from a tank truck of 2 tanks every month.

To meet water requirements every year, a *cubang* model with a capacity of 50 (Type 1) is needed; 100 (Type 1) and 124 m3 (Type 1) for families with 2 members and 1 livestock each; 4 people and 2 livestock; and 5 people and 2 livestock. The ideal *cubang* model can be made of bricks equipped with a roof as rainwater harvesters and can be added to the roof of the house, to meet the required catchment area according to the height of the rain, at the cost of IDR 44,600,000 (USD 3075) for Type1; Type 2 is IDR 66,100,000 (USD 4,558; and Type 3 is IDR 74,700,000 (USD 5,150).

Leaking cavity conditions can be repaired with ferrocement layers to function properly and last for a long time, at the cost of IDR 7,800,000 (USD 538) for a diameter of 3 meters and in 3 meters or IDR 219,718 (USD 15.1) for every ferrocement m2.

Suggestions

It is necessary to test the model by making it directly in accordance with the size of the family that uses it and observed for at least one year starting from the beginning of November until the beginning of November the following year. If the *cubang* model is not ideal, it needs to be modified as needed and then it can be mass-produced for those in need. It is necessary to make an model of repairing *cubangs* that leak with ferocement. The participation and support of the government and the private sector are very much needed to help realize *cubang* in an effort to meet the needs of the community for drinking water in Kubu District, especially for those who are categorized as poor.

5. Acknowledgments

This research was funded by the Study Program Featured Research grant from the Institute of Research and Community Service of Udayana University, for which we express our deepest gratitude to the Dean of the

Faculty of Engineering and staff as well as the Chairperson and Staff of the Research and Community Service Institute of Udayana University.

References

BPS Kabupaten Karangasem, (2016), Curah Hujan Kabupaten Karangasem 2012-2016 (Rainfall in Karangasem Regency 2012-2016), https://karangasemkab.bps.go.id/statictable/2016/08/01/3/jumlah-curah-hujan-2012-2016.html

BPS Kabupaten Karangasem (2017), Kecamatan Kubu Dalam Angka 2017 (Kubu Subdistrict in Numbers 2017), https://kuburayakab.bps.go.id/publication/2017/09/22/4d7199157c94ccaec173142e/kecamatan-kubu-dalam-angka-2017.html

Beritabali.com. (2016), Warga Kubu Karangasem Butuh *Cubang* Air (People of Kubu Karangasem need Cubang), https://www.beritabali.com/read/2016/12/05/201612070010/DPRD-Bali--Warga-Kubu-Karangasem-Butuh-*Cubang*-Air.html

JICA, (2006), The Comprehensive Study on Water Resources Development and Management in Bali Province in The Republic of Indonesia, JICA-PU Bali Province

Geredeg I Wayan, (2011), Rencana Pembangunan Jangka Menengah (RPJM) Daerah Kabupaten Karangasem 2010-2015 (Medium-Term Development Plan of Karangasem Regency 2010-2015), Government of Karangasem Regency.

Mediatataruang.com, (2016), Standar Kebutuhan Air (Standard of Water Ned), http://mediatataruang.com/standar-kebutuhan-air-menurut/

Waskom, R (2008), Graywater Reuse and Rainwater Harvesting, Colorado Water Resources Research Institute, Colorado State University

ASIAN INSTITUTE OF RESEARCH
Connecting Scholars Worldwide

The Asian Institute of Research
Engineering and Technology Quarterly Reviews
Vol.2, No.1, 2019: 62-67
ISSN 2622-9374

The Effect of Time, Price of Stock Research and Development, and Number of Bugs on Net Revenue for Intel Corporation

Ceyhun Ozgur[1], Li Shen, Yiming Shen, Haojie Chen, Abby Bridwell

[1] College of Business, Valparaiso University

Abstract
Intel Corporation studied the effect of bugs in the revenue of the company. In this paper, we look at the factors affecting the revenue of Intel Corporation with respect to how bugs affect the revenue. By doing research on the development and number of Intel employees, we examined the effect it has on stock price, and how bugs affect this in the corporation.

Key Words: Net Revenue, Intel Corporation, Price of Stock Research

Introduction

In a computer, software and hardware work hand-in-hand. Computer software is a collection of data and instructions that tell the computer how to function. On the contrary, computer hardware is actually computer system that is built and performs the work. Computer software includes computer programs, libraries, and data. Both computer hardware and software are necessarily for each other in order for the computer program to work properly.

In computer software, an error or failure in the computer program can occur that causes it to produce an incorrect result, also known as a software bug. In this failure, the computer program can crash and will not operate properly for the user. These bugs are often caused by human errors in the source code or design ("Software Bug", n.d.). Hardware bugs work similarly, but instead they attack the hardware portion of a computer system ("What is a Bug?", 2017). Problem with the Bloomberg Businessweek's report claiming that Chinese government agents used the supply chain of server hardware vendor Supermicro, during an interview with BuzzFeed News (Sanders, J, 2018).

Intel Corporation is a technology company that is the world's largest semiconductor chip maker based on revenue. They work with companies to produce needed technology like integrated circuits for computing and communication. Their website on www.intel.com aims to instruct their viewers about annual progress reports and safety/health compliance. Intel works to provide many products for their customers that range from

[1] Dr. CEYHUN OZGUR, CPIM is a professor of Information and Decision Sciences in the College of Business at Valparaiso University. He co-authored a textbook by McGraw-Hill entitled *Introduction to Management Science with Spreadsheets.* Among others, Dr. Ozgur has published in *Operations Management Research, Journal of Modern Applied Statistical Methods, Journal of Data Science, Decision Sciences Journal of Innovative Education, Interfaces,and OMEGA,* He is a member of the Decision Sciences Institute, and APICS. He is is an area editor *for Operations Management Research, associate* editor for *Decision Sciences Journal of Innovative Education*

microprocessors with few processor cores to software products and services that help enable and advance the computing ecosystem (Intel Reports, n.d.).

1) Discussion of the effects of meltdown on this corporation
2) Methodology (using XLSTAT to get the OLS model)

Intel Corporation has a security dimension in its protocol mentioned on their website. Specifically, Intel builds hardware-enabled security capabilities directly into their silicon in order to help protect all layers of the computer including hardware, firmware, operating systems, applications, networks and the cloud ("hard-ware enabled security", 2019).

However, in 2018, there was evidence for a flaw in the security of Intel's chips. One of Intel's security measures, called Software Guard Extensions, allows programs to establish "secure" enclaves on Intel processors. This secured enclave creates a safe-haven against malware or other comprises to the computer. Recently, researchers have found that SGX mostly repels Spectre and Meltdown attacks and a related attack can bypass its defenses (Newman, 2018).

Yuriy Bulygin, the former Intel Corporation chief threat researcher, has recently discovered that hackers can exploit previously discloses problems in microprocessors to access a computer's firmware to get the most sensitive information (Robertson, 2018).

Academic partnership for Intel Corporation is a very high priority for them. Specifically, they are committed to being an active partner in the security ecosystem and do so by strengthening cybersecurity partnerships with academia to advance research. Intel has paired with Purdue to continue to strive for this goal (Echevarria, 2018).

Data

Database compiled for this paper source from Intel's annual report from year 2007 to year 2017. In this paper, it is reasonable to set Bugs as dummy variable since it is not a continual data. When the number of bugs is larger or equal to 2, it's set as 1, which means bugs exist during this period; otherwise, it doesn't necessarily have a bug.

Figure 1: Descriptive Statistics _ Bugs (Mean 1.75; Median 1.00)

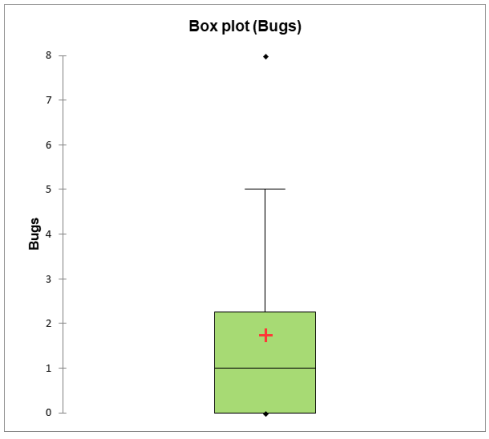

Methodology

The least square model is used in this paper. There are two models to illustrate the relationship between Bugs and other commercial factors like revenue and the number of employees.
Firstly, estimating whether the bugs can affect Intel's net revenue:

$$ln\_Revenue_i = \beta_0 + \beta_1 Time_i + \beta_2 Stock\_price_i + \beta_3 Bugs_i + \varepsilon_i$$

Where, ln_Revenuei is the net revenue Intel Corporate gets each quarter; $Bugs_i$ is a dummy variable.

Next, examining how the number of employees and the amount of Research and Development affect Bugs:

$$Bugs_i = \beta_0 + \beta_1 Employees_i + \beta_2 ln\_Research_i + \varepsilon_i$$

Where, $Bugs_i$ represents whether there are bugs or not.

Empirical Findings

Tables 1 shows the results of OLS (Ordinary Least Square) regressions. It tells that Time is significantly positive and affects the net revenue of Intel Corporation; when the stock price increases by 1 unit, net revenue will have 0.003 more likely chance to increase. However, there is an opposite relationship between the Bugs and the Revenue; also, this is not statistically significant which means that even though the number of bugs have a relationship with the net revenue for Intel Corporation, the relationship of the number of bugs to revenue for Intel is not significant. It seems that the only significant independent variable to predict the net revenue for Intel Corporation are time and price of stock. However, the price of stock is only significant at less than 0.057.

Table 1: estimates for Net Revenue [a,b]

Independent Variables	Coef. Estimate	Std. Error	Pr > |t|
Intercept	9.895	0.0303	**< 0.0001**
Time	0.005	0.0009***	**< 0.0001**
Stock_price	0.003	0.002	0.057
Bugs	-0.016	0.015	0.282

a. The dependent is natural logarithm of net worth Intel Corporation price of stock;
b. The symbols (***), (**) and (*) indicate statistical significance at $p < 0.01$, $p < 0.05$ and $p < 0.10$, respectively.

ln_Revenue = 9.89517+0.00491*Time+0.00335*Stock_price-0.01597*Bugs

Table 2: In-Revenue

Source	Value	Standard error	t	Pr > |t|	Lower bound (95%)	Upper bound (95%)
Time	0.691	0.131	5.279	**< 0.0001**	0.426	0.955
Stock_price	0.256	0.131	1.956	0.057	-0.009	0.521
Bugs	-0.086	0.079	-1.090	0.282	-0.246	0.074

Figure 2. Graph of In-Revenue

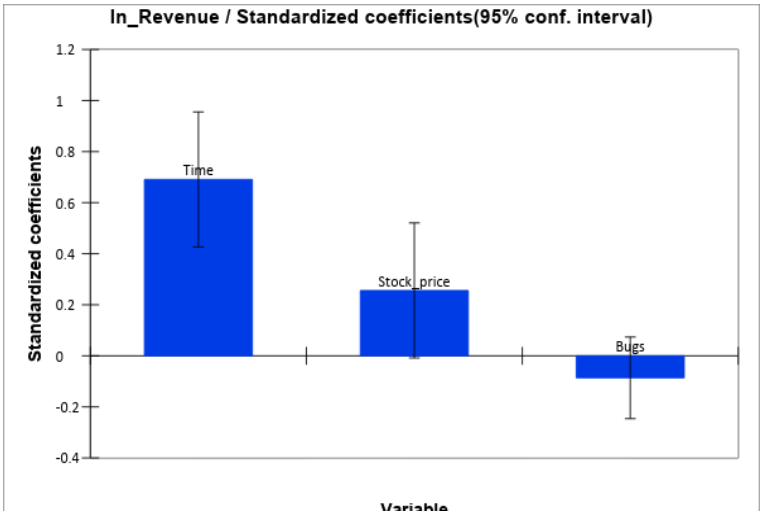

Figure 3: Standardized residuals vs. in-revenue

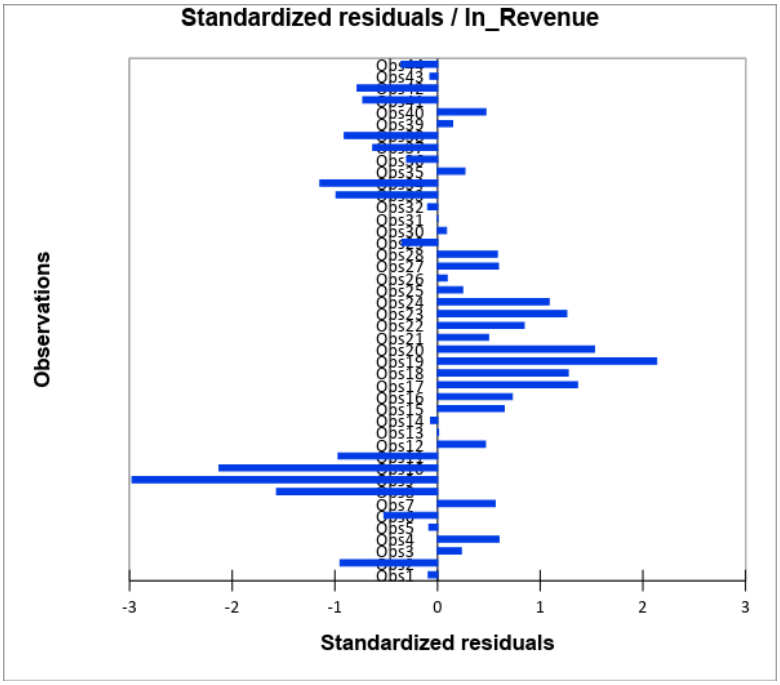

Table 3 shows how the Intel Corporation related factors effect the bugs. It tells that Time does not influence the number of bugs. The estimate of Employees, -0.00007, indicated that if the Intel Corporation has one than more employee, it has 0.00007 possibility to avoid having a problem concerning bugs and effects the net revenue of the corporation significantly. However, the more funds are in Research & Development, it become more likely to have an effect on the bugs significantly. Specifically, the more money invested in Research and Development indicates a possibility of fewer bugs. For example, in this model the independent variables are time, number of employees, and investment in research and development to predict Intel Corporation's number of hardware bugs.

Table 3: estimates for Bugs [a,b]

Independent Variables	**Coef. Estimate**	**Std. Error**	**Pr > |t|**
Intercept	-46.411	8.963	**< 0.0001**
Time	0.000	0.000	
Employees	-0.00007	0.00001***	**< 0.0001**
Research & Development	5.738	1.097***	**< 0.0001**

c. The independent variable of Research is natural logarithm of net worth Intel Corporation price of stock;
d. The symbols (***), (**) and (*) indicate statistical significance at $p < 0.01$, $p < 0.05$ and $p < 0.10$, respectively.

Bugs = -46.41094-0.00007*Employees+5.73817*ln_Research

Table 4: Standardized coefficients (Bugs)

Source	Value	Standard error	t	Pr > |t|	Lower bound (95%)	Upper bound (95%)
Time	0.000	0.000				
Employees	-1.563	0.324	-4.828	**< 0.0001**	-2.217	-0.909
ln_Research	1.692	0.324	5.227	**< 0.0001**	1.039	2.346

Figure 4. Bugs/ Standardized coefficients (95% conf. interval)

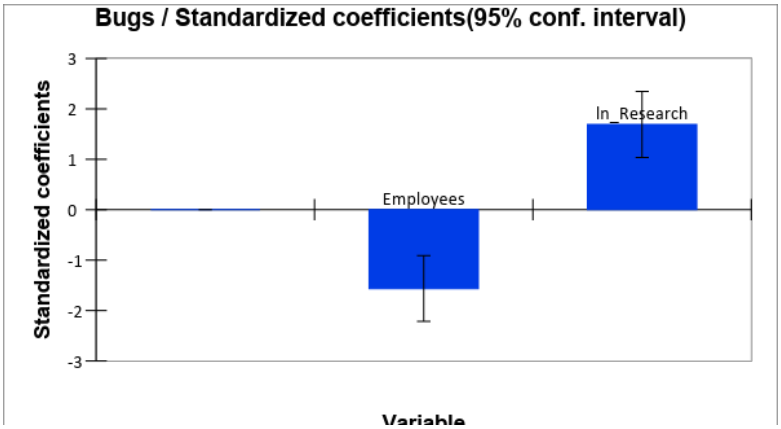

Figure 5: Standardized residuals vs. Bugs

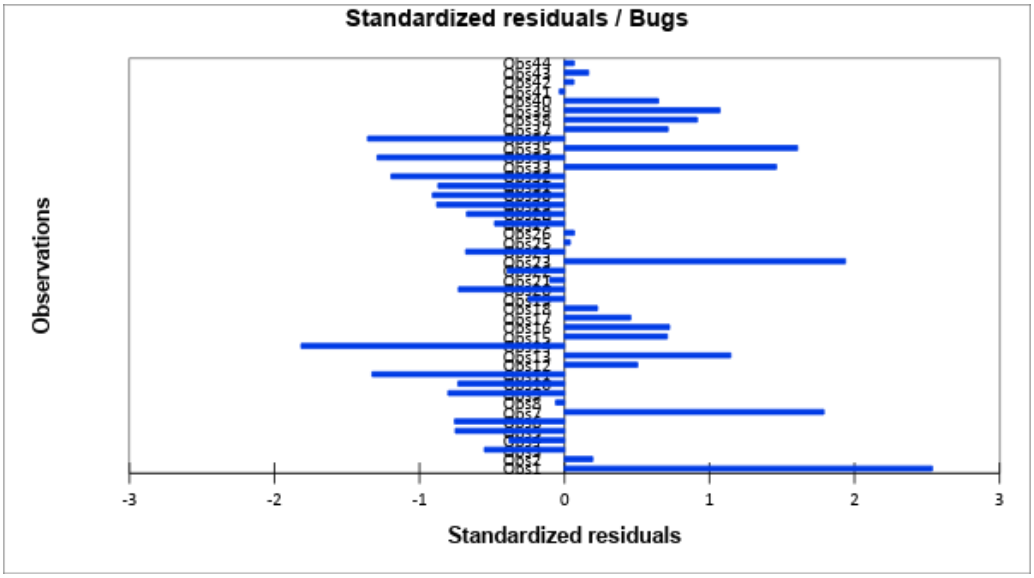

Conclusion

We try to show in this paper how the bugs, time, number of employees and amount of research development affects the net revenue of Intel Corporation. We were able to show that both time and price of stock of Intel Corporation significantly affects the net revenue of Intel Corporation. However, most importantly, we were able to show that Research & Development significantly affects the number of bugs in Intel Corporation.

References

Bloomberg.com, Bloomberg, www.bloomberg.com/news/articles/2018-05-17/millions-of-computers-are-at-risk-from-the-next-gen-spectre-bug.

"Hardware-Enabled Security." *Intel*, www.intel.com/content/www/us/en/security/hardware/hardware-security-overview.html.

Intel Corporation. (n.d.). Retrieved from http://www.annualreports.com/Company/intel-corporation

(n.d.). Retrieved from https://www.intc.com/investor-relations/financials-and-filings/earnings-results/default.aspx

(n.d.). Retrieved from https://www.sec.gov/Archives/edgar/data/50863/000005086316000105/a10kdocument12262015q4.ht

m(n.d.). Retrieved from https://www.capitaliq.com/CIQDotNet/company.aspx?companyId=21127

Newman, Lily Hay. “Critical Flaw Undermines Intel CPUs' Most Secure Element.” *Wired*, Conde Nast, 20 Aug. 2018, www.wired.com/story/foreshadow-intel-secure-enclave-vulnerability/.

“Securing the Digital World: Intel Announces Silicon-Level Security Technologies, Industry Adoption at RSA 2018.” *Intel Newsroom*, newsroom.intel.com/editorials/securing-digital-world-intel-announces-silicon-level-security-technologies-industry-adoption-rsa-2018/#gs.9kpyqi.

Sanders, J. (n.d.).(Oct,2018) How to detect hardware-based server bugs. Retrieved from https://www.techrepublic.com/article/detecting-hardware-based-server-bugs-heres-how/

What is a Bug? (2017, September 15). Retrieved from https://www.computerhope.com/jargon/b/bug.htm

What is Software Bug? - Definition from Techopedia. (n.d.). Retrieved from https://www.techopedia.com/definition/24864/software-bug-

The Asian Institute of Research
Engineering and Technology Quarterly Reviews
Vol.2, No.1, 2019: 68-81
ISSN 2622-9374

Oxidative Clearing of Polyester Cotton Blended Fabric by Hydrogen Peroxide: An Alternative to Reduction Clearing

Abul Fazal Mohammad Fahad Halim[1], Roy Ajoy[2], Mohammad Muzammel Hossen[3], Arpan Chakma[4]

[1] Textile Engineering, World University of Bangladesh, Dhaka, Bangladesh
[2] Textile Engineering, World University of Bangladesh, Dhaka, Bangladesh
[3] Textile Engineering, Zhejiang Sci-Tech University, Hangzhou, China
[4] Textile Engineering, Zhejiang Sci-Tech University, Hangzhou, China

Abstract
Reduction clearing is commonly carried out as an after-treatment to remove deposits of disperse dye and other residual impurities from the surface of dyed polyester. Because of certain environmental and economical disadvantages associated with traditional reduction clearing, there is industrial interest in alternative processes. In this study the P/C blended fabric was dyed with disperse dyes in grey state and then treated with H2O2 at different concentration for oxidation clearing. Another process was carried out conventionally where pre-treated P/C blended fabric was dyed with disperse dyes and reduction cleared. Fabrics from both processes were dyed with reactive dyes. The performance was evaluated through assessing the changes in absorbency, Kubelka-monk theory (K/S value), wash fastness, rubbing fastness, bursting strength test and by comparing the obtained results. The overall results showed that, the test results of oxidation clearing process were quite similar to reduction clearing process. But after reactive dyeing oxidation cleared samples showed better results than reduction cleared samples.

Key Words: Reduction Clearing, Oxidative Clearing, PC, Disperse Dye, Reactive Dye

1. Introduction

Polyester (polyethylene terephthalate, PET) fibres have emerged as having a leading share among natural and synthetic fibres when production and consumption of different fibres in the world is compared. It enjoys this dominant position due to its desirable properties, the most important of which are versatility and ease of use. It is also blended with natural fibres such as cotton and wool, mainly due to these characteristics, which are lacking in most natural fibres. Polyester and its blends find applications in a range of markets, such as apparel, upholstery and work wear as well as technical textiles, for example, non-woven.

Polyester is dyed with disperse dyes. Disperse dyes are non-ionic molecules with limited solubility in water at room temperature. They are usually applied to polyester from a fine aqueous dispersion at relatively high temperatures where the solubility in water becomes sufficient to allow individual molecules in solution to come into contact with the fibres. Polyester fibres are relatively hydrophobic with a highly crystalline structure and are consequently difficult to dye at low temperatures. Dyeing is generally carried out at high temperatures, often around 130°C, above a temperature referred to as the dyeing transition temperature, which is closely aligned with the glass transition temperature and where higher segmental mobility of the polymer chains enables the dye

molecules to penetrate into the fibre. Because of the low solubility of disperse dyes in water and the tendency for particles in the dye dispersion to aggregate during the course of dyeing, some residual dye commonly remains on the fibre surface at the end of the dyeing phase. These surface deposits may have an adverse effect on the colour fastness and properties of the dyed fabrics, if present, and an after treatment to remove them is generally introduced into the dyeing process. The washing process which is used traditionally to remove the deposits of disperse dye from the surface of the polyester after dyeing is referred to as reduction clearing. This process involves treatment of the dyed polyester with an aqueous solution of a reducing agent in alkaline conditions (DM 1979, Park and Shore 2004). Because of the hydrophobic character of polyester and since the process is conducted below the glass transition temperature, the reducing agent and alkali, both ionic species, cannot penetrate into the interior of the polyester. Thus, only dye on the surface is removed while dye molecules that have diffused into the polymer during dyeing remain unaffected (Aspland 1992).

In addition to the dye, there may be surface deposits of oligomers, which are only soluble in water at the dyeing temperature and may crystallize as a white powder on the fabric and in dyeing machinery as the dyebath is cooled. These oligomers may also be removed by the clearing process.

Reduction clearing is of technical importance in polyester dyeing in order to improve the brightness of the color and the fastness properties of the dyed fabric, especially to wet treatments.

There are, however, certain environmental, technological and economic disadvantages associated with the traditional reduction clearing process. The environmental disadvantage of the process is that it generates sulphur-containing degradation products derived from sodium dithionite which appear in the effluent with potentially toxic effects, notably sulphite, sulphate and thiosulphate. Waste water containing sulphites and sulphates are corrosive and can cause severe damage in waste lines. The oxidation products of sodium dithionite may also cause oxygen depletion in water streams resulting in an increase in chemical oxygen demand. Another technical issue is the sensitivity of sodium dithionite to air oxidation in an alkaline medium at high temperatures, so that an excess is used to compensate for the loss. In addition, the after treatment requires pH adjustment from the acidic conditions during dyeing to the strongly alkaline clearing conditions for reduction clearing, followed by a final neutralization, and this increases the time and cost of the overall dyeing process. Nevertheless, reduction clearing currently retains industrial importance especially for medium to heavy depths of shade, for package dyeing and the dyeing of loose fibres. In addition, it is important in the dyeing of polyester microfibers which require more dye than regular denier fibres to achieve equivalent depth (Aleem 2013).

2. Experimental Equipment

In this project we used Datacolor Ahiba IR (James. H. Heal Co Ltd, UK), Datacolor SF650 Benchtop Spectrophotometer, Hydraulic Diaphragm Bursting Strength Tester (Mesdan, Italy), Gyro Wash Machine (James. H. Heal Co Ltd, UK), Crock Meter (James. H. Heal Co Ltd, UK), Grey Scale S.D.C, England).

3. Materials and Methods

The fabric was collected from Mymun Textiles Ltd. (DBL Group).

Table 3. 1: Specification of Fabric

Type	60/40 PC blend knitted Fabric
Wales Per Inch (WPI)	34
Course Per Inch (CPI)	58
Yarn Count (Ne)	38
G.S.M	120

Chemicals used for pre-treatment NaOH 40 g/mol (Merck, India), H_2O_2 34 g/mol, stabilizer SOF (Switzerland), wetting agent (Archroma Bd Ltd.), EDTA (Archroma Bd Ltd.), Non-ionic detergent (Archroma Bd Ltd.), Disperse dye T/D: Red EFB (Dysin-Chem Ltd., china), Anionic Dispersing agent Setamol WS, Anionic levelling agent (Jintex, Taiwan), Acetic acid 60.05 g/mol (Vosol), Sodium acetate anhydrate as buffer 82.03 g/mol, Reactive red-D-2B bifunctional, mono-azo type (Dysin-Chem Ltd., china), Soda ash 106 g/mol (Merck, India), Sodium sulphate anhydrous 142.04 g/mol (Merck, India), Sodium hydrosulphate solid, Sulphuric acid (95-97%), Meta Cresol 108.14 g/mol (Merck, India), Direct dye blue (Dysin-Chem Ltd., china).

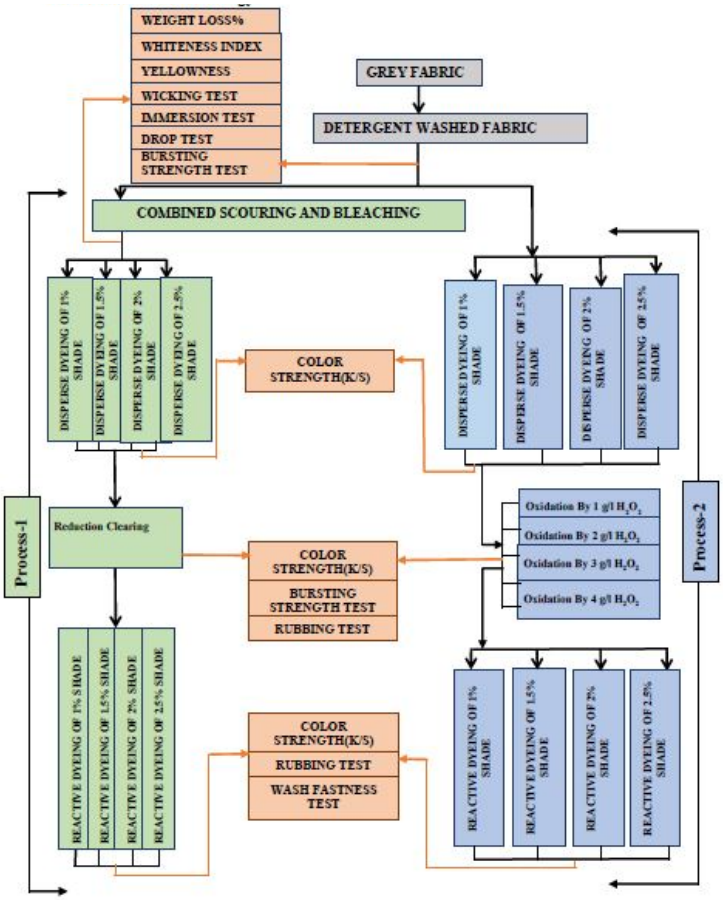

Figure 3.1. Research Methodology

4. Results and Discussion

4.1. Data analysis of Pretreated Samples

Table 4.1. Weight loss (%), Whiteness Index (WI), Yellowness Index (YI), Wicking Test, Immersion Test, Drop Test, Strength Loss (%) of Differently Treated Fabric

Fabric Type	Weight Loss%	WI	YI	Wicking Test (mm)	Immersion Test (sec)	Drop Test	Strength Loss%
Detergent Washed Fabric	0.36	70.13	4.88	71	4.2	Even and Complete	1.03
Combined Scoured and Bleached Fabric	1.81	78.98	2.90	80	3.2	Even and Complete	3.17

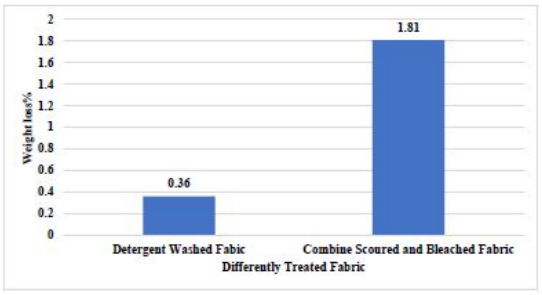

Figure 4.1. Weight loss (%) of Differently Treated Fabric

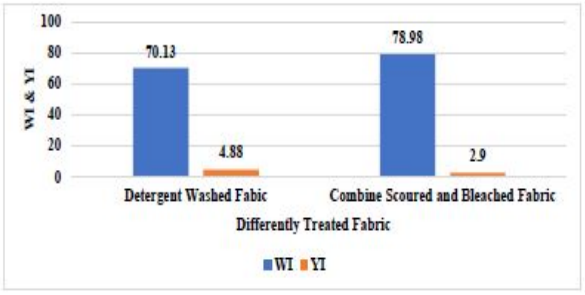

Figure 4.2. Whiteness Index (WI) and Yellowness Index (YI) of Differently Treated Fabric

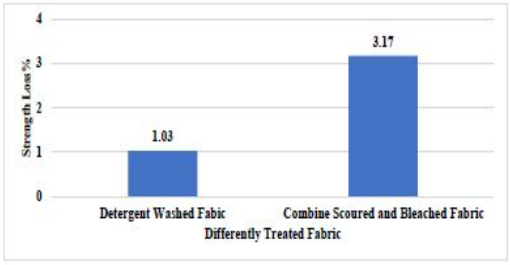

Figure 4.3. Strength Loss (%) of Differently Treated Fabric

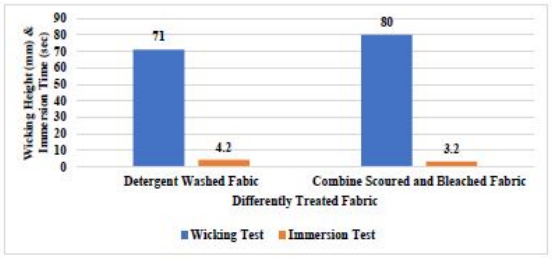

Figure 4.4. Wicking Test and Immersion Test of Differently Treated Fabric

The results show that, after combine Scouring and bleaching weight loss percentage was higher because more impurities removed in combined scouring and bleaching process which results in increased absorbency. After combined scouring and bleaching whiteness index increased and yellowness index decreased as natural color of fabric destroyed during bleaching. After combined scouring and bleaching wicking height is increased to 80 mm and immersion time is decreased to 3.2 second. After combined scouring and bleaching impurities had been removed that is why wicking height increased as well as immersion time decreased. After combined scouring and bleaching strength loss percentage was increased. This is because after combined scouring and bleaching the fabric strength is reduced due to treatment with hydrogen peroxide.

4.2. Analysis of Conventionally Treated Samples

4.2.1. Data Analysis of Process-1 Disperse Dyed Samples

Table 4.2. Color Strength of Disperse Dyed Process-1 Samples

Shade%	K/S value
1	3.759
1.5	4.389
2	4.991
2.5	5.709

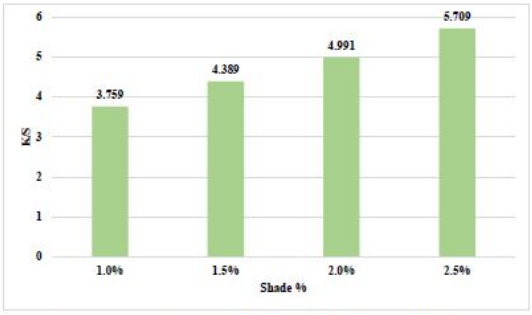

Figure 4.5. Color Strength of Disperse Dyed Process-1 Samples

The results show that, the color strength is increased with shade percentage. It can be explained that, with the increasing of shade percentage, dye concentration increases that is why K/S value increased.

4.2.2. Data Analysis of Process-1 Reduction Cleared Samples

Table 4.3. Color Strength, Strength Loss (%), Rubbing Tests of Process-1 Reduction Cleared Samples

Shade%	Reduction Clearing with $Na_2S_2O_4$	K/S value	Strength Loss%	Rubbing Test	
				Dry	Wet
1	2 g/l	3.494	1.10	5	5
1.5		3.991	1.12	5	5
2		4.441	1.09	5	5
2.5		5.020	1.17	5	5

The results show that, color strength increased with increased shade percentage. Strength loss % remain quite similar for all shade percentage. Excellent rubbing fastness achieved for all shade percentage.

4.2.3. Data Analysis of Process-1 Disperse/Reactive Dyed Samples

Table 4.4. Color Strength, Rubbing Test of Process-1 Disperse/Reactive Dyed Samples

Shade%	K/S value	Rubbing Test	
		Dry	Wet
2 (1%D+1%R)	5.96	5	4/5
3(1.5%D+1.5%R)	8.446	5	4/5
4 (2%D+2%R)	10.272	5	4/5
5(2.5%D+2.5%R)	11.922	5	4/5

Table 4.5. Wash Fastness (Staining of multifibre fabric) of Process-1 Disperse/Reactive Dyed Samples

Shade %	Di-acetate	Bleached Cotton	Nylon	Polyester	Acrylic	Wool
2 (1%D+1%R)	4	4/5	4	4/5	4/5	5
3 (1.5%D+1.5%R)	3/4	4/5	3/4	4/5	4/5	5
4 (2%D+2%R)	3/4	4/5	3/4	4/5	4/5	4/5
5 (2.5%D+2.5%R)	3	4/5	3	4/5	4/5	4/5

The results show that, color strength increased with increased shade percentage. Excellent dry rubbing fastness achieved for all shade percentage. Good to excellent wet rubbing fastness achieved for all shade percentage.

The results show that, di-acetate and nylon are the most highly stained among the six fibre types and other showed quite similar result.

Table 4.6. Change in Color of Process-1 Disperse/Reactive Dyed Samples

Shade %	Change in Color
2 (1%D+1%R)	4/5
3 (1.5%D+1.5%R)	4
4 (2%D+2%R)	3/4
5 (2.5%D+2.5%R)	3

The results show that by increasing the depth of the shades wash fastness rating is decreasing.

4.3. Analysis of Process-2 Samples

4.3.1. Data Analysis of Process-2 Disperse Dyed Samples

Table 4.7. Color Strength of Disperse Dyed Process-2 Samples

Shade%	K/S value
1	3.813
1.5	4.541
2	5.132
2.5	5.896

Figure 4.6. Color Strength of Disperse Dyed Process-2 Samples

The results show that, by the increasing concentration of dye, color strength increasing.

4.3.2. Data Analysis of Process-2 Oxidation Cleared Samples

Table 4.8. Color Strength, Strength Loss (%), Rubbing fastness Tests of Process-2 Oxidation Cleared Samples Dyed with 1% Disperse Dye

Shade%	Oxidation Clearing with H_2O_2	K/S value	Strength Loss%	Rubbing Test	
				Dry	Wet
1	1 g/l	3.601	1.06	5	5
	2 g/l	3.596	2.01	5	5
	3 g/l	3.540	3.11	5	5
	4 g/l	3.515	6.91	5	5

Table 4.9. Color Strength, Strength Loss (%), Rubbing fastness Tests of Process-2 Oxidation Cleared Samples Dyed with 1.5% Disperse Dye

Shade%	Oxidation Clearing with H_2O_2	K/S value	Strength Loss%	Rubbing Test	
				Dry	Wet
1.5	1 g/l	4.332	1.08	5	5
	2 g/l	4.231	2.15	5	5
	3 g/l	4.147	3.23	5	5
	4 g/l	4.147	7.68	5	5

Table 4.10. Color Strength, Strength Loss (%), Rubbing fastness Tests of Process-2 Oxidation Cleared Samples Dyed with 2% Disperse Dye

Shade%	Oxidation Clearing with H_2O_2	K/S value	Strength Loss %	Rubbing Test	
				Dry	Wet
2	1 g/l	4.700	1.09	5	5
	2 g/l	4.689	3.26	5	5
	3 g/l	4.600	4.35	5	5
	4 g/l	4.539	8.35	5	5

Table 4.11. Color Strength, Strength Loss (%), Rubbing fastness Tests of Process-2 Oxidation Cleared Samples Dyed with 2.5% Disperse Dye

Shade%	Oxidation Clearing with H_2O_2	K/S value	Strength Loss%	Rubbing Test	
				Dry	Wet
2.5	1 g/l	5.400	1.26	5	5
	2 g/l	5.365	3.52	5	5
	3 g/l	5.225	5.02	5	5
	4 g/l	5.139	8.51	5	5

From the results it has been clear that, by the increasing concentration of H_2O_2 more surface dye removed and strength loss percentage increasing.

Excellent rubbing fastness results found for all oxidation cleared samples.

Table 4. 12 : Absorbency of Oxidation Cleared Samples

Shade% (Disperse Dye)	Oxidation Clearing with H_2O_2	Wicking Height (mm)	Immersion Time (sec)	Drop Test
1	1 g/l	90	2.38	Even and Complete
	2 g/l	89	2.45	Even and Complete
	3 g/l	90	2.35	Even and Complete
	4 g/l	91	2.19	Even and Complete
1.5	1 g/l	92	2.11	Even and Complete
	2 g/l	89	2.43	Even and Complete
	3 g/l	88	2.56	Even and Complete
	4 g/l	90	2.37	Even and Complete
2	1 g/l	86	2.75	Even and Complete
	2 g/l	88	2.61	Even and Complete
	3 g/l	89	2.43	Even and Complete
	4 g/l	91	2.23	Even and Complete
2.5	1 g/l	90	2.33	Even and Complete
	2 g/l	91	2.20	Even and Complete
	3 g/l	93	2.03	Even and Complete
	4 g/l	91	2.29	Even and Complete

The results show that, after oxidation clearing wicking height and immersion time remain more or less similar for all concentration. But, if we compare with detergent washed fabric it can obviously be said that, wicking height increased and immersion time decreased. That means, absorbency increased after oxidation process.

4.3.3. Data Analysis of Process-2 Disperse/Reactive Dyed Samples

Table 4.13. Color Strength, Rubbing Test of Process-2 Samples Dyed with 2% (1%D+1%R) Disperse/Reactive

Shade%	Oxidation Clearing with H_2O_2	K/S value	Rubbing Test	
			Dry	Wet
2	1 g/l	7.4	5	4/5
	2 g/l	7.333	5	4/5
	3 g/l	7.51	5	4/5
	4 g/l	7.702	5	4/5

Table 4.14. Color Strength, Rubbing Test of Process-2 Samples Dyed with 3% (1.5%D+1.5%R) Disperse/Reactive Dye

Shade%	Oxidation Clearing with H_2O_2	K/S value	Rubbing Test	
			Dry	Wet
3	1 g/l	10.555	5	4/5
	2 g/l	10.364	5	4/5
	3 g/l	10.288	5	4/5
	4 g/l	10.497	5	4/5

Table 4.15. Color Strength, Rubbing Test of Process-2 Samples Dyed with 4% (2%D+2%R) Disperse/Reactive Dye

Shade%	Oxidation Clearing with H_2O_2	K/S value	Rubbing Test	
			Dry	Wet
4	1 g/l	12.219	5	4/5
	2 g/l	12.303	5	4/5
	3 g/l	12.33	5	4
	4 g/l	12.514	5	4/5

Table 4.16. Color Strength, Rubbing Test of Process-2 Samples Dyed with 5% (2.5%D+2.5%R) Disperse/Reactive Dye

Shade%	Oxidation Clearing with H_2O_2	K/S value	Rubbing Test	
			Dry	Wet
5	1 g/l	13.353	5	4
	2 g/l	13.609	5	4
	3 g/l	13.881	5	3/4
	4 g/l	13.65	5	3/4

Table 4.17. Wash Fastness Rating of Process-2 Samples Dyed with Disperse/Reactive Dye

Shade %	Oxidation Clearing with H_2O_2	Di-acetate	Cotton	Nylon	Polyester	Acrylic	Wool
2	1 g/l	3	4	3	4	4	4/5
	2 g/l	3/4	4	3/4	4	4	4/5
	3 g/l	4	4	3/4	4	4	4/5
	4 g/l	3/4	4	3/4	4	4	4/5
3	1 g/l	3/4	4	3	4	4	4/5
	2 g/l	3/4	4	3/4	4	4	4/5
	3 g/l	3/4	4	3/4	4	4	4/5
	4 g/l	3	4	3	4	4	4/5
4	1 g/l	3/4	4	3	4	4	4/5
	2 g/l	3/4	4	3	4	4	4/5
	3 g/l	3/4	4	3/4	4	4	4/5
	4 g/l	3/4	4	3/4	4	4	4/5
5	1 g/l	3/4	4	3/4	4	4	4/5
	2 g/l	3/4	4	3/4	4	4	4/5
	3 g/l	3/4	4	3/4	4	4	4
	4 g/l	3/4	4	3/4	4	4	4

From the results it has been clear that, after reactive dyeing color strength increased with increasing shade percentage but it remains nearly similar for different concentration of H_2O_2. From rubbing fastness (wet) results, 2%, 3% oxidation cleared samples showed good to excellent. For 4% shade OC-3 g/l showed good, others showed good to excellent. For 5% shade OC-1 g/l, OC-2 g/l showed good to excellent and other samples showed fair to good rating. Excellent dry rubbing fastness results found for all oxidation cleared samples. The wash fastness results show that, di-acetate and nylon are the most highly stained among the six fibre types.

Table 4.18. Change in color of Process-2 Samples Dyed with Disperse/Reactive Dye

Shade %	Oxidation Clearing with H_2O_2	Change in Color
2	1 g/l	4
	2 g/l	4
	3 g/l	4/5
	4 g/l	4
3	1 g/l	4
	2 g/l	4
	3 g/l	4
	4 g/l	4
4	1 g/l	4
	2 g/l	3/4
	3 g/l	3/4
	4 g/l	4
5	1 g/l	3/4
	2 g/l	3
	3 g/l	3/4
	4 g/l	3/4

The results show that, by increasing the depth of the shades, change in color of the dyed samples decreases.

4.4. Comparison of Process-1 and Process-2 Samples

4.4.1. Comparison of Disperse Dyed Samples

Table 4. 19 : Comparison of Process-1 (P-1) and Process-2(p-2) disperse dyed Samples

Shade%	K/S value (P-1)	K/S value (P-2)
1	3.759	3.813
1.5	4.389	4.541
2	4.991	5.132
2.5	5.709	5.896

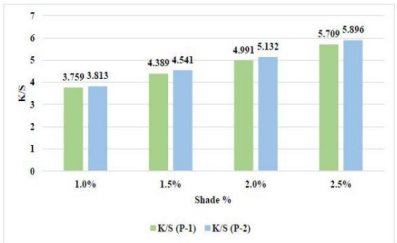

Figure 4. 7 : Graphical Representation of K/S of Process-1 (P-1) and Process-2(p-2) Disperse Dyed Samples

From the results, it can be seen that K/S value is increasing with increasing shade percentage. It is also clear that K/S value of process-1 and process-2 samples remain quite similar.

4.4.2. Comparison of Reduction Cleared/Oxidation Cleared Samples

Table 4. 20 : Comparison of Process-1 and Process-2 Reduction cleared/Oxidation Cleared Samples Dyed with 1% Disperse Dye

Shade%	Processes	Chemical Concentration		K/S value	Strength Loss%	Rubbing Test	
						Dry	Wet
1	Process-1	$Na_2S_2O_4$ (2 g/l)		3.494	1.10	5	5
	Process-2	H_2O_2	(1 g/l)	3.601	1.06	5	5
			(2 g/l)	3.596	2.01	5	5
			(3 g/l)	3.54	3.11	5	5
			(4 g/l)	3.515	6.91	5	5

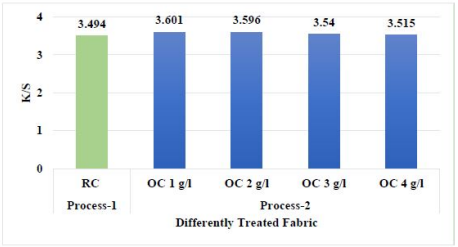

Figure 4. 8 : Graphical Representation of K/S of Process-1 and Process-2 Reduction Cleared (RC)/Oxidation Cleared (OC) Samples Dyed with 1% Disperse Dye

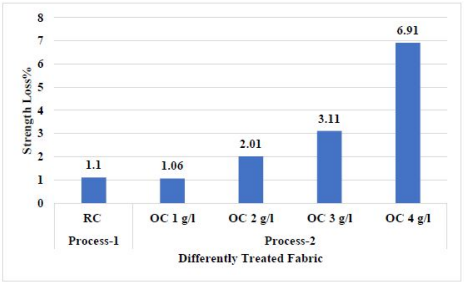

Figure 4. 9 : Graphical Representation of Strength Loss (%) of Process-1 and Process-2 Reduction Cleared (RC)/Oxidation Cleared (OC) Samples Dyed with 1% Disperse Dye

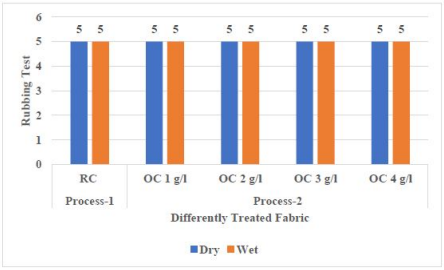

Figure 4. 10: Graphical Representation of Rubbing Test of Process-1 and Process-2 Reduction Cleared (RC)/Oxidation Cleared (OC) Samples Dyed with 1% Disperse Dye

Table 4. 21 : Comparison of Process-1 and Process-2 Reduction cleared/Oxidation Cleared Samples Dyed with 1.5% Disperse Dye

Shade%	Processes	Chemical Concentration		K/S value	Strength Loss%	Rubbing Test	
						Dry	Wet
1.5	Process-1	$Na_2S_2O_4$ (2 g/l)		3.991	1.12	5	5
	Process-2	H_2O_2	(1 g/l)	4.332	1.08	5	5
			(2 g/l)	4.231	2.15	5	5
			(3 g/l)	4.147	3.23	5	5
			(4 g/l)	4.119	7.68	5	5

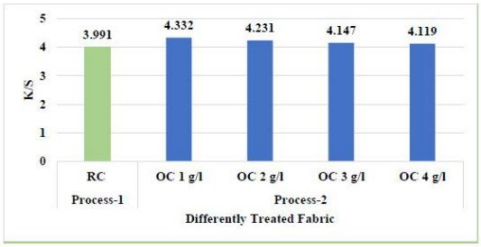

Figure 4. 11 : Graphical Representation of K/S of Process-1 and Process-2 Reduction Cleared (RC)/Oxidation Cleared (OC) Samples Dyed with 1.5% Disperse Dye

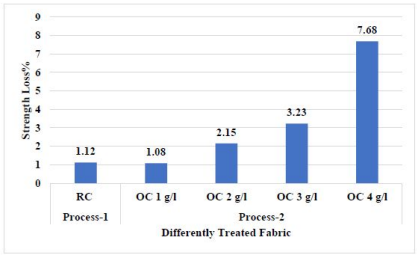

Figure 4. 12 : Graphical Representation of Strength Loss (%) of Process-1 and Process-2 Reduction Cleared (RC)/Oxidation Cleared (OC) Samples Dyed with 1.5% Disperse Dye

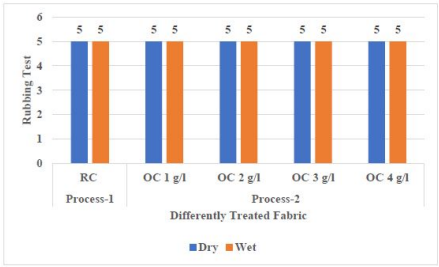

Figure 4. 13: Graphical Representation of K/S of Process-1 and Process-2 Reduction Cleared (RC)/Oxidation Cleared (OC) Samples Dyed with 1.5% Disperse Dye

Table 4. 22 : Comparison of Process-1 and Process-2 Reduction cleared/Oxidation Cleared Samples Dyed with 2% Disperse Dye

Shade%	Processes	Chemical Concentration		K/S value	Strength Loss %	Rubbing Test	
						Dry	Wet
2	Process-1	$Na_2S_2O_4$ (2 g/l)		4.441	1.09	5	5
	Process-2	H_2O_2	(1 g/l)	4.700	1.09	5	5
			(2 g/l)	4.689	3.26	5	5
			(3 g/l)	4.600	4.35	5	5
			(4 g/l)	4.539	8.35	5	5

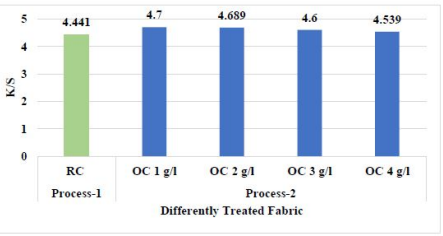

Figure 4. 14 : Graphical Representation of K/S of Process-1 and Process-2 Reduction Cleared (RC)/Oxidation Cleared (OC) Samples Dyed with 2% Disperse Dye

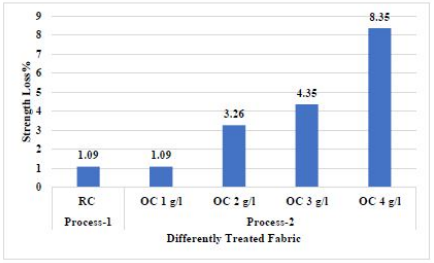

Figure 4. 15 : Graphical Representation of Strength Loss (%) of Process-1 and Process-2 Reduction Cleared (RC)/Oxidation Cleared (OC) Samples Dyed with 2% Disperse Dye

Figure 4. 16: Graphical Representation of K/S of Process-1 and Process-2 Reduction Cleared (RC)/Oxidation Cleared (OC) Samples Dyed with 2% Disperse Dye

Table 4. 23 : Comparison of Process-1 and Process-2 Reduction cleared/Oxidation Cleared Samples Dyed with 2.5% Disperse Dye

Shade%	Processes	Chemical Concentration		K/S value	Strength Loss %	Rubbing Test	
						Dry	Wet
2.5	Process-1	$Na_2S_2O_4$ (2 g/l)		5.020	1.17	5	5
	Process-2	H_2O_2	(1 g/l)	5.400	1.26	5	5
			(2 g/l)	5.365	3.52	5	5
			(3 g/l)	5.225	5.02	5	5
			(4 g/l)	5.139	8.51	5	5

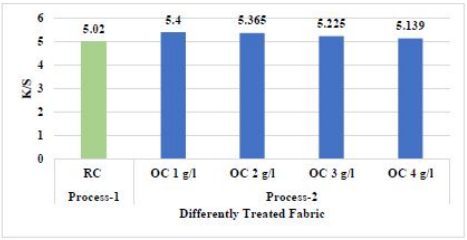

Figure 4. 17 : Graphical Representation of K/S of Process-1 and Process-2 Reduction Cleared (RC)/Oxidation Cleared (OC) Samples Dyed with 2.5% Disperse Dye

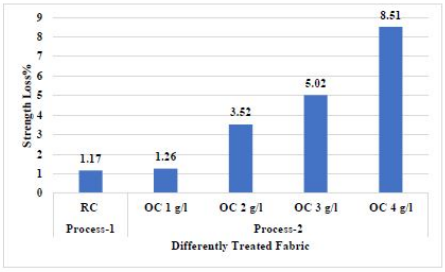

Figure 4. 18 : Graphical Representation of Strength Loss (%) of Process-1 and Process-2 Reduction Cleared (RC)/Oxidation Cleared (OC) Samples Dyed with 2.5% Disperse Dye

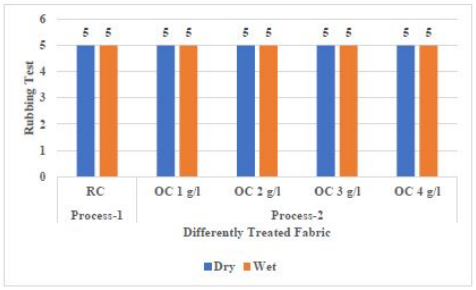

Figure 4. 19: Graphical Representation of K/S of Process-1 and Process-2 Reduction Cleared (RC)/Oxidation Cleared (OC) Samples Dyed with 2.5% Disperse Dye

From the results, it has been clear that by the increased concentration of H_2O_2 the K/S value decreased as well as strength loss (%) increased. It can be explained that as peroxide concentration increased more surface dye removed that is why K/S value decreased. On the other hand, strength reduced due to using H_2O_2 as oxidizing agent which can damage fabric.

Excellent dry and wet rubbing fastness rating found for all shade percentage.

4.4.3. Comparison of Disperse/Reactive Dyed Samples

Table 4. 24 : Comparison of Process-1 and Process-2 Samples Dyed with 2%(1%D+1%R) Disperse/Reactive Dye

Shade %	Processes	Chemical Concentration		K/S value	Rubbing Test	
					Dry	Wet
2	Process-1	$Na_2S_2O_4$ (2 g/l)		5.96	5	4/5
	Process-2	H_2O_2	(1 g/l)	7.4	5	4/5
			(2 g/l)	7.333	5	4/5
			(3 g/l)	7.51	5	4/5
			(4 g/l)	7.702	5	4/5

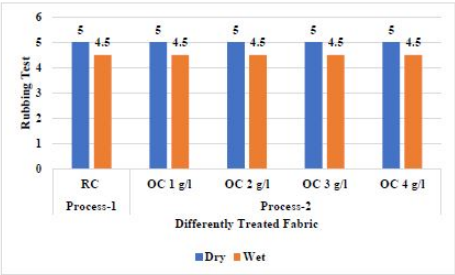

Figure 4. 21 : Graphical Representation of Rubbing Test Rating of Process-1 and Process-2 Reduction Cleared (RC)/Oxidation Cleared (OC) Samples Dyed with 2%(1%D+1%R) Disperse/Reactive Dye

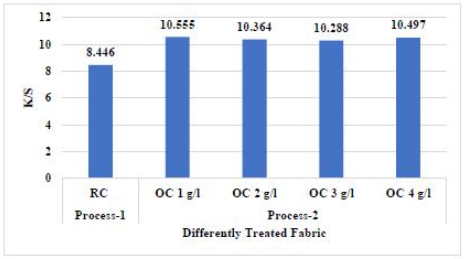

Figure 4. 22 : Graphical Representation of K/S of Process-1 and Process-2 Reduction Cleared (RC)/Oxidation Cleared (OC) Samples Dyed with 3%(1.5%D+1.5%R) Disperse/Reactive Dye

Table 4. 26 : Comparison of Process-1 and Process-2 Samples Dyed with 4%(2%D+2%R) Disperse/Reactive Dye

Shade%	Processes	Chemical Concentration		K/S value	Rubbing Test	
					Dry	Wet
4	Process-1	$Na_2S_2O_4$ (2 g/l)		10.272	5	4/5
	Process-2	H_2O_2	(1 g/l)	12.219	5	4/5
			(2 g/l)	12.303	5	4/5
			(3 g/l)	12.33	5	4
			(4 g/l)	12.514	5	4/5

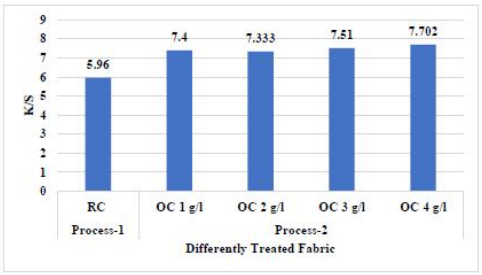

Figure 4. 20 : Graphical Representation of K/S of Process-1 and Process-2 Reduction Cleared (RC)/Oxidation Cleared (OC) Samples Dyed with 2%(1%D+1%R) Disperse/Reactive Dye

Table 4. 25 : Comparison of Process-1 and Process-2 Samples Dyed with 3%(1.5%D+1.5%R) Disperse/Reactive Dye

Shade%	Processes	Chemical Concentration		K/S value	Rubbing Test	
					Dry	Wet
3	Process-1	$Na_2S_2O_4$ (2 g/l)		8.446	5	4/5
	Process-2	H_2O_2	(1 g/l)	10.555	5	4/5
			(2 g/l)	10.364	5	4/5
			(3 g/l)	10.288	5	4/5
			(4 g/l)	10.497	5	4/5

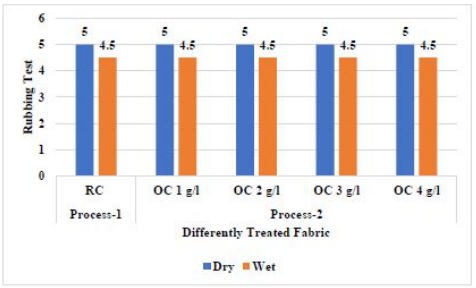

Figure 4. 23 : Graphical Representation of Rubbing Test Rating of Process-1 and Process-2 Reduction Cleared (RC)/Oxidation Cleared (OC) Samples Dyed with 3%(1.5%D+1.5%R) Disperse/Reactive Dye

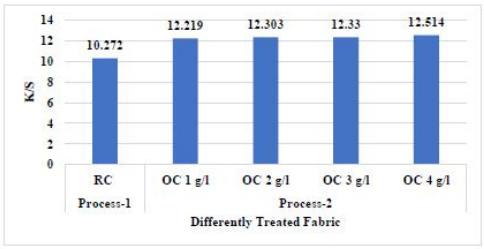

Figure 4. 24 : Graphical Representation of K/S of Process-1 and Process-2 Reduction Cleared (RC)/Oxidation Cleared (OC) Samples Dyed with 4%(2%D+2%R) Disperse/Reactive Dye

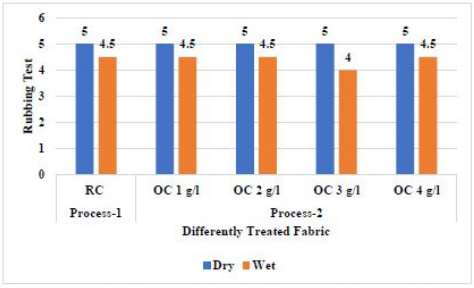

Figure 4. 25 : Graphical Representation of Rubbing Test Rating of Process-1 and Process-2 Reduction Cleared (RC)/Oxidation Cleared (OC) Samples Dyed with 4%(2%D+2%R) Disperse/Reactive Dye

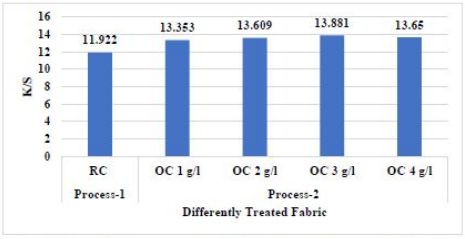

Figure 4. 26 : Graphical Representation of K/S of Process-1 and Process-2 Reduction Cleared (RC)/Oxidation Cleared (OC) Samples Dyed with 5%(2.5%D+2.5%R) Disperse/Reactive Dye

Table 4. 27 : Comparison of Process-1 and Process-2 Samples Dyed with 5%(2.5%D+2.5%R) Disperse/Reactive Dye

Shade%	Processes	Chemical Concentration		K/S value	Rubbing Test	
					Dry	Wet
5	Process-1	$Na_2S_2O_4$ (2 g/l)		11.922	5	4/5
	Process-2	H_2O_2	(1 g/l)	13.353	5	4
			(2 g/l)	13.609	5	4
			(3 g/l)	13.881	5	3/4
			(4 g/l)	13.65	5	3/4

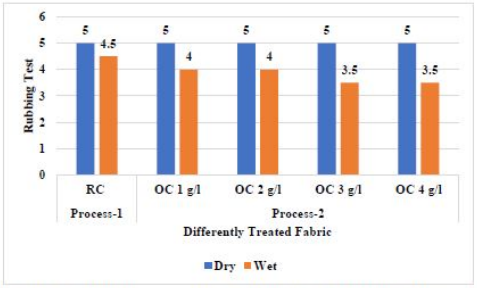

Figure 4. 27 : Graphical Representation of Rubbing Test Rating of Process-1 and Process-2 Reduction Cleared (RC)/Oxidation Cleared (OC) Samples Dyed with 5%(2.5%D+2.5%R) Disperse/Reactive Dye

The results show that, K/S value increased with the increased shade percentage and also color strength is higher in process-2 samples comparing to process-1 samples. This is because in process-2 absorbency increased as a result color strength got higher. From the results of wet rubbing fastness it was found that, for 2%, 3% shade process-1 and process-2 samples showed good to excellent result. For 4% shade OC-3 g/l showed good rating and others showed good to excellent result but process-1 sample showed good to excellent result. For 5% shade, OC-1 g/l, OC-2g/l showed good rating but others showed fair to good rating and process-1 sample showed good to excellent rating.

Table 4. 28 : Comparison of Wash Fastness Rating of Process-1 and Process-2 samples

Process-1						
Shade %	Di-acetate	Bleached Cotton	Nylon	Polyester	Acrylic	Wool
2	4	4/5	4	4/5	4/5	5
3	3/4	4/5	3/4	4/5	4/5	5
4	3/4	4/5	3/4	4/5	4/5	4/5
5	3	4/5	3	4/5	4/5	4/5

Process-2							
Shade %	Oxidation Clearing with H_2O_2	Di-acetate	Bleached Cotton	Nylon	Polyester	Acrylic	Wool
2	1 g/l	3	4	3	4	4	4/5
	2 g/l	3/4	4	3/4	4	4	4/5
	3 g/l	4	4	3/4	4	4	4/5
	4 g/l	3/4	4	3/4	4	4	4/5
3	1 g/l	3/4	4	3	4	4	4/5
	2 g/l	3/4	4	3/4	4	4	4/5
	3 g/l	3/4	4	3/4	4	4	4/5
	4 g/l	3	4	3	4	4	4/5
4	1 g/l	3/4	4	3	4	4	4/5
	2 g/l	3/4	4	3	4	4	4/5
	3 g/l	3/4	4	3/4	4	4	4/5
	4 g/l	3/4	4	3/4	4	4	4/5
5	1 g/l	3/4	4	3/4	4	4	4/5
	2 g/l	3/4	4	3/4	4	4	4/5
	3 g/l	3/4	4	3/4	4	4	4
	4 g/l	3/4	4	3/4	4	4	4

The results show that acetate and nylon are the most highly stained among the six fibre types. This can be explained on the basis that acetate, nylon were stained for using disperse dyes in polyester dyeing and cotton and wool stained for using reactive dye in cotton part dyeing.

Table 4. 29 : Comparison of Change in Color of Process-1 and Process-2 samples

Process-1		
Shade %	**Change in Color**	
2	4/5	
3	4	
4	3/4	
5	3	
Process-2		
Shade %	**Oxidation Clearing with H_2O_2 (g/l)**	**Change in Color**
2	1	4
	2	4
	3	4/5
	4	4
3	1	4
	2	4
	3	4
	4	4
4	1	4
	2	3/4
	3	3/4
	4	4
5	1	3/4
	2	3
	3	3/4
	4	3/4

The results show that, by increasing the shade percentage, fastness rating is decreasing.

5. Conclusions

In traditional process, the surface deposits of disperse dye is removed by reduction clearing. Reduction clearing has adverse effect on environment. Sodium dithionate is an inorganic compound and not bio-degradable. As, sodium dithionate is not bio-degradable, its presence in the effluent increases the COD of water. In this study, oxidation clearing with H_2O_2 was done as an alternative to reduction clearing. From different research work it has been found that, in oxidation process, ecological advantages were significant and further advantage is that pre-treatment can be eliminated.

References

DM, N. 1979. The dyeing of synthetic-polymer and acetate fibres. Dyers Company Publications Trust.
Broadbent, A.D. 2001. Basic principles of textile coloration. Bradford: Society of Dyers and Colourists.
Hawkyard, C. 2004. Synthetic fibre dyeing. Society of Dyers and Colourists.
Park, J. and J. Shore. 2004. Practical dyeing. Society of Dyers & Colourists.
Aspland, J. 1992. Disperse dyes and their application to polyester. Textile Chemist and Colorist. 24: p. 18-18.
Ul Aleem, A. 2013. An Investigation of Alternatives to Reductive Clearing in the Dyeing of Polyester. Heriot Watt University.
Gomes, J.R., C. Lima, and J. Almeida. 2000. Oxidative clearing of polyester and post-bleaching of cotton: a novel shorter process with better fastness. Colourage: annual edition, 47: p. 49-52.
Anis, P. and H.A. Eren. 2004. Examining The Effectiveness of Oxidative Clearing in One-Step Dyeing of Polyester/Cotton Fabrics. University of Uludag.
McIntyre, J.E. 2005. Synthetic fibres: Nylon, polyester, acrylic, polyolefin. Taylor & Francis US.
Deopura, B., et al. 2008. Polyesters and polyamides. Elsevier.
Perepelkin, K. 2001. Polyester Fibres Abroad in the Third Millennium. Fibre Chemistry. 33(5): p. 333-339.
Krichevskii, G. 2001. Textile Materials Made from Polyester Fibres:a Most Difficult Material to Color. Fibre chemistry. 33(5): p. 364-367.
Needles, H.L. 1986. Textile fibres, dyes, finishes, and processes: a concise guide. Park Ridge, N.J.: Noyes Publications.
Moncrieff, R.W. 1975. Man-made fibres. 6th ed. London: Newnes-Butterworths.

Bendak, A. and S. El-Marsafi. 1991. Effects of chemical modifications on polyester fibres. Journal of Islamic Academy of Sciences, 4(4): p. 275-284.
Shore, J. 1995. Cellulosic dyeing. Bradford: Society of Dyers and Colourists.
Choudhury, A.R. 2006. Textile preparation and dyeing. Science publishers.
Canal, J., et al. 2004. Effect of various bio-scouring systems on the accessibility of dyes into cotton. Coloration technology. 120(6): p. 311-315.
Hearle, J. 2007. Physical structure and properties of cotton, Cotton: science and technology. Woodhead Publishing Limited Cambridge; p. 35-67.
Gordon, S. and Y.-l. Hsieh. 2006. Cotton: Science and technology. Woodhead Publishing.
Cook, J.G. 1984. Handbook of textile fibres: Volume I. Natural Fibres. Cambridge: Woodhead Publishing Ltd.
Chao, N.P.C. 1963. Blending cotton and polyester fibres: effects of processing methods on fibre distribution and yarn properties. Georgia Institute of Technology.
Baykal, P.D., O. Babaarslan, and R. Erol. 2006. Prediction of strength and elongation properties of cotton polyester-blended OE rotor yarns. Fibres and Textiles in Eastern Europe. 14(1): p. 18.
Cyniak, D., J. Czekalski, and T. Jackowski. 2006. Quality analysis of cotton/polyester yarn blends spun with the use of a rotor spinning frame. Fibres & Textiles in Eastern Europe. 3(57): p. 33-37.
Sevkan, A. and H. Kadoglu. 2012. An investigation on ring and open-end spinning of flax/cotton blends. Journal of Textile & Apparel/Tekstil ve Konfeksiyon. 22(3).
Hegde, R.R., et al. 2011. Cotton fibres.
Wardman, R.H.a., an Introduction to Textile Coloration: Principles and Practice. 1st ed.
Shore, J. 1998. S.o. Dyers, and c. Blends dyeing. Bradford: Society of Dyers and Colourists.
Chakraborty, J.N.a., Fundamentals and practices in colouration of textiles.
Karmakar, S., Chemical Technology in The Pre-Treatment Processes of Textiles. 1st. Amsterdam. Elsevier.
Disperse Dyes | Properties of Disperse Dye. 2012, April 25. Available from: http://textilefashionstudy.com/disperse-dyes-properties-of-disperse-dye/ Access Date: 20/01/2018.
Avinc, O. 2011. Clearing of dyed poly (lactic acid) fabrics under acidic and alkaline conditions. Textile Research Journal. 81(10): p. 1049-1074.
Shore, J. 2002. Colorants and auxiliaries organic chemistry and application properties: Volume 2: Auxiliaries.
Dr. Naresh M. Saraf, D.A.G.S. Save Natural Resources: Adopt Acid Reduction Clearing. Available from: https://www.google.com/url?sa=t&rct=j&q=&esrc=s&source=web&cd=1&ved=0ahUKEwjuiJ3n_vnZAhXLPY8KHZmpB9QQFggmMAA&url=http%3A%2F%2Fwww.sarex.com%2Ftextile%2Fwp-content%2Fuploads%2F2015%2F08%2FART138.pdf&usg=AOvVaw1Zh69J7dvXbiasbaDctVnT Access Date: 2/02/2018.
Roessler, A. and X. Jin. 2003. State of the art technologies and new electrochemical methods for the reduction of vat dyes. Dyes and pigments. 59(3): p. 223-235.
Baumgarte, U. 1987. Developments in vat dyes and in their application. Coloration Technology. 17(1): p. 29-38.
Tiedemann, W. and J. Schad. 1998. Reduction clearing of polyester dyeings from its ecological and economic aspects. Melliand Textilberichte International Textile Reports. 79: p. 852-855.
Clarke, E. and D. Steinle. 1995. Health and environmental safety aspects of organic colorants. Coloration Technology.; 25(1): p. 1-5.
Bhaskar, M., et al. 2003. Analyses of carcinogenic aromatic amines released from harmful azo colorants by Streptomyces sp. SS07. Journal of Chromatography A. 1018(1): p. 117-123.
Chung, K.T. 2000. Mutagenicity and carcinogenicity of aromatic amines metabolically produced from azo dyes. Journal of Environmental Science & Health Part C.18(1): p. 51-74.
Zee, F. 2002.Anaerobic azo dye reduction. Netherlands: Wegeningen University.
Pandey, A., P. Singh, and L. Iyengar. 2007. Bacterial decolorization and degradation of azo dyes. International Bio-deterioration & Biodegradation.; 59(2): p. 73-84.
Eren, H.A. 2006. Afterclearing by ozonation: a novel approach for disperse dyeing of polyester. Coloration technology. 122(6): p. 329-333.
Chinta, S. and S. VijayKumar. 2013. Technical facts & figures of reactive dyes used in textiles. International Journal of Engineering and Management Sciences. 4(3): p. 308-312.
Clark, M. 2011. Handbook of textile and industrial dyeing. Woodhead Publishing Series in Textiles. Oxford; Philadelphia: Woodhead Publishing Limited